



Skeletal ultrastructure and phylogeny of cyclostome bryozoans

PAUL D. TAYLOR FLS* AND MICHAEL J. WEEDON

Department of Palaeontology, The Natural History Museum, London SW7 5BD

Received September 1998; accepted for publication January 1999

Recent research on the ultrastructure of the calcareous skeleton in the bryozoan order Cyclostomata is summarized and updated, based on field emission SEM studies of 87 species. Six fundamental ultrastructural fabrics are recognized which differ in the crystallographic orientations, shapes and prevailing growth directions of the constituent crystallites. During the growth of individual walls a succession of fabrics is secreted, defining a fabric suite. Five fabric suites are described in interior walls and four in exterior walls. Nine ultrastructural characters were combined with 37 other skeletal characters in a PAUP analysis of the relationships between 28 post-Palaeozoic cyclostomes chosen to include representatives of all suborders. A single tree of length 142 steps was found. Comparison of tree statistics for three categories of characters showed ultrastructural characters to be more homoplastic than zooidal characters, and the latter more homoplastic than colonial characters. Rooting the tree on the paleotubuliporine *Cuffeyella* gave four transitions from fixed- to free-walled organization and no reversals. With respect to the five extant suborders of cyclostomes, this first, preliminary analysis implies that Rectangulata and Cancellata are monophyletic groups, whereas Articulata are diphyletic, and both Tubuliporina and Cerioporina paraphyletic.

© 2000 The Linnean Society of London

ADDITIONAL KEY WORDS:—Stenolaemata – calcite – biomineralization – morphology – palaeontology – cladistics – systematics.

CONTENTS

Introduction	338
Cyclostome taxonomy, biology and anatomy	339
Skeletal ultrastructure	342
Previous studies	342
Terminology	345
Fabrics	346
Fabric suites	366
Fine-scale structures	371
Summary and new findings	372
Phylogenetic analysis	373
Taxa selected	373
Characters	374
Character descriptions	375
Tree rooting	381

* Corresponding author. E-mail: pdt@nhm.ac.uk

Results	382
Comments on some character state transitions	382
Suborders and their inter-relationships	386
Comparisons with earlier, non-cladistic phylogenies	387
Discussion	388
Acknowledgements	391
References	391
Appendix 1	396
Appendix 2	398

INTRODUCTION

The Bryozoa are a phylum of colonial, coelomate metazoans comprising nearly 6000 described living species. All bryozoans are aquatic suspension feeders, employing the ciliated tentacle crowns (lophophores) of individual zooids in the colony to capture plankton, and most species are benthic and sessile. Bryozoan zooids are divisible into two primary components: the body walls or cystid, and the polypide with tentacles and gut. In most groups the polypide undergoes cycles of degeneration and regeneration whereas the cystid persists.

Four major groups of bryozoans are recognized at the present day. Phylactolaemates are a low diversity, exclusively freshwater class, whose relationship with the other bryozoan groups is obscure. Another group with some freshwater representatives although overwhelmingly marine is the Order Ctenostomata. Phylogenetic analysis of ctenostomes based on cystid morphology (Todd, in press) strongly suggests that they are a primitive paraphyletic grouping of marine bryozoans within which the other two living orders—Cheilostomata and Cyclostomata—are nested. Both of these latter orders possess calcareous skeletons, acquired independently (Taylor & Larwood, 1990), and it is skeletal morphology which historically has been and still is the basis for their taxonomy. Cheilostome and cyclostome skeletons can be complex at all hierarchical levels, from the colony to the zooid to the ultrastructure of individual skeletal walls. New studies have succeeded in revealing a wide diversity of ways in which bryozoan species can use small crystallites of calcite and/or aragonite in particular patterns to construct their skeletons. These ultrastructural patterns provide useful additional characters for systematics.

Knowledge of inter-relationships within bryozoan orders is in its infancy. Attempts to infer cladistic relationship rigorously within cheilostomes have been made recently using data from skeletal morphology (Gordon, in press) and from molecular sequences (Dick, Williams & Coggeshall-Burr, in press). However, our understanding of relationships among the less diverse cyclostomes is extremely poor. A computer-generated cladistic phylogeny has yet to be published for cyclostomes—indeed very few explicit phylogenies, cladistic or otherwise, can be found in the literature on this bryozoan order.

Following a brief introduction to cyclostome taxonomy, biology and anatomy, the two principal aims of this paper are addressed. The first objective is to review and synthesize recently completed work on the skeletal ultrastructure of cyclostomes. This will include some previously unpublished data as well as re-interpretations of published data. Secondly, we use these ultrastructural characters together with larger-scale characters of cyclostome skeletons to make a preliminary analysis of phylogenetic relationships within the order. The implications of this phylogeny are

explored with regard to traditional classifications, although formal changes to cyclostome classification are deferred until much needed data from soft parts and molecular sequences becomes available for incorporation in future phylogenetic analyses.

CYCLOSTOME TAXONOMY, BIOLOGY AND ANATOMY

The Order Cyclostomata was established by Busk (1852) when dividing the living marine bryozoans into 'Polyzoa infundibulata' and Cyclostomata, the former group now recognized as the Class Gymnolaemata and comprising Ctenostomata + Cheilostomata. Although the name Tubuliporata has been proposed to circumvent homonymy of the bryozoan Order Cyclostomata with the vertebrate Order Cyclostomata (Boardman, Cheetham & Cook, 1983), this replacement name has not met with general acceptance and is not used here for the following reasons: (1) the International Rules of Zoological Nomenclature (IRZN) do not require homonyms above family level to be replaced; (2) confusion may result from use of Tubuliporata because similar names with the same root are already applied widely at lower taxonomic ranks for cyclostomes (i.e. Suborder Tubuliporina, Family Tubuliporidae, Genus *Tubulipora*); and (3) the vertebrate Order Cyclostomata (hagfish + lampreys) is paraphyletic and has fallen out of use (P. L. Forey, pers comm., May 1998).

Among living bryozoans, the Cyclostomata are a monophyletic clade (Taylor, in press). This conclusion is founded on several characters regarded as synapomorphies which are known to be present in disparate recent cyclostomes but are not found in the living outgroup (Ctenostomata). Cyclostome synapomorphies are: (1) polyembryony, whereby the primary embryo divides repeatedly to produce clonal secondary and tertiary embryos (Harmer, 1893); (2) the membranous sac, a muscular internal membrane enclosing an inner body cavity (entosaccal coelom), interpreted as a detached peritoneum and functioning in tentacle protrusion (Nielsen & Pedersen, 1979); (3) lack of or rudimentary frontal cilia on the tentacles (Nielsen, 1987; Riisgård & Manríquez, 1997; Nielsen & Riisgård, 1998); (4) a poorly-developed funicular system which does not link to communication pores in the walls between zooids; (5) larval brooding in enlarged polymorphic zooids (gonozooids) or apparently derivative 'zoarial brood chambers' (see Silén, 1977b; Schäfer, 1991) (polymorphic brooding zooids appear to have been secondarily lost in the Cinctiporidae, see p. 54); (6) absence of a larval apical organ (Nielsen, 1995: 202); (7) larval metamorphosis to give a calcified, dome-shaped protoecium, otherwise referred to as the primary disk (Nielsen, 1970); (8) a calcitic adult skeleton with a predominantly lamellar fabric; (9) interior skeletal walls containing pores lined by inward growing spines.

Cyclostomes have a good fossil record due to the resistant calcareous skeletons present in all known species. The oldest recorded cyclostomes come from the Arenig Stage of the Early Ordovician (Taylor, 1993), but the order did not become common until the Mid Jurassic when they underwent an evolutionary radiation (Taylor & Larwood, 1990). From then until the early part of the Late Cretaceous, cyclostomes were the dominant group of bryozoans present in most fossil assemblages (Lidgard *et al.*, 1993; McKinney *et al.*, 1998). Most, if not all, post-Palaeozoic cyclostomes can be accommodated within the cyclostome crown-group; they had, or can reasonably be inferred to have had, the full suite of synapomorphies listed above.

However, Palaeozoic cyclostomes are better accommodated within the cyclostome stem-group because they all apparently lacked polymorphic brooding zooids (synapomorphy 5). Additionally, some Palaeozoic cyclostomes appear not to have had interzooidal pores (synapomorphy 9).

As argued by Taylor (in press), several extinct groups which are conventionally regarded as orders of equivalent rank to the Cyclostomata and placed within the Class Stenolaemata, nest within the cyclostome total-group. These predominantly Palaeozoic 'orders'—Cystoporata, Trepostomata, Cryptostomata and Fenestrata—probably constitute an extinct clade branching off the cyclostome stem-lineage.

An alternative interpretation of stenolaemate relationships views post-Palaeozoic cyclostomes as polyphyletic, with some taxa being most closely-related to Palaeozoic cyclostomes but others to two or more of the 'extinct' stenolaemate orders. Boardman (1984, 1998) suggested that post-Palaeozoic cyclostomes originated from four sources: Palaeozoic cyclostomes, trepostomes, cystoporates and cryptostomes. Viskova (1992) favoured a diphyletic origin of post-Palaeozoic cyclostomes, some of which she thought were derived from Palaeozoic cyclostomes but others from trepostomes. Neither of these theories of cyclostome polyphyly can be accepted until supporting evidence is forthcoming from a rigorous phylogenetic analysis incorporating data from all relevant stenolaemate groups. Furthermore, synapomorphies numbers (5) and (9) listed above for extant cyclostomes support cyclostome monophyly as these characters are present in post-Palaeozoic fossil cyclostomes but lacking in the extinct stenolaemate orders.

There are an estimated 850 species of cyclostomes living at the present-day (Horowitz & Pachut, 1996). The group as a whole has a worldwide distribution, spanning latitudes from the Arctic (e.g. Kluge, 1975) to the Antarctic (e.g. Borg, 1944). Although tropical occurrences are known, including on coral reefs (e.g. Winston, 1986), the relative and absolute importance of cyclostomes in benthic communities tends to increase in higher latitudes. Some environments in the temperate zone, such as the continental shelf off south-eastern New Zealand (Probert *et al.*, 1979) and the western Mediterranean Sea (Harmelin, 1976a), contain relatively diverse and abundant cyclostome assemblages. The modern British fauna numbers 36 cyclostome species (Hayward & Ryland, 1985), 49 species are known to occur in the Mediterranean (Zabala & Maluquer, 1988), and an estimated 90 species in New Zealand (D. P. Gordon, pers. comm., 1995). Cyclostomes are stenohaline, and their depth distribution ranges from the low intertidal, where species of *Crisia* are important constituents of 'zoophyte turfs' (Hayward & Ryland, 1985), down to 4400 metres (Harmelin & d'Hondt, 1982). However, the great majority inhabit shelf depths.

Cyclostomes invariably have curved, tubular zooids which are narrowest proximally, broaden in width distally, and have a terminal aperture which is either subcircular or polygonal in shape. Colony-form varies widely between species and in some cases intraspecifically (Harmelin, 1973, 1976a). Encrusting colonies of living species are usually small, ramifying, sheet-like or dimple-like, whereas erect colonies tend to be larger and may be articulated, bushy with delicate or robust bifurcating branches, or, more rarely, bilamellar and foliaceous in form.

Zooidal polymorphism is not as well-developed in cyclostomes as in cheilostome bryozoans. However, brooding gonozooids are almost ubiquitous, and many species possess supportive and/or space-filling kenozooids which lack functional polypides. Nanozooids, distinguished by minute apertures and polypides with a single tentacle,

occur in some taxa and possibly fulfil a cleaning function (Silén & Harmelin, 1974). In addition, an extinct clade of cyclostomes—melicerititids—which are unusual in having operculate autozooids, frequently develop polymorphic zooids with hypertrophied opercula (Taylor, 1986, 1994). These eleozooids resemble the avicularia found in living cheilostomes and are most likely to have been defensive.

Cyclostome larvae are ciliated, have invaginations at oral and aboral poles, and lack a functional gut. They settle a short time after release. Although described fully in relatively few species, available evidence indicates that larval morphology is relatively uniform across the group (Nielsen, 1970). Adult soft part anatomy is known in only a small minority of cyclostome species. Tentacle number varies between species from 6 to 17, but other features of the gut and tentacles seem relatively uniform, except that a small minority of investigated species have gizzards (Schäfer, 1986). A greater degree of interspecific variability is found in polypide attachment organs and other structures associated with the mechanics of polypide protrusion (Boardman, 1998). In all known cyclostomes, feeding zooids have a distal vestibule lined by a vestibular membrane. Continuous with the vestibular membrane in some taxa is a distinct terminal membrane which closes across the skeletal aperture when the tentacles are retracted. An exosaccal pseudocoel occurs as a body cavity between the vestibular membrane and the epithelium forming the body walls of the zooid. This pseudocoel also continues into the proximal part of the zooid beyond the attachment structures which anchor the tentacle sheath and membranous sac to the zooidal body walls. As in other bryozoans, the tentacle sheath is everted hydrostatically to protrude the tentacle crown. The muscular action needed to be achieved eversion occurs mainly, if not exclusively, by contraction of muscles in the membranous sac. Withdrawal of the tentacles is brought about by contraction of the retractor muscle anchored to the base of the tentacle crown, probably supplemented by contraction of funicular muscles attached to the base of the polypide.

Budding of new zooids usually occurs in discrete regions at the outer edges of colonies. Borg (1926) used the term 'common bud' to describe these zooidal budding zones. Polypide buds are initially differentiated from clusters of ectodermal cells of the terminal membrane, move inwards taking with them some mesodermal cells, and are eventually enclosed by the upward growing walls of the zooidal cystid (Borg, 1926). Groups of sex cells become associated with the polypide rudiments, some being primary oogonia eventually to develop into ovaries, and others primary spermatogonia which aggregate in testes. While cyclostome colonies are usually regarded as hermaphroditic, the comments of Harmer (1891: 145) on *Crisia eburnea* appear to imply that separate male and female colonies exist in this species (cf. Wasson & Newberry, 1997).

Cycles of polypide degeneration and regeneration occur in cyclostomes as in other marine bryozoans. Knowledge of these processes, however, is very limited. In at least some cyclostome species, small polypides can be found at colony growing edges and full-sized polypides do not appear until later stages of zooidal ontogeny. According to species, successive polypides may be attached to the zooid body walls at the same position, or may migrate distally as the zooid grows in length during its ontogeny. These two alternatives have been named stationary and non-stationary polypide cycles respectively by Boardman (1998).

As in other bryozoans, an important distinction can be made between exterior body walls and interior body walls. Exterior walls are located at the boundary between bryozoan and external environment, whereas interior walls form internal

partitions within the bryozoan, subdividing the body cavity. Both wall types may or may not include calcareous mineralized layers. In the case of exterior walls, the mineralized layer is sandwiched between an organic cuticle and the epithelium that secretes it. Interior walls have no such cuticle and instead have epithelium on both sides which secretes the mineralized components of the wall. Calcified exterior walls occur as basal and frontal walls, whereas interior walls usually occur as vertical walls but less often as frontal walls or as basal walls in erect bifoliate colonies.

SKELETAL ULTRASTRUCTURE

Previous studies

Although the skeletal microstructure of cyclostomes and other stenolaemates as revealed by thin sections has been studied for many years (see Boardman, 1983), information on the ultrastructure of the skeleton only became accessible with the advent of scanning electron microscopy (SEM). Söderqvist (1968) was the first to study the skeletal ultrastructure of cyclostome bryozoans using SEM in a study mainly of the articulate *Crisia eburnea* Linnaeus. He characterized the skeleton as consisting of two layers, a thin outer 'prismatic' layer and a thicker layer of lamellar fabric. According to Söderqvist, the outer layer consisted of bundles of crystals, with each bundle comprising 20–50 prisms lacking intracrystalline structure, whereas the inner layer comprised "polygonal tabular crystals . . . stacked like roofing tiles" (Söderqvist, 1968: 117). Sections through the wall showed the 'crystals' to be arranged in lamellae of uniform thickness. Söderqvist stated that interzooidal walls, initiated as "septa", are constructed of the same lamellar fabric and, importantly (see below, p. 368), that these walls differed from those of some other cyclostomes in lacking a central 'hyaline' zone. He interpreted the septa of *C. eburnea* as having a comparatively narrow "growing front", and noted that "crystals non-parallel to the growth direction are either entirely absent or too few crystals are present in this deflected region to be detectable . . ." (Söderqvist, 1968: 117). Söderqvist was able to confirm Borg's (1926: 256, fig. 14) observation of parallel, longitudinal strips in the outer layer. He also recorded the presence of stacked tabular crystals in the walls of the tubuliporines *Stomatopora* sp., *Diplosolen intricaria* (Smitt), *Idmonea* [*Idmidronea*] *atlantica* Forbes in Johnston and also the cerioporine *Heteropora pelliculata* Waters.

In their broad survey of bryozoan skeletal ultrastructures, Tavener-Smith & Williams (1972) studied a range of tubuliporine, rectangulate and articulate cyclostomes. They stated that the skeletal succession of cyclostomes was less variable than that of cheilostomes, skeletons almost invariably comprising "two calcitic layers of primary crystallites and secondary laminae" (Tavener-Smith & Williams, 1972: 122). In the Recent tubuliporines *Plagioecia* [*Berenicea*] *patina* and *Tubulipora phalangea*, they found the skeletons to have a primary layer 6 μm thick in basal [exterior] walls and up to 12 μm thick in zooecial [interior] walls. This layer comprised gently inclined or vertically oriented acicular crystallites up to 2.5 μm wide and more than 10 μm long. The primary layer was succeeded by lenses of more granular calcite (up to 0.5 μm thick and 15 μm wide) arranged more-or-less parallel to zooecial wall surfaces. This fabric they described as a precursor to regular 'banding' about 0.25 μm thick which, when seen on internal wall surfaces, comprised tabular laminae with rhombic

or dihexagonal corner angles and spiral growth patterns. A similar ultrastructural succession was found in another Recent tubuliporine *Entalophora* sp., but in this species the 'secondary' layer had more elongate, imbricated, fibrous calcite tablets, often bearing keeled surfaces. Tavener-Smith & Williams (1972) also described the basal wall of *Lichenopora radiata* which they said comprised a thin 'primary shell' composed of vertically stacked calcitic granules, and a secondary shell of laminated structure. The secondary shell, forming the remainder of the skeleton, was said to consist of bladed crystallites with rare screw dislocations. Their work on the skeletal ultrastructure of the articulate *Crisidia cornuta* (Linnaeus) corroborated the findings of Söderqvist (1968) on the related *Crisia eburnea*. The outer or 'primary' layer was described as comprising long, parallel strips of gently inclined, acicular crystallites, 0.3 μm thick and up to 1.2 μm long, which are aligned roughly parallel to the long axis of the zooecium. This layer was succeeded abruptly by a laminar secondary layer comprising partly fused tablets with rhombic or dihexagonal corners. They identified a second constituent of the secondary layer resembling a keeled fibre, and noted that both fibres and tablets can occur on the same wall surfaces and are arranged like overlapping tiles, with frequent spiral growth. They also contrasted the slit-like outer surface of the 'canals' (pseudopores) with their elliptical shapes on inner surfaces, and characterized the articulation surfaces of the jointed colonies as finely granular. A granular primary layer and a well-developed laminar secondary layer were identified in the Eocene articulate *Crisia cobini* Canu.

Brood (1972) expanded the description of cyclostome skeletal ultrastructure, recognising three types of wall structure which he termed tubuliporidean, cancellate and cerioporoid wall structures, with the latter comprising the subtypes pseudocerioporoid, densiporid and disporellid wall structures. Tubuliporidean wall structure—recorded by Brood in the families Diastoporidae, Tubuliporidae, Pustuloporidae, Cytidae, Filisparsidae and Theonidae—comprised three structural units: a middle granular layer and inner and outer laminar layers. His description concerns interior walls only, and the term 'middle' refers to the central layer of the double wall. The initial laminar layers have an 'orally diverging' arrangement, whereas the laminae of the outer laminar layer approximate to wall parallel.

According to Brood (1972), cancellate wall structure (occurring in the Suborder Cancellata) also comprises three layers (middle granular layer, inner and outer laminar layers), though here the inner laminar layer is much thinner and nearly wall parallel, with the outer layer forming a thick unit of secondary thickening. Cerioporid wall structure, Brood stated, comprises one main structural unit—the inner laminar layer—consisting of frontally diverging laminae, with an occasional vestigial middle granular layer. With maturity the laminae become wall-parallel. Cerioporid wall structure proper occurs in the Cerioporidae and Radioporidae. Pseudocerioporid wall structure (in *Pseudoceriopora*) consists entirely of laminated layers, with primary frontally oblique laminae and "a distal secondary part with laminae oriented transversely to the growth direction of the zooecial wall" (Brood, 1972: 39). Brood's densiporid wall structure is essentially similar to typical cerioporid structure, but differs in having large spiny processes. Also similar to cerioporid structure is Brood's disporellid structure, except for the presence at each autozooidal aperture of a "pseudolunarium", a process with a reverse cone-in-cone structure.

Brood (1976) further described the secretion of the calcified skeleton in cyclostomes. He noted the calcification of the basal lamina beginning with a thin primary layer of acicular crystallites which appear granular in fossil specimens. This 'primary

layer' is succeeded by a 'secondary layer' of "well-defined, lath-like laminar crystals" (Brood, 1976: 379). Similarly, Brood described the double-walled interior walls as initiating with an acicular fabric layer succeeded by a lath-like laminar layer. The laminae, he noted, are generally orally divergent or parallel to wall growth direction. Interestingly, he suggested that polymorphic zooids with a supportive function may have a different pattern of growth, with growth of laminae transverse to wall growth direction. Such a pattern of kenozooidal growth was identified in species belonging to the Corymboporidae, Crisinidae and Cytidae. Skeletal structure was used as one character in the construction of a tentative phylogenetic diagram (Brood, 1976: fig. 11; see also Fig. 18 herein), although no clear distinctions were made between the constituent ultrastructural fabrics of the different cyclostome suborders.

Ross (1975, 1976, 1977) proposed a mechanism for formation of the cyclostome skeleton whereby the calcareous tablets were secreted within the skeletal wall, associated with a system of 'canals'. Her unconventional model has failed to receive support: some of the crucial structures she identifies are evidently misinterpreted (see Weedon & Taylor, 1996). Ross (1975) described the tubuliporine *Diplosolen obelium* as having an outer cuticular layer of protein-chitin with acicular crystallites, and an inner layer of regularly ordered, overlapping laminate platelets. She identified similar skeletal structures in the articulate *Crisia*, the cerioporine *Heteropora*, and the rectangulates *Disporella* and *Lichenopora* (Ross, 1976, 1977).

Bigey (1977, 1982) illustrated skeletal ultrastructures in the tubuliporines *Fron dipora verrucosa* (Lamouroux) and *Diaperoecia floridana* (Smitt) for comparison with ultrastructures in Palaeozoic bryozoans. She also confirmed the granular and laminar structure found by Tavener-Smith & Williams (1972) in a species of *Lichenopora*, and described and illustrated a similar fabric in the related *Disporella buski* (Harmer).

In her paper on cyclostome brood chambers, Schäfer (1991) referred to the ultrastructure of the interior vertical walls of, for example, lichenoporids as having a fundamentally laminar structure, with laminae arranged subparallel or distally divergent to a slight degree. The fabric was described as comprising platey, lath-like crystallites, increasing in size towards the outside of the wall.

More recent studies involving the current authors are only briefly reviewed here because the findings are synthesized in the sections that follow. Boardman, McKinney & Taylor (1992) described the skeletal ultrastructure of the Cinctiporidae, here regarded as a family of 'tubuliporines' (see below, p. 389). Cinctiporids were shown to have interior walls consisting of an inner layer of transverse fibrous crystallites, overlain by a laminated layer of distally-imbricated, lath-like crystallites.

Taylor & Jones (1993) contrasted the two-layered cinctiporid skeleton with the skeleton of the cancellates *Hornera robusta* and *H. squamosa*. These free-walled cyclostomes have skeletal walls consisting of laminae of one fabric type: sub-hexagonal tablets, often with distinctive triple spikes located at their centres. Secretion of tablets was shown to be concentrated at the distal growing edge of the wall. Here seed crystallites are about 0.5 μm in diameter and may have radial sectoring with six sectors having alternately rough and smooth surfaces. Screw dislocations were also common near the distal edges of walls. With increasing maturity the crystallites were inferred to broaden and coalesce to give a fabric of predominantly proximally imbricated crystallites. Taylor & Jones (1993) suggested that this mature fabric was regularly foliated in the sense of Carter *et al.* (1990), whereas Weedon & Taylor (1995) equated the early fabric with the calcitic semi-nacre of the same authors.

Taylor, Weedon & Jones (1995) described the skeletal ultrastructure of species in

the family Lichenoporidae (Suborder Rectangulata). Precursory wedge-shaped or irregular granular fabrics are succeeded by a predominantly distally foliated fabric. A similar fabric succession was later found in the majority of studied species belonging to the Suborder Cerioporina (Weedon & Taylor, 1996). However, two cerioporine species (*Heteropora parapelluculata* and *H. neozelanica*) were unusual in having transverse fibres like those previously found in cinctiporids. Mesozoic fossil meliceritids (Family Eleidae) and their inferred primitive sister-group were found also to have transverse fibres (Taylor & Weedon, 1996).

Four distinct fabric successions or suites were identified by Weedon & Taylor (1997) in the diverse fixed-walled suborder Tubuliporina. The remaining cyclostome suborder, the Articulata, was studied by Weedon & Taylor (1998) who demonstrated that most species had a simple fabric suite comprising hexagonal semi-nacre only. The one exception was *Crisulipora* which was found to have a complex fabric suite incorporating transverse fibres.

The most recent investigation into the skeletal ultrastructure of cyclostomes focused on the earliest-formed skeleton in the protoecium (Weedon, 1998). A remarkable consistency of protoecial fabrics across all suborders was found but with differences in skeletal ultrastructure between roofs and floors.

Terminology

The terminology of this paper follows that used in previous papers on the skeletal ultrastructure of the specific cyclostome orders and families. Some of these terms were introduced and defined by Taylor *et al.* (1995) and are summarized and elaborated here.

True crystallites are the products of discrete seeding events. They are presumed to represent single crystals. With the exception of small, newly-seeded crystallites, and the minute crystallites in granular fabrics, most of the surface area of each crystallite is hidden beneath overgrowing crystallites, with only the distalmost parts of the crystallites being visible on the surface of the wall.

Surficial crystallites are the apparently discrete crystallites visible on wall surfaces but which are not necessarily distinct crystallites, originating from separate seeding events. Instead they may be *lobes* of a branching crystallite, or different layers of a crystallite undergoing *screw dislocation* (spiral overgrowth) or *stepping* (localized thickening and formation of a new growing edge on the crystallite surface).

Crystallite domains are areas on wall surfaces where surficial crystallites have a consistent growth direction distinguishable from adjacent areas of different growth direction. In at least some cases, domains represent single true crystallites split by screw dislocation, branching or stepping. *Convergent*, *divergent*, or *transform zones* are regions on the wall surface where domains of different orientation make contact and can be likened to similar boundaries in plate tectonics. In convergent zones the crystallites of adjacent domains grow directly opposed to each other; in divergent zones the crystallites of adjacent zones grow away from one another; and in transform zones they grow in opposite directions parallel to the domain boundary.

Fibrils are tiny parallel strips forming an apparent substructure to the crystallite. Slight grooves mark the boundaries of adjacent fibrils, and the growing edge of the crystallite may be jagged or stepped at these boundaries.

Fabric suite refers to a consistent succession of ultrastructural fabrics in a skeletal

wall. Up to five separate ultrastructural fabrics can be layered to form one fabric suite.

Fabrics

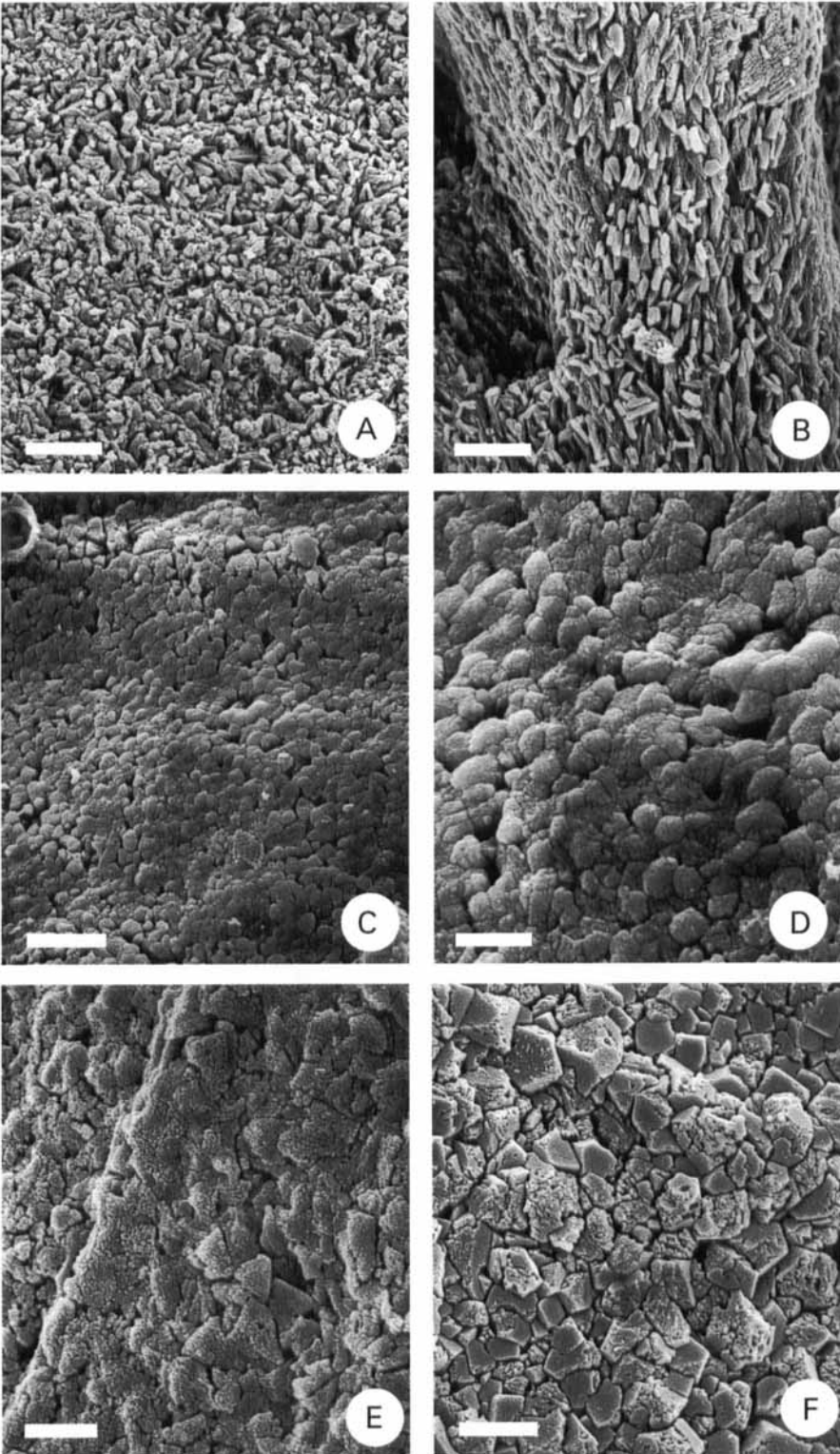
The results reported in the next two sections represent a synthesis, with additions and some reinterpretations, of findings published by Boardman *et al.* (1992), Taylor & Jones (1993), Taylor *et al.* (1995), Taylor & Weedon (1996), Weedon & Taylor (1995, 1996, 1997, 1998), and Weedon (1997, 1998). Details of material used and methods can be found in these papers. However, it is worthwhile reiterating that the work has mostly entailed high resolution, field emission SEM, and has concentrated on the ultrastructures visible on the surfaces of bleached walls. Wherever possible, only pristine material has been used. A particular focus has been on regions close to the distal growing edges of walls because individual fabric types are best developed here and those formed during early stages of wall growth can be seen before they become overgrown by later fabrics. All figured SEM stubs are stored in the collections of The Natural History Museum, London.

Six fundamental ultrastructural fabrics constitute the building blocks of cyclostome skeletons. When developed, granular and planar spherulitic fabrics always occur as the first-formed fabric in the walls. The rest of the wall is invariably formed from lamellar fabrics parallel to the wall surface or more often inclined at a very low angle with a tile-like imbrication. Of the four lamellar fabrics, three (transverse fibrous, foliated and rhombic semi-nacre) are based on identical crystallographic orientations, whereas the fourth (hexagonal semi-nacre, and the derivative pseudo-foliated fabric) has a unique orientation. In addition to these fundamental wall fabrics, the mural spines and spikes found in many cyclostomes have a distinct 'moulded' fabric described at the end of this section.

Granular fabric

Granular fabric (Fig. 1) usually forms the first mineralized unit in the walls of cyclostomes, and normally consists of minute wedge-shaped crystallites (Fig. 1A, B). It is secreted directly against the cuticle in most exterior walls, and forms the initial layer in many interior wall fabric suites. In exterior walls, granular fabric is most thickly developed in fabric suites which lack planar spherulitic structure (Weedon & Taylor, 1997: figs 6b, 7d, e). Granular fabric is the precursory layer of interior fabric suites which have predominantly foliated fabric, and also occurs in the predominantly semi-nacreous fabric suite of tubuliporines. The fabric varies in

Figure 1. Granular fabrics in cyclostome skeletal walls. A, *Disporella gordonii*; partially disarticulated, wedge-shaped granules in roof of protoecium (outer surface of an exterior wall); note discrete nature of crystallites which mostly lie in plane of wall surface but are not aligned. B, *Patinella radiata*; wedge-shaped granules on edge of zooidal aperture (interior wall), aligned parallel to apertural rim. C, *Patinella radiata*; underside of exterior basal wall with blebby granular fabric; area at top right shows roughly triangular granules, interpreted as transversely sectioned wedge-shaped crystallites. D, *Patinella radiata*; detail of C. E, *Tubulipora* sp.; tightly-packed, wedge-shaped granules in outer layer of protoecium (outer surface of an exterior wall); note ridge on left formed by slight thickening of granular layer. F, *Diaperoecia purpurascens*; detail of the large, irregular, blocky crystallites forming outer layer of protoecium. (Scale bars: 1.5 µm in A; 3.6 µm in B; 1.3 µm in C; 0.5 µm in D; 0.75 µm in E; 1 µm in F).



thickness, but most commonly comprises a very thin layer of one or a few crystallites in thickness. However, granular fabric is not universally developed in cyclostome walls: it has not been found in the semi-nacre dominated interior walls of cancellates or articulates, and a re-assessment of ultrastructures shows that granular fabric is apparently absent from the tubuliporine fabric suites which incorporate transverse fibres.

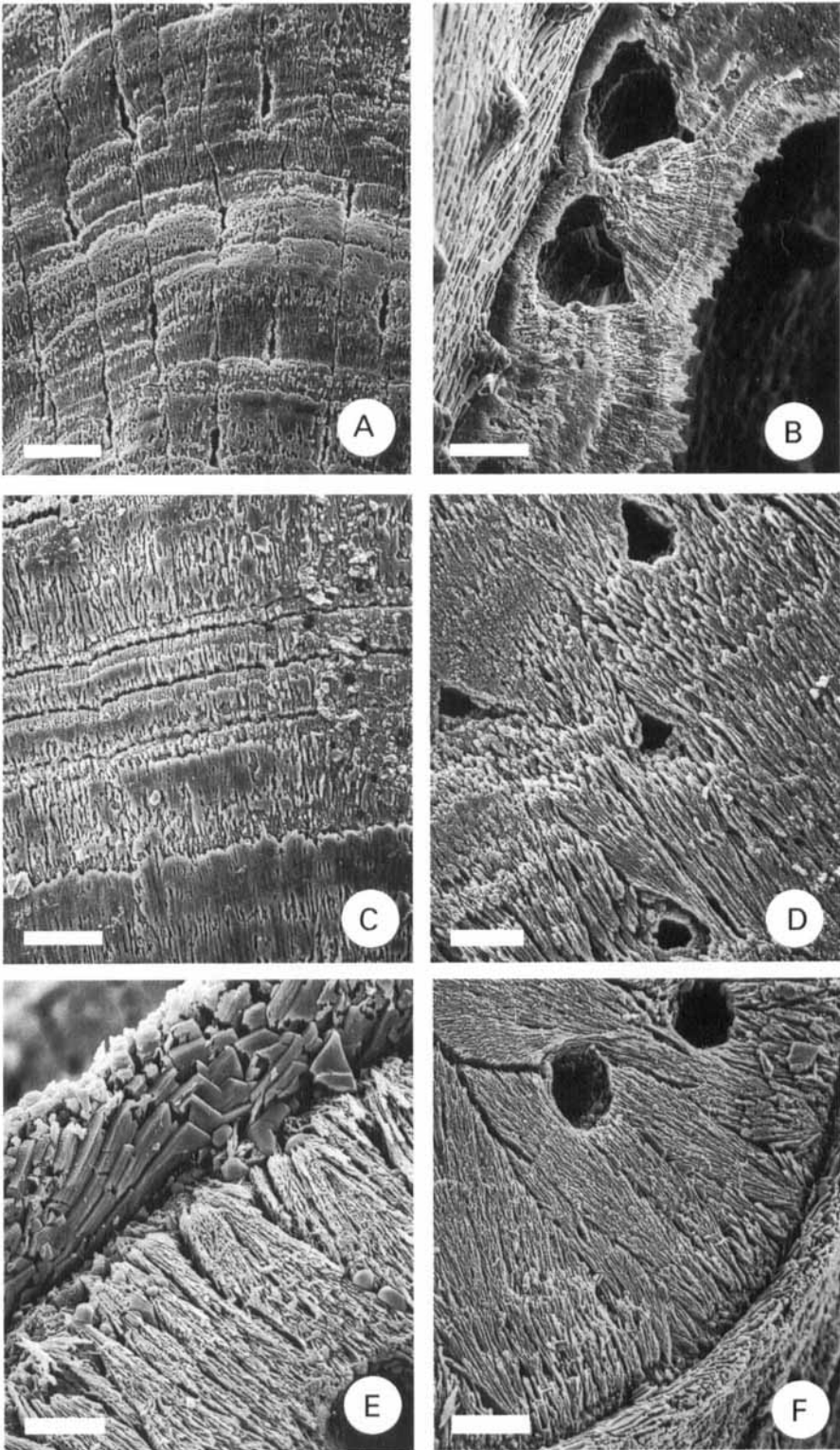
Initiation of granular fabric entails the secretion of tiny, discrete (though closely-packed) crystallites, either directly upon the cuticle (exterior walls) or directly upon existing crystallite surfaces, as with septa (new interior walls) originating on basal walls. Crystallites in granular fabrics are minute, 1–2 μm long and 0.2–1 μm wide, and most commonly wedge-shaped, with a three-dimensional, four-faced form which has elongate subtriangular or fan-shaped surfaces (Fig. 1B). The crystallites have a roughly equilateral triangular transverse section, usually with a slight concavity of the sides. High magnifications of individual crystallites reveal a compound 'fractal' substructure of similar, wedge-shaped fibrils, each <0.05 μm in width.

In newly formed septa, growing directly on basal walls, the first wedge-shaped crystallites are very tiny and often have a disordered and loose arrangement, suggesting high intercrystalline organic content (Fig. 1A). As the septum develops, the wedge-shaped crystallites become more tightly packed and acquire a crude alignment parallel to the septum (Fig. 1B).

Frontal walls with an outer layer of entirely granular fabric are characteristic of some tubuliporine species, e.g. *Plagioecia dorsalis*, *P. patina*, *Platonea stoechas* and '*Cardioecia*' *watersi*. When pristine, frontal walls show a densely-packed, finely granular fabric of wedge-shaped crystallites which was deposited directly against the cuticle. In other species, however, the constituent crystallites are more irregular in shape or have a rounded outline (Fig. 1C, D). This fabric forms a very thin exterior layer only a few crystallites deep, and in many specimens is wholly or partly lost during bleaching and cleaning. Striations parallel to wall growth direction and 7–10 μm apart are present in *Plagioecia patina*. They appear to mark slight differences in the surface topography of the frontal wall. The strip-like units of calcification between adjacent striations resemble those seen in frontal walls with a planar spherulitic fabric as described below.

A granular outer layer, with an absence of planar spherulitic fabric, is found in the roof of all protoecia studied (Weedon, 1998; Fig. 1A, E, F). High magnification reveals the exterior walled outer surface of the protoecium roof to comprise a relatively coarse granular fabric (Fig. 1A, E, F). The constituent crystallites are often

Figure 2. Planar spherulitic fabrics in cyclostome skeletal walls. A, *Crisia sigmoidea*; strips of planar spherulitic fabric in exterior frontal wall with slit-like pseudopores at strip boundaries; note convex fronts marking growth bands; smoother areas represent unetched finely granular, outer fabric. B, *Tubulipora elegans*; new terminal diaphragm growing from interior wall with transverse fibrous fabric (left); note fan-shaped units which wrap around subtriangular pseudopores. C, *Tubulipora liliacea*; growth banding in partially etched strips of planar spherulitic fabric from exterior frontal wall. D, *Coronopora truncata*; acicular crystallites forming fan-like spherulitic strips interrupted by subtriangular pseudopores. E, *Diaperoecia purpurascens*; units of planar spherulitic fabric originating from point sources to form a terminal diaphragm growing centripetally from a peristome with pseudofoliated fabric (upper left). F, *Diaperoecia purpurascens*; fully-formed terminal diaphragm with planar spherulitic units truncating against their neighbours. (Scale bars: 12 μm in A; 15 μm in B; 10 μm in C; 7.5 μm in D; 3.5 μm in E; 7.5 μm in F).



slightly elongate and wedge-shaped, 0.2–0.4 μm long and about 0.1–0.15 μm wide (Fig. 1A). Crystallites have a substructure of minute ‘blebby’ units which are less than 0.01 μm in diameter (Fig. 1E). They are often aligned, with their long axes roughly parallel to the 0.2–0.4 μm wide ridges defining strip boundaries. Ridges have an identical granular fabric to the rest of the strip and are distinguished only by their slight elevation, usually less than 0.2 μm (Fig. 1E). In some protoecia, notably the very large protoecia of tubuliporines such as *Diaperoecia*, the granular crystallites are rather blocky in shape and are larger than in other species, ranging up to 1 μm in maximum diameter (Fig. 1F). These crystallites are tightly packed and form an almost smooth outer surface which, in partially abraded specimens, breaks up into a more loosely organized structure.

In many species, crystallites forming granular fabrics have relatively non-angular outlines and instead are equant, rounded or rather anhedral in appearance. For example, the extreme distal growing tips of apertural spines in rectangulates such as *Disporella gordonii* can be only 1–3 μm in diameter with a granular texture. The irregular granules here are minute (<0.02 μm). During spine growth they become aggregated into fibrils one grain thick and up to 0.5 μm in length, and ultimately coalesce to form the foliated fabric of the main part of the skeleton.

Planar spherulitic fabric

Planar spherulitic fabric occurs as a layer immediately following the thin layer of granular fabric in most exterior walls (Fig. 2). The fabric is almost universal in exterior basal and frontal walls, including the roofs of gonozooids, terminal diaphragms and peristomes. In exterior walls where chemical etching has removed the granular layer, planar spherulitic fabric may appear to be the outer fabric of exterior walls. Although previously regarded as a fabric restricted to exterior walls, a type of planar spherulitic fabric is recognizable as the first formed fabric of at least some (perhaps all) interior walls with fabric suites including transverse fibres (Fig. 3).

Planar spherulitic fabric comprises strip-like units of acicular crystallites which are flat against the wall surface. Each unit originates from a point source from which the very fine crystallites (*c.* 0.05 μm wide) radiate and grow in a predominantly distal direction within the plane of the wall. The radiating growth pattern resembles the spherulitic fabrics found in other biomineralizing organisms but is essentially two dimensional, hence the name planar spherulitic (see Bryan & Hill, 1941; Sandberg, 1983). Crystallites of one unit truncate against adjacent units along relatively straight boundaries which are aligned parallel to the direction of wall growth. Initiation of planar spherulitic units occurs at transverse growth checks spaced at least 5–20 μm apart (Fig. 2A, C). The planar spherulitic layer is very thin (<2 μm).

There are three main modes of planar spherulitic fabric in exterior walls according to growth direction. In most frontal walls and peristomes, the outer wall layers comprising granular and planar spherulitic fabrics grow as distinct strips of calcification (2–20 μm wide though most commonly 5–10 μm), parallel to the distal growth direction of the wall (Fig. 2A, C). The strips usually show distally convex growth bands mirroring the underlying ‘fan-shaped’ growth fronts of the planar spherulitic units (Fig. 2A). In a few tubuliporines, the strips of planar spherulitic fabric grow obliquely towards the centre of the zooid. For example, in the tubuliporine *Fasciculipora ramosa*, the fascicle-bounding frontal walls have planar spherulitic units

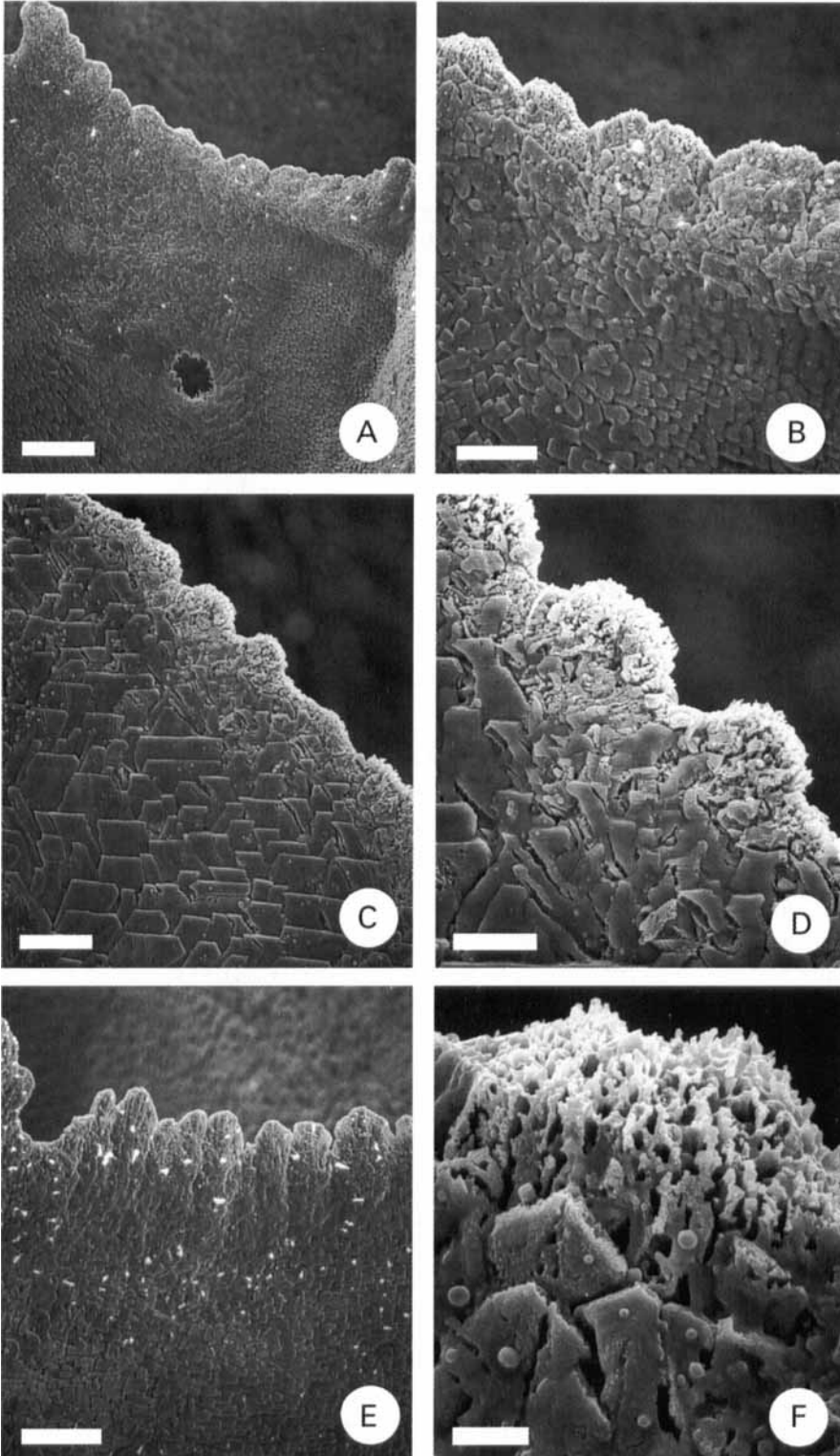
which originate along zooidal boundaries and grow obliquely distally at about 45° to these boundaries. Units growing from either side of the zooid meet to form a 'suture' along the midline of the zooid. Growth checks in the planar spherulitic layer are here defined by irregularly-spaced, v-shaped 'grooves' (Fig. 2A). The third main growth mode adopted by planar spherulitic fabrics occurs in terminal diaphragms and some exterior-walled brood chambers (Fig. 2B, E, F). Here the units of planar spherulitic fabric grow centripetally. Lightly etched examples of terminal diaphragms show that the planar spherulitic units originate from point sources around the inner edge peristomes or other walls which support the growing diaphragm (Fig. 2E, F). From each of these point sources, very fine acicular crystallites radiate as fan-shaped arrays within the plane of the diaphragm. Initially these radiating units have rounded growth fronts, but with continued growth towards the centre of the zooid they meet adjacent units obliquely and truncate against them (Fig. 2F).

The identification of planar spherulitic fabric in interior walls was made possible by careful collection of fresh material and protection of the delicate branch growth tips from damage, so that the extremely thin distalmost edges of the skeletal walls survived intact (Fig. 3). Thin sections of the interior walls of *Cinctipora elegans* and other species with transverse fibrous fabrics had previously revealed a central, initial layer of dark, organic rich material with little definite structure (Boardman *et al.*, 1992). However, this layer had not been unequivocally characterized using SEM. Pristine walls protected from damage show that the distalmost part of the wall, here less than 0.5 µm thick, has a finely scalloped edge with a series of minute convex lobes. The lobes are rather variable in width, ranging from about 2 µm to over 16 µm, although most are between 6 and 8 µm. Contacts between adjacent lobes are often marked by shallow grooves, oriented parallel to the direction of wall accretion, suggesting the lobes are growth fronts of narrow strip-like units. Lobes have a distinctive ultrastructural fabric, comprising very fine, fibrous crystallites aligned predominantly in the direction of wall growth. Individual fibres are as little as 0.05–0.2 µm in width. The outer surface of some lobes comprises flattened, elongate strip-like structures about 1 µm wide (Fig. 2E) and up to 10 µm long. These fan-shaped strips have fundamentally the same ultrastructure as the planar spherulitic fabric of exterior walls. This initial layer of interior walls, which is located deep within the centre of the wall and is only visible at the surface in specimens with pristine preservation, was previously interpreted as a form of granular fabric (e.g. Weedon & Taylor, 1996).

Transverse fibrous fabric

In both exterior and interior walls, transverse fibrous fabric invariably succeeds a layer of planar spherulitic layer. Transverse fibrous fabric comprises imbricated, highly elongated crystallites which grow in the plane of the wall surface but with their long axes transverse to the distal direction of wall growth (Figs 4, 7). Surficial crystallites vary in width from 0.5 µm to more than 15 µm, although most are 1–5 µm wide. Owing to the strong imbrication of the crystallites, their full lengths are masked and far exceed fibre lengths of 30 µm which can be measured on wall surfaces.

Fibres sometimes have triangular growing tips, with three principal interfacial angles (Fig. 4B). More commonly, however, the growing tips of fibres have one edge



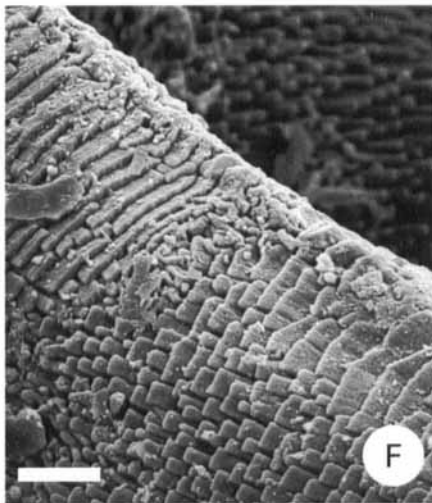
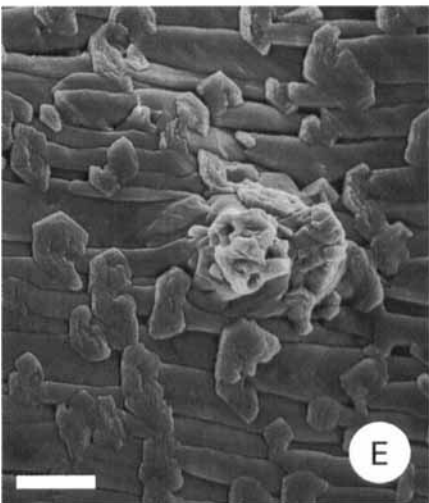
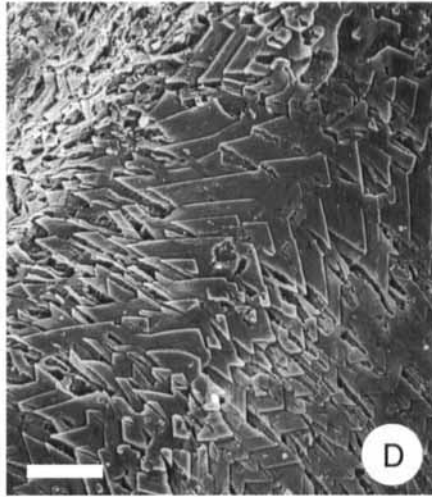
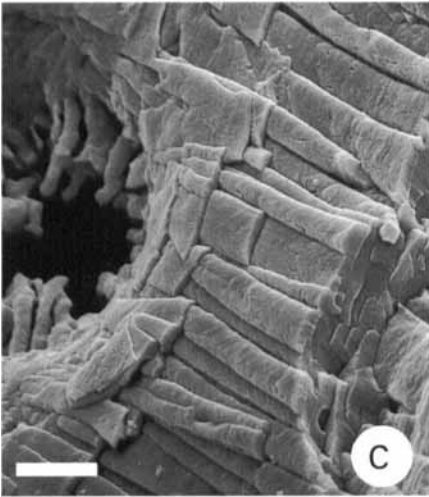
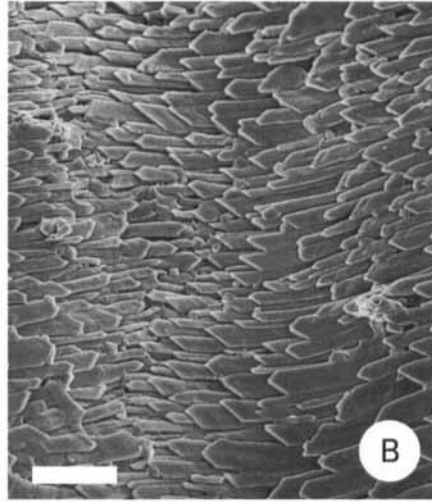
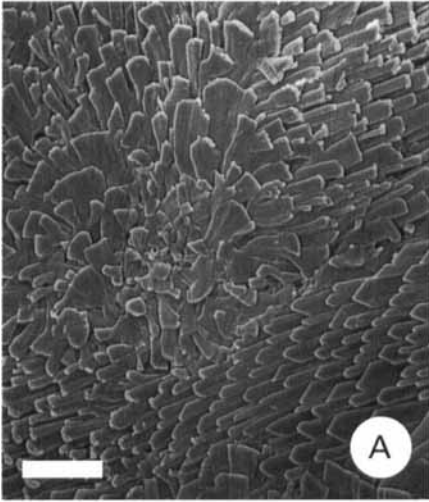
perpendicular to fibre growth direction, flanked by two angled edges (Fig. 4F). The principal angle (a) between these angled edges has the following mean values: 72.6° and 74.1° in the cerioporines *Heteropora parapelluculata* ($n=39$) and *H. neozelanica* ($n=22$) respectively; 76.9° and 73.4° in the tubuliporines *Diaperocia purpurascens* ($n=18$) and *Telopora watersi* ($n=30$) respectively; and 70.4° in the cancellate *Pseudidmonea fissurata* ($n=20$). These angles imply that the two edges correspond to the acute angles of the calcite rhomb, with the rhombic $(10\bar{1}1)$ face lying on the plane of the wall (Fig. 7; and see Runnegar, 1984). Hence the c -axes of the fibres are inclined at 45° to the crystallite surface, in a plane perpendicular to that of the growth direction of the fibre itself (i.e. a plane parallel to the distal/proximal direction of wall growth). Optical microscopy shows remarkable uniformity of extinction throughout the transverse fibrous layer in a wall, suggesting common crystallographic orientation and perhaps a common origin of fibres.

Fibres increase rapidly in width during the early stages of their growth, but soon achieve a maximum width after which they continue to grow with parallel-sided edges. They undergo frequent subdivision or 'splitting' into lobes forming separate surficial crystallites. Domains (*sensu* Taylor *et al.*, 1995) of crystallites contact other domains with different orientations at divergent, convergent and transform zones (cf. Taylor *et al.*, 1995: fig. 2a–e; Fig. 4A, B, D, F). Divergent zones have a wide range of morphologies, including those with a spreading, sinuous "fountain-like" appearance, consisting of branching crystallites, distally-oriented at the centre of the zone but becoming progressively more transversely oriented away from the centre, giving rise to domains of fibres with different, typically opposite, directions of growth (Fig. 4A). Alternatively, divergent zones may have fibres radiating from a sub-circular surficial crystallite source. In some taxa (e.g. *Telopora watersi*) the fibres originate from screw dislocations of a subtriangular central crystallite (Fig. 4D). In all types, however, fibres maintain a growth direction transverse to distal wall growth.

In some heteropodid cerioporines, the apertural edges of more mature zooids with thick walls often possess a modified form of transverse fibrous structure where the individual, predominantly transversely growing crystallites are very broad, almost as wide as the thickness of the wall (i.e. 20–30 μm wide; Fig. 4F).

Fractured or exfoliated walls expose sections through transverse fibres. These reveal a tightly-packed arrangement, each crystallite typically having a convex upper surface and a lower surface with two concave sides meeting at a central ridge (Fig. 4C). The concavities on the lower surface fit precisely over adjacent halves of the convex upper surfaces of two immediately underlying crystallites. Crystallites thus interlock tightly with those above and below them. The shape of these interlocking crystallites resembles those seen in "anvil-type fibrous prismatic structure" as defined by Carter & Clark (1985). This occurs in the bivalve *Mytilus edulis* (e.g. Travis, 1968;

Figure 3. Planar spherulitic fabric as a precursory ultrastructure of interior walls in *Cinctipora elegans*. All photomicrographs show the fan-shaped growth fronts of planar spherulitic fabric at extreme distal growing edge of walls. A–D, note the finely fibrillar structure of the lobe-shaped leading edges of the planar spherulitic fabric, contrasting with the succeeding transverse fibrous fabric seen in older, more proximal parts of wall. E, fan-shaped units of planar spherulitic fabric forming teeth-like lobes along the distal wall edge. F, detail of fibrils of planar spherulitic unit succeeded by partially etched rhombic crystallites, representing newly developing transverse fibres. (Scale bars: 20 μm in A; 7.5 μm in B; 7.5 μm in C; 3 μm in D; 12 μm in E; 1.5 μm in F).



Suzuki, 1979) and in some articulate brachiopods (Williams, 1966, 1968a, b; Brunton, 1972).

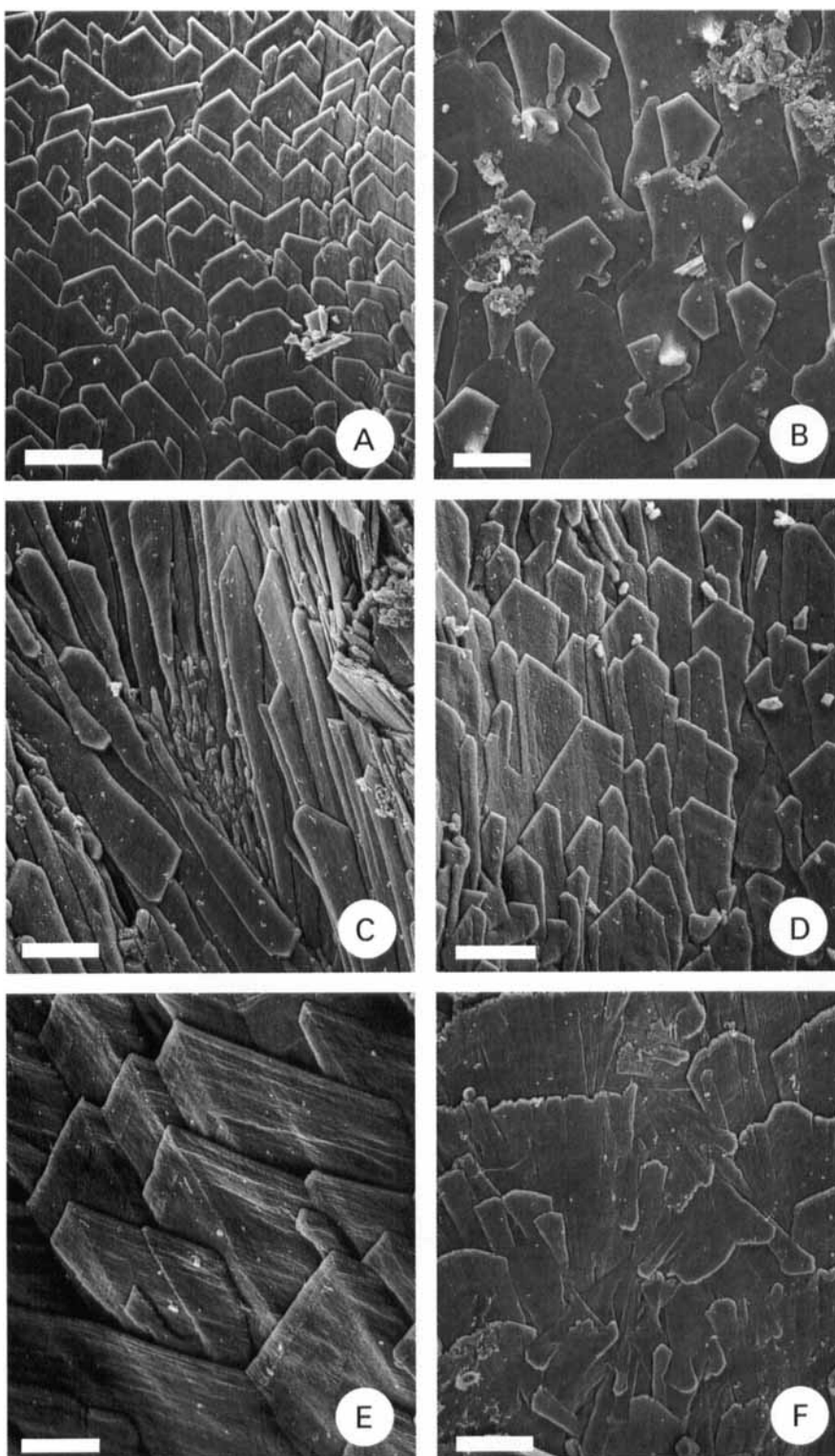
Fibres etched during the bleaching process may lose the central area, causing the fibre to appear to be divided into two halves, each half often having well-defined, sharply angular terminations (Fig. 4D). Another common effect of over-bleaching is the etching of the fibres to form jagged, tooth-like edges.

Foliated fabric

Foliated fabric consists of flattened, imbricated crystallites growing parallel to the proximal-distal direction of wall growth (Fig. 5). Crystallographically, it is closely related to transverse fibrous fabric: the growth of both fabrics is based around the accretion of (10 $\bar{1}$ 1) faces of the calcite rhomb (Fig. 7). The dominant alignment of the rhombic crystallite form is constant in both transverse fibrous and foliated fabrics, with the acute angle transverse to wall growth direction. However, whereas transverse fibrous fabric originates by growth along the two faces which make an acute angle (*c.* 78°), foliated fabric originates by growth along the two adjacent faces which make an obtuse angle (*c.* 102°). Interfacial angles measured from growing edges of foliated crystallites have mean values for the α angle of 108° in *Fasciculipora ramosa* ($n=52$) and 102° in *Idmidronea obtecta* ($n=47$). These α angle measurements, combined with optical microscopy, suggest that the c-axis is oriented parallel to the growth direction of the crystallites, but inclined at an angle of 45° to the wall surface (Fig. 7).

Foliated fabric is the dominant wall ultrastructure in all rectangulates, most cerioporines and a few tubuliporines. It also occurs locally in mature walls consisting mainly of other fabrics, such as transverse fibres and semi-nacre. Where it forms the dominant wall fabric, foliated fabric succeeds granular or planar spherulitic fabrics in exterior walls, and granular fabric in interior walls. In distal wall areas, immediately proximal to the precursory layer, there is a zone of laminar crystallites which are small (less than 2 μm in width), subtriangular, fan-shaped or irregular, and have seemingly random growth directions. In older, more proximal parts of walls, the overlapping crystallites become successively broader, attaining a typical width of 5 μm at a distance of 30 μm from the growing edge. Crystallite size continues to increase proximally, and the crystallites become more regularly subtriangular or fan-shaped and attain a predominantly distal growth direction, overlying one another in a low-angled imbricated pattern (Fig. 5A–E). Further proximally still, surficial

Figure 4. Transverse fibrous fabrics in cyclostome skeletal walls. A, *Cinctipora elegans*; divergent crystallites at source area of transverse fibrous fabric; note irregular crystallites at centre, with surficial crystallites growing in many directions; a transform zone where domains of transverse fibres of opposite growth direction pass each other is visible centre right. B, *Cinctipora elegans*; two domains of crystallites of opposing direction contact each other along a convergent zone. C, *Heteropora neozelanica*; partially fractured wall showing transverse sections through fibres (right); note bicusperate cross-sections and close-packing of crystallites; the hole on the left is an interzooidal pore partly occluded by pore spines. D, *Telopora watersi*; divergent zone in which light etching during the bleaching process has removed the central section of the transverse fibres, producing a striking triangular effect. E, *Cinctipora elegans*; area of transition between transverse fibres and foliated fabric; growth direction of the tips of the crystallites rotates through 90°, whilst the crystallographic orientation is maintained. F, *Heteropora parapelluculata*; apertural rim with very broad transverse fibres meeting at a convergent zone. (Scale bars: 7 μm in A; 7.5 μm in B; 3.5 μm in C; 7.5 μm in D; 3 μm in E; 5 μm in F).



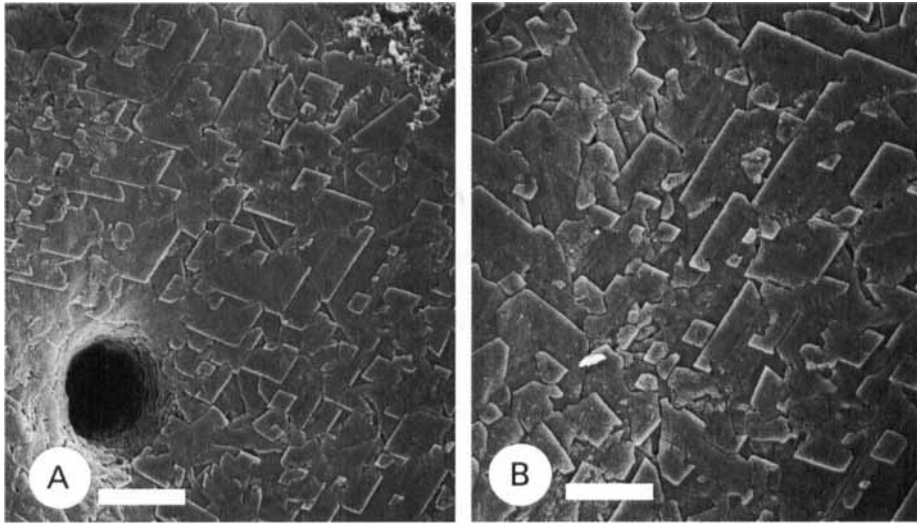


Figure 6. Rhombic semi-nacreous fabric in skeletal walls of *Heteropora magna*. Wall surfaces consist of rhombic tablets with frequent screw dislocations and scattered small, newly-formed crystallites. (Scale bars: 5 μm in A; 7.5 μm in B).

crystallites can be up to 15 μm in width, although crystallite widths are usually highly variable on any given surface, sometimes with 3 μm and 15 μm wide crystallites adjacent to one another. Much larger and more elongate and angular surficial crystallites *c.* 5–25 μm in width occur in older parts of walls (Fig. 5F). At least some of the size variability is a function of the branching or splitting of crystallites into finer lobe-like surficial crystallites. Such splitting, sometimes incorporating screw dislocations, is very common on all surfaces (Fig. 5B, C, F). Most daughter lobes grow parallel to and in the same direction as the parent crystallite, although oblique growth or reversals, which may give local areas of proximal growth, are common (Fig. 5B, C, F). Newly divided surficial crystallites usually undergo a rapid expansion in width and are therefore wedge-shaped in plan view (Fig. 5B), in contrast to more mature surficial crystallites with approximately parallel sides.

Various styles of contact between adjacent crystallite domains of foliated fabric have been observed. Domains with opposite growth directions diverge from each other along typically linear divergent zones. Here tiny surficial crystallites develop

Figure 5. Foliated fabrics in cyclostome skeletal walls. A, *Fasciculipora ramosa*; regularly foliated fabric formed of imbricated, euhedral, distally-growing crystallites. B, *Idmidronea oblecta*; splitting of surficial crystallites of foliated fabric; note the occurrence of proximally-growing crystallites in this predominantly distally imbricated fabric, and spikes on surfaces of some crystallites. C, *Idmidronea oblecta*; area of origination of elongate surficial crystallites which are initially bipolar, growing in two opposite directions. D, *Fasciculipora ramosa*; euhedral, regularly-foliated crystallites and scattered areas of reversed growth direction. E, unidentified lichenoporphid (“blue disporellid” of Taylor *et al.*, 1995); fine growth banding in euhedral foliated crystallites. F, *Patinella radiata*; mature foliated fabric from older wall proximal of growing edge; individual crystallites are less well-defined, of lower profile, and lack a strongly preferred growth direction, and crystallite splitting is common. (Scale bars: 7.5 μm in A; 4 μm in B; 4 μm in C; 5 μm in D; 3 μm in E; 7.5 μm in F).

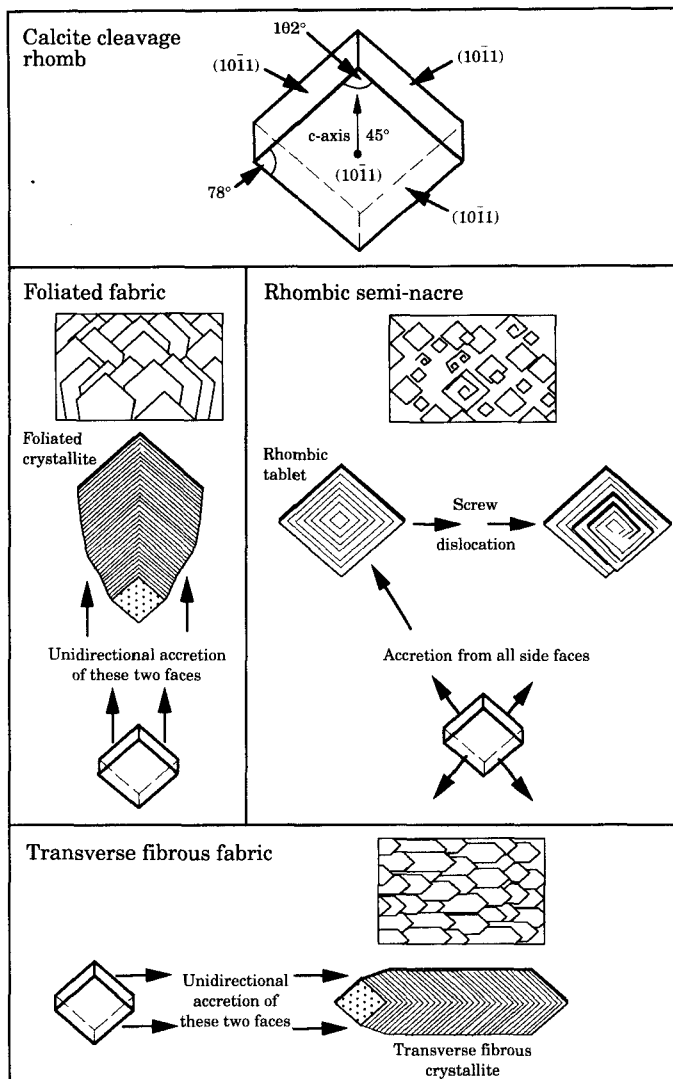


Figure 7. Diagrammatic representation of the growth of laminal fabrics from the calcite cleavage rhomb aligned with one of the $(10\bar{1}1)$ faces parallel to the wall surface, and with the c-axis at 45° to the wall surface. Three fabrics (foliated, transverse fibrous and rhombic semi-nacreous) form by accretion of the oblique $(10\bar{1}1)$ faces of the rhomb, with the upper surface parallel to a further $(10\bar{1}1)$ face. The fabric type is determined by the direction of accretion.

on the surface of 'host' crystallites by formation of steps on the crystallite surface or by screw dislocation. Crystallite domains may also converge, with crystallite fronts meeting obliquely or 'head-on'. At these convergent zones crystallites of one growth direction sometimes dominate and overlap crystallites growing in the other direction. The third style of contact, which occurs most commonly at septal margins and on pustulose basal walls, is a transform structure where crystallite domains of opposite growth direction pass one another.

In the rectangulate *Disporaella gordoni*, areas of apparent rejuvenation of growth

have been observed within foliated fabric of the basal wall. Crystallites with fibrillar substructures sometimes form a well-defined front overgrowing older, smooth textured crystallites. The fibrillar crystallites resemble 'immature' crystallites normally seen much closer to the distal edge of the basal wall (Fig. 5F). In other cases, new seeding zones form proximally of the edge of the basal wall and lift slightly above the rest of the basal wall. It seems possible that cuticle is present beneath the uplifted edge.

Individual crystallites sometimes comprise many fibrils and therefore have a 'compound' appearance (Fig. 5F). Their growing edges have 'ragged' margins, with each of the fibrils terminating at an angular front. The upper surface of the crystallites in these early growth stages may have a distinctive speckly texture, with bright raised spots about 1 μm in diameter arranged in a seemingly random pattern, each spot usually $>0.2 \mu\text{m}$ from its neighbours. In *D. gordonii* the apertural spines have an initial granular fabric transitional to fibrils (up to 0.5 μm in length) which coalesce to form foliated crystallites growing distally parallel to spine length. Further down the spine, crystallites become broader, such that by about 30–50 μm from the spine tip the individual distally growing crystallites are very long and narrow, with 5–10 μm of the length of each crystallite exposed. About 100 μm from the spine tip, near the spine base, some of the crystallites begin to imbricate in the opposite direction. The remainder of the spine surface and the aperture of the zooid are characterized by frequent alternations of the direction of growth of the crystallites.

On some wall surfaces in the erect tubuliporine *Idmidronea obtecta* tiny subtriangular spikes form locally on the surfaces of crystallites (Fig. 5B). These spikes are usually less than 2 μm in height and width. Most spikes are perpendicular to the crystallite surface but some grow obliquely or even subparallel to the wall. Spacing of spikes is variable, with distances between nearest neighbours ranging from 2–5 μm . Oblique spikes occasionally appear to broaden to become minute foliated crystallites, implying that spikes may have a role in the generation of new surficial crystallites. In an unidentified species of the rectangulate *Disporella* (Taylor *et al.*, 1995), thorn-like spinelets pointing distally are developed on the surfaces of foliated fabric crystallites forming apertural spines.

Rhombic semi-nacreous fabric

Rhombic semi-nacre can be regarded as a modified form of foliated fabric which occurs on some mature wall surfaces (Fig. 6). However, it warrants separate description because extremely similar fabrics occur in cheilostome bryozoans, as well as in the shells of some calcified craniacean inarticulate brachiopods (e.g. *Neocrania anomala*) and have been interpreted as "semi-nacreous structure" by Carter & Clark (1985; see also Lee & Brunton, 1986). However, unlike true semi-nacre (see below, p. 360), rhombic semi-nacre has the same crystallographic orientation as transverse fibrous and foliated fabrics. But instead of accreting linearly through addition of calcite along two adjacent growing faces, growth in rhombic semi-nacre is equal on all four sides of the rhombic (10 $\bar{1}$ 1) tablet (Fig. 7).

Rhombic tablets are often less than 0.5 μm in diameter and have frequent four-sided screw dislocations (Fig. 6A, B). The α interfacial angles of these tablets measured in *Heteropora magna* averages 102.9° ($n=26$) and equates with the interfacial angles corresponding to the face with the Bravais–Miller index (10 $\bar{1}$ 1) of the cleavage rhombohedron. In this crystallographic orientation the c-axis is inclined at 45° to

the tablet surface in a plane bisecting the obtuse angles of the tablet, contrasting with the perpendicular c-axes of hexagonal semi-nacre tablets (Fig. 7).

Hexagonal semi-nacreous (and pseudofoliated) fabric

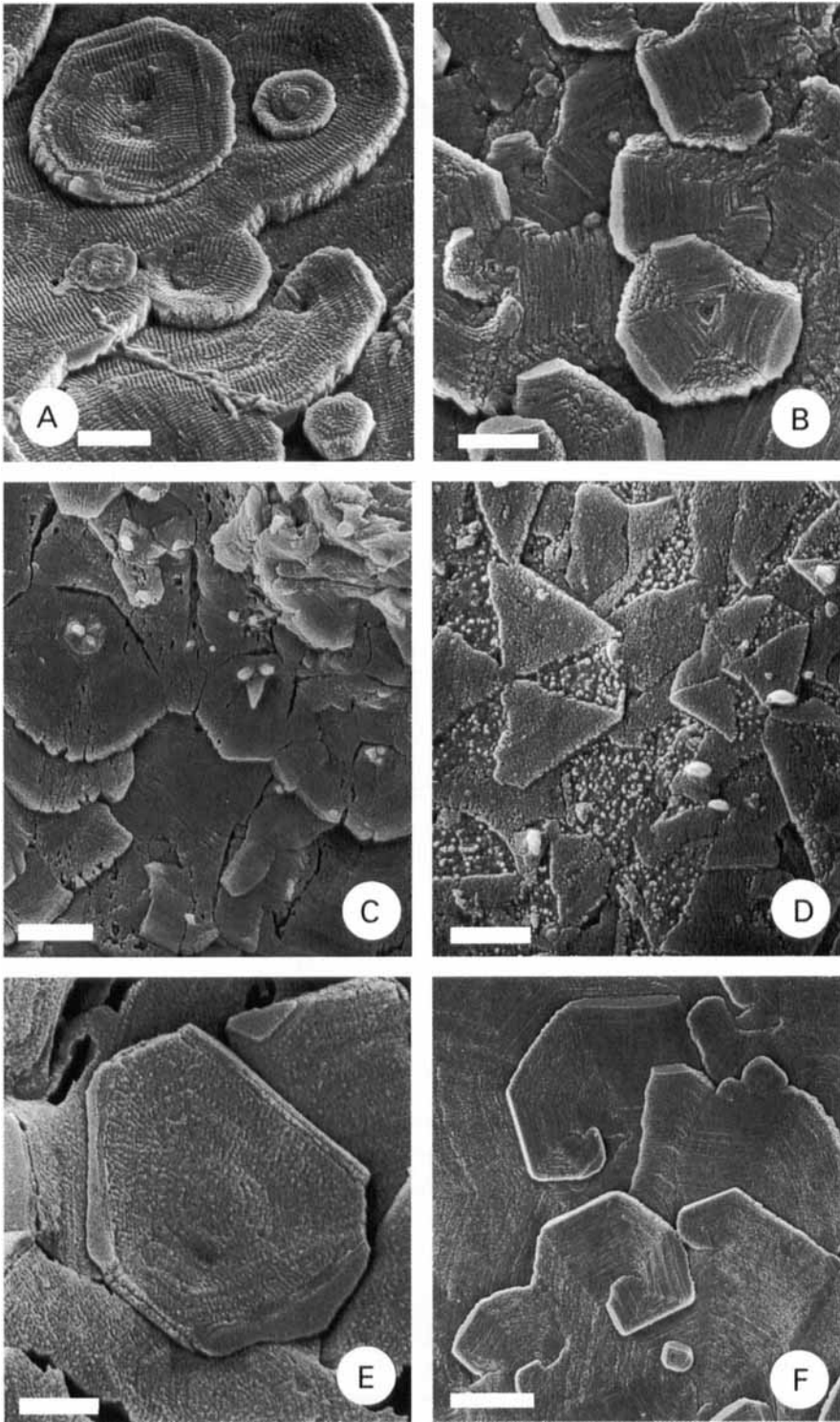
This fabric (Figs 8–11) employs a different crystallographic orientation from the other laminar fabrics found in cyclostomes. It is based on hexagonal tablets of calcite, with the c-axis perpendicular to the tablet (and wall) surface. The uppermost surface corresponds to the (0001) face (Fig. 9).

Hexagonal semi-nacre forms the only fabric of the interior walls of most articulates and cancellates. In the interior walls of other taxa, it may succeed wedge-shaped granular fabric, transverse fibrous fabric, and locally foliated fabric. When present, hexagonal semi-nacre, or its derivative pseudofoliated fabric, usually forms the zoecial lining, although in some tubuliporines foliated fabric may succeed it locally.

In walls with hexagonal semi-nacre succeeding wedge-shaped granular fabric, there is a transitional zone of tiny crystallites (<2 µm diameter), immediately proximal of the wedge-shaped crystallites and overlying them. The flat crystallites are about 0.2 µm thick, with no preferred growth direction. Boundaries between crystallites are poorly-defined. Overlap and fusion with adjacent crystallites is common. More mature tablets typically have a well-defined, euhedral, six-sided shape (Fig. 8A, B, D). However, there is some local and perhaps taxonomic variation in the precise shapes of the hexagonal tablets: on some wall surfaces tablets are angular and euhedral with straight edges, meeting at sharp angles while on others they are anhedral or subcircular in outline (Fig. 8A). The latter variety is particularly common in some crisiid articulate species.

Hexagonal tablets of semi-nacre have interfacial angles consistently approximating to 120°. In *Platonea stoechas* a mean value of 121.3° was determined (SD = 7.57°; range = 108–137°; n = 56). Tablet surfaces often have fine concentric growth lines whose spacing demonstrates that tablet growth rates were equal in all directions (Fig. 8A, B). Surfaces may also have a conjugate series of fine striations perpendicular to these growth lines (Fig. 8A). Tablets usually have a gently concave upper surface with a slight depression at the centre (up to 1 µm in diameter on larger tablets; Fig. 8A, B). Newly seeded tablets less than 0.5 µm in diameter are distributed without apparent pattern over the surfaces of larger, older tablets. Tablet size varies considerably on any given surface. Individual six-sided tablets can be reasonably interpreted as true crystallites. Where neighbouring tablets meet they frequently appear to 'fuse' to form continuous wall parallel laminae or sheets. Lines of fusion

Figure 8. Hexagonal semi-nacreous fabrics in cyclostome skeletal walls. A, *Diaperoecia* sp. 1 (of Weedon, 1997); tablets of hexagonal semi-nacre with well-defined, growth-parallel striations; note fusion of adjacent tablets to form sheets. B, unidentified tubuliporine; partially etched hexagonal semi-nacre; hexagonal tablet at lower right has well-defined sectoring, with three well-etched and three poorly-etched sectors; poorly-etched sectors have downward-sloping growing edges. C, *Homera robusta*; typical cancellate hexagonal semi-nacre with triple spikes at centres of tablets. D, *Platonea stoechas*; heavily etched wall showing the well-defined tablet sectoring. E, *Tubulipora* sp.; single tablet of hexagonal semi-nacre showing the outward sloping edges of three of the sectors. F, unidentified tubuliporine; screw dislocations and a tiny, newly-seeded tablet (bottom). (Scale bars: 1 µm in A; 1 µm in B; 1.5 µm in C; 1.5 µm in D; 1 µm in E; 2.5 µm in F).



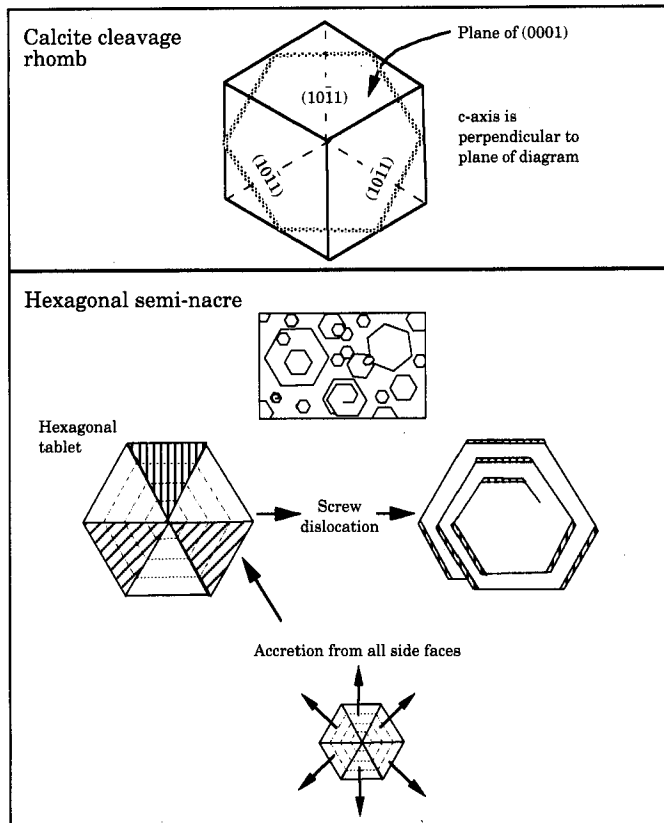


Figure 9. Diagrammatic representation of the growth of hexagonal semi-nacre (and pseudofoliated fabric) from the calcite cleavage rhomb aligned with the c-axis perpendicular to the wall surface. The upper surface of the hexagonal tablets correspond to the (0001) face, and the oblique side edges to (1011) faces.

between adjacent crystallites are marked by very narrow furrows or disruptions in the growth lines.

Screw dislocations (or spiral overgrowths) are common on many wall surfaces and may be either dextral or sinistral (Fig. 8F). Two screw dislocations with opposite coiling directions are often linked together to form a double spiral. Crystallite growing edges in screw dislocations precisely parallel those of the underlying 'parental' crystallite. Local areas of wall surfaces often have groups of screw dislocations with precisely parallel edges suggesting they are related to a single true crystallite. Screw dislocations allow wall thickening without seeding of new crystallites and become commoner in more mature walls where seeding is less frequent.

The surfaces of six-sided tablets are sometimes differentially etched to reveal six alternating triangular sectors (Fig. 8B, D). In the three more soluble sectors the tablet surface is normally pimply, whereas the surface of the less soluble sectors is smooth with well-defined growth lines. However, in some instances (see Taylor & Jones, 1993) the more etched sectors may appear smooth, and the less etched sectors coarsely granular. Persistent bleaching for long periods (or other etching processes) may cause the complete removal of the more soluble sectors, leaving the three less

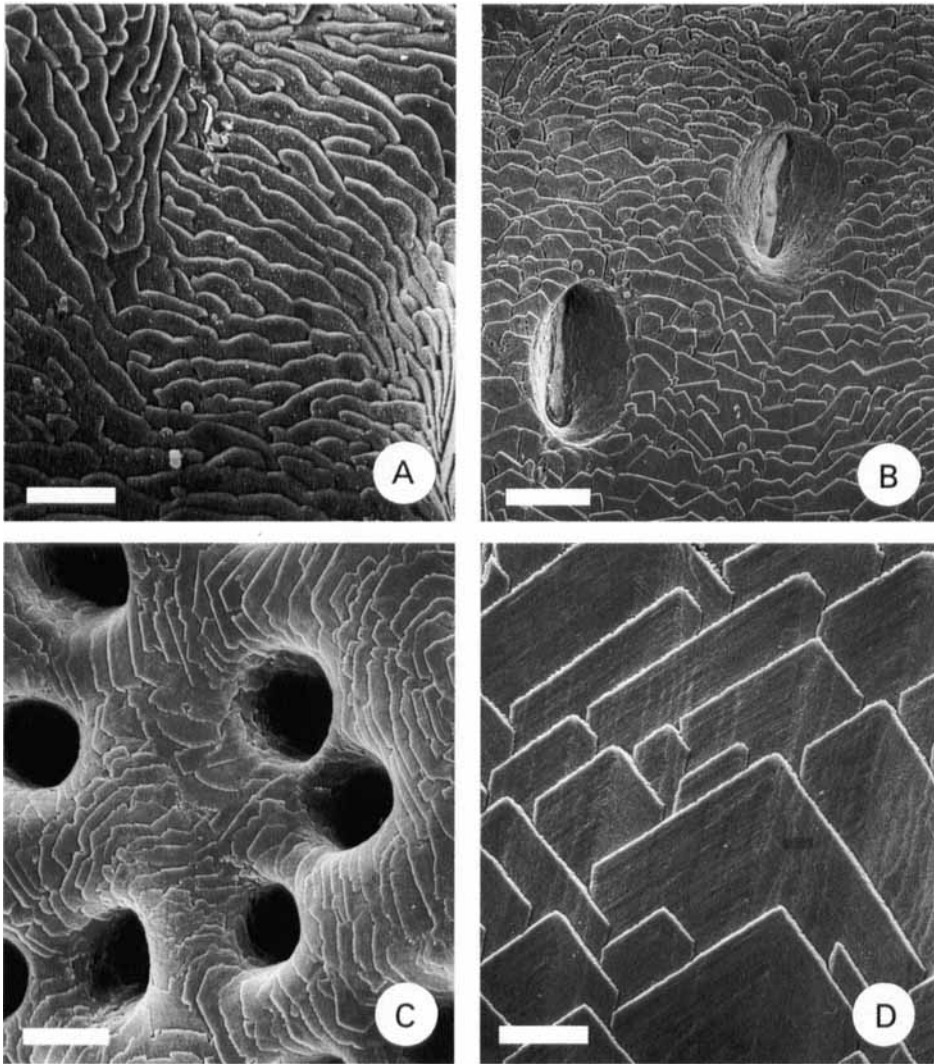


Figure 10. Distally imbricated pseudofoliated fabrics in cyclostome skeletal walls. This is a mature, imbricated derivative of hexagonal semi-nacre. A, *Entalophorecia deflexa*; broad fronts of imbricated crystallites from an interior wall. B, *Crisia* sp.; inner surface of exterior frontal wall with pseudofoliated fabric; note scattered, tiny tablets of hexagonal semi-nacre, and two elliptical pseudopores. C, *Plagioecia dorsalis*; inner surface of exterior wall forming roof of a gonozoid; pseudopores are numerous and closely-spaced. D, *Filicrisia franciscana*; localized area on inner surface of exterior frontal wall with pseudofoliated crystallites having 90° interfacial angles. (Scale bars: $5\ \mu\text{m}$ in A; $9\ \mu\text{m}$ in B; $7.5\ \mu\text{m}$ in C; $3\ \mu\text{m}$ in D).

soluble sectors (Fig. 8D). On unetched wall surfaces sectoring may still be detected because the more soluble sectors have a darker shade under SEM, and the less soluble sectors usually appear to be raised and have better defined growth lines and striations. In many six-sided tablets three of the growing edges are slightly longer than the other three, giving three narrow sectors alternating with three broad sectors. The more soluble sectors in these cases are the narrow sectors, the less soluble the

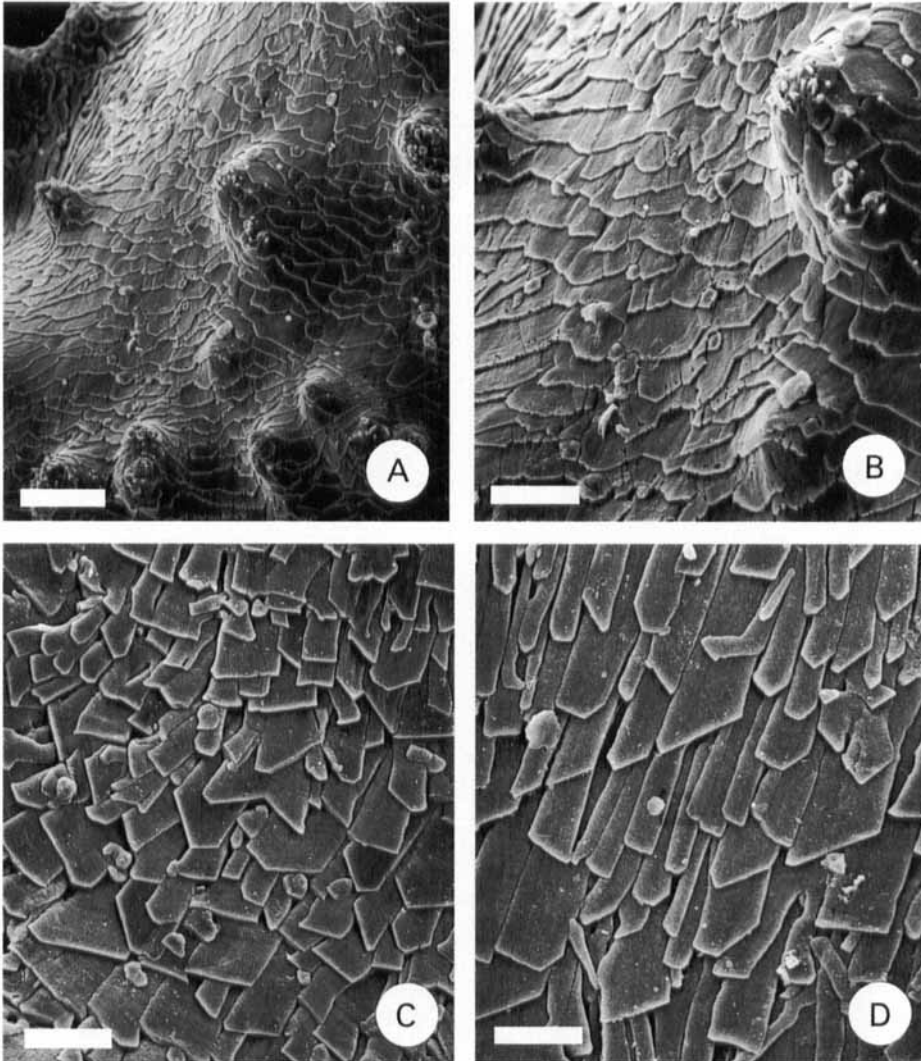


Figure 11. Proximally imbricated pseudofoliated fabrics in cyclostome skeletal walls. A, B, *Homera frondiculata*; pustulose wall with broad crystallite fronts of proximally imbricated pseudofoliated fabric; note tiny spikes on tubercles which are associated with crystallite origins. C, *Homera lichenoides*; proximally-imbricated crystallites with scattered, newly-formed tablets. D, *Crisina radians*; elongate proximally-imbricated crystallites. (Scale bars: 10 μm in A; 5 μm in B; 5 μm in C; 4 μm in D).

broad sectors. Only the three less soluble sectors reach the very centre of the tablets. Here the three sectors are separated by sutures in a 'trilete' pattern. The three more soluble sectors first appear about 0.1–0.3 μm outward from the centres of the tablets. Growing edges of semi-nacre tablets are not perpendicular to the upper surface but are inclined such that the edges of the three more soluble sectors slope inwards to form an overhang, whereas those of the three less soluble sectors slope outwards (Fig. 8B, E).

In some species (e.g. *Platonea stoechas*, *Crisia* spp.), tiny spikes occur on the surfaces of tablets (Fig. 8D). The spikes are up to 1 μm long and form in highest concentrations

inside interzooidal pores and around pustules. The great majority of spikes occur on the less soluble sectors and sometimes can be observed to originate along the growing edges of the tablets. Spikes are also characteristic of the semi-nacreous fabric of many hornerid cancellates. However in these species, the spikes often occur in triplet arrangements on the less etched, downward sloping faces of the hexagonal tablets (Fig. 8C). The triple spikes always form very near the centre of the tablets, and are angled away from each other, pointing roughly towards the mid point of the tablet side growing edge (Fig. 8C). Single spikes are also widespread in these species, and are particularly common on less etched sectors; they reach maximum abundance in areas where pustules or crystallite seeds are present.

Pseudofoliated fabric is a modified form of hexagonal semi-nacre where the overlapping of fused tablets creates an imbricated fabric which is reminiscent of true foliated fabrics (Figs 10, 11). This imbricated sub-division of hexagonal semi-nacre occurs in two distinct forms. Most common is distally-imbricated pseudofoliated fabric which can be found in tubuliporines, articulates and cerioporines (Fig. 10). Proximally-imbricated pseudofoliated fabric occurs in most cancellates, and in the tubuliporine *Fenestulipora* (Fig. 11).

On wall surfaces typically well proximal of growing edges, large areas can be covered by crystallites that have undergone multiple divisions by screw dislocation or stepping. These surfaces of pseudofoliated fabric may show regular imbrication in a predominantly distal direction (Fig. 10). Pseudofoliated fabric is able to conform to strongly curved surfaces; for example, laminae can wrap around the inner surface of pseudopores in exterior walls (Fig. 10C).

Distally-imbricated pseudofoliated fabrics usually have broad growth fronts comprising many fused surficial crystallites. Although few interfacial angles are available for measurement, most are obtuse, corresponding to the angles of the hexagonal semi-nacre tablets. However, in exceptional cases, such as an unidentified species of *Crisia*, areas of wall surfaces occur where there are consistent and unusual interfacial angles. These may include regions where the primary angle is very nearly 90° (Fig. 10D), corresponding with the $(10\bar{1}2)$ face found in the calcitic foliated fabric of molluscs *Anomia* and *Placuna* by Runnegar (1984). In this structure, the c -axis would be inclined at 64° to the crystallite surface in a plane parallel to the growth direction. More commonly, surficial crystallites of distally-imbricated pseudofoliated fabrics have α angles close to 102° , suggesting localized $(10\bar{1}1)$ faces, similar to those found in foliated fabrics.

Proximally-imbricated pseudofoliated fabric occurs in hornerid cancellates and in the tubuliporine *Fenestulipora cassiformis* (Harmer), a deep-water species with an unusual fenestrate colony-form (Taylor & Gordon, 1997). The fabric is essentially the same as distally-imbricated pseudofoliated fabric except that the dominant growth direction is proximal. Growth fronts may be broad, comprising many fused surficial crystallites, usually with large interfacial angles. However, in some species (e.g. *Pseudidmonea fissurata*, *Crisina radians* and *Hornera lichenoides*) the proximally growing crystallites may accrete in a characteristic pattern, becoming very elongate and growing as separate surficial crystallites which do not fuse with their neighbours (Fig. 11C, D). The interfacial angles of the elongate crystallites are highly variable, often with a squared-off growing tip. Interestingly α angles of $c. 90^\circ$ are quite common in this fabric, corresponding to possible $(10\bar{1}2)$ faces (see above).

In *Fenestulipora cassiformis*, crystallites are up to $10\ \mu\text{m}$ in width and have interfacial angles averaging 98° ($n=20$). Crystallites have a variety of interfacial angles from

77–122°, with most in the range 100–105°, suggesting a variety of orientations, with the (10 $\bar{1}$ 1) rhombic face dominant. Some wall areas have variably-oriented, narrower, more fibrous crystallites which bifurcate and may develop screw dislocations.

Moulded fabric

Found in all cyclostomes, moulded or homogeneous fabric is the ultrastructure from which many fine-scale structures are formed. These structures include the tooth-like spines projecting into interzooidal pores and pseudopores (Fig. 4C); the long spikes developing the surfaces of some crystallites; and the tiny thorn-like spikes which cover the heads of some mural spines (Fig. 10D). In all cases the fabric has a dense, uniform appearance, and lacks angular crystal faces.

Fabric suites

Individual skeletal walls of cyclostomes comprise the ultrastructural fabrics described above in combinations of between one and five distinct fabric layers. The arrangement of the fabrics follows set patterns termed fabric suites (Fig. 12). Each species possesses skeletons of only one fabric suite for interior walls, one for exterior walls, and one for the protoecium. However, the precise thicknesses of the constituent layers may vary locally, and localized areas of skeletons may occasionally develop unusual crystallite morphologies and/or growth directions. Some particular fabrics (e.g. hexagonal semi-nacre) occur in more than one interior or exterior wall fabric suite; others, such as transverse fibrous fabric, occur in only one suite.

Interior walls

Five fabric suites can be recognized in interior walls: (1) planar spherulitic → transverse fibrous → foliated → hexagonal semi-nacre and distally-imbricated pseudofoliated; (2) precursory granular → foliated; (3) precursory granular → hexagonal semi-nacre and distally-imbricated pseudofoliated; (4) hexagonal semi-nacre and distally-imbricated pseudofoliated; (5) hexagonal semi-nacre and proximally-imbricated pseudofoliated.

Interior wall fabric suite 1 (with transverse fibres). This fabric suite is characteristic of about half of the tubuliporine species, and two of the heteropodid cerioporines (Fig. 12A; Appendix 1). When fully developed, the skeletal succession is:

(1) *Precursory planar spherulitic fabric.* As described above, this fabric is only clearly visible on pristine growing edges as it forms an extremely thin delicate layer barely protruding beyond the distal tip of the growing wall. Although only clearly imaged in *Cinctipora*, from similarities in fractured surfaces and thin sections it is inferred that this fabric forms the initial layer in all interior walls with transverse fibres.

(2) *Transverse fibrous fabric.* The precursory planar spherulitic fabric is succeeded directly by a fabric comprising imbricated, extremely long fibres with their long axes perpendicular to the distal direction and oriented in the plane of the wall. The thickness of the transverse fibrous layer is highly variable between species; e.g. in *Tubulipora notomale* it is up to 20 μm and in *Mecynoecia delicatula* less than 5 μm .

(3) *Distally-imbricated foliated fabric.* The transition between transverse fibres and the succeeding foliated fabric is complex, variable and has yet to be studied in detail.

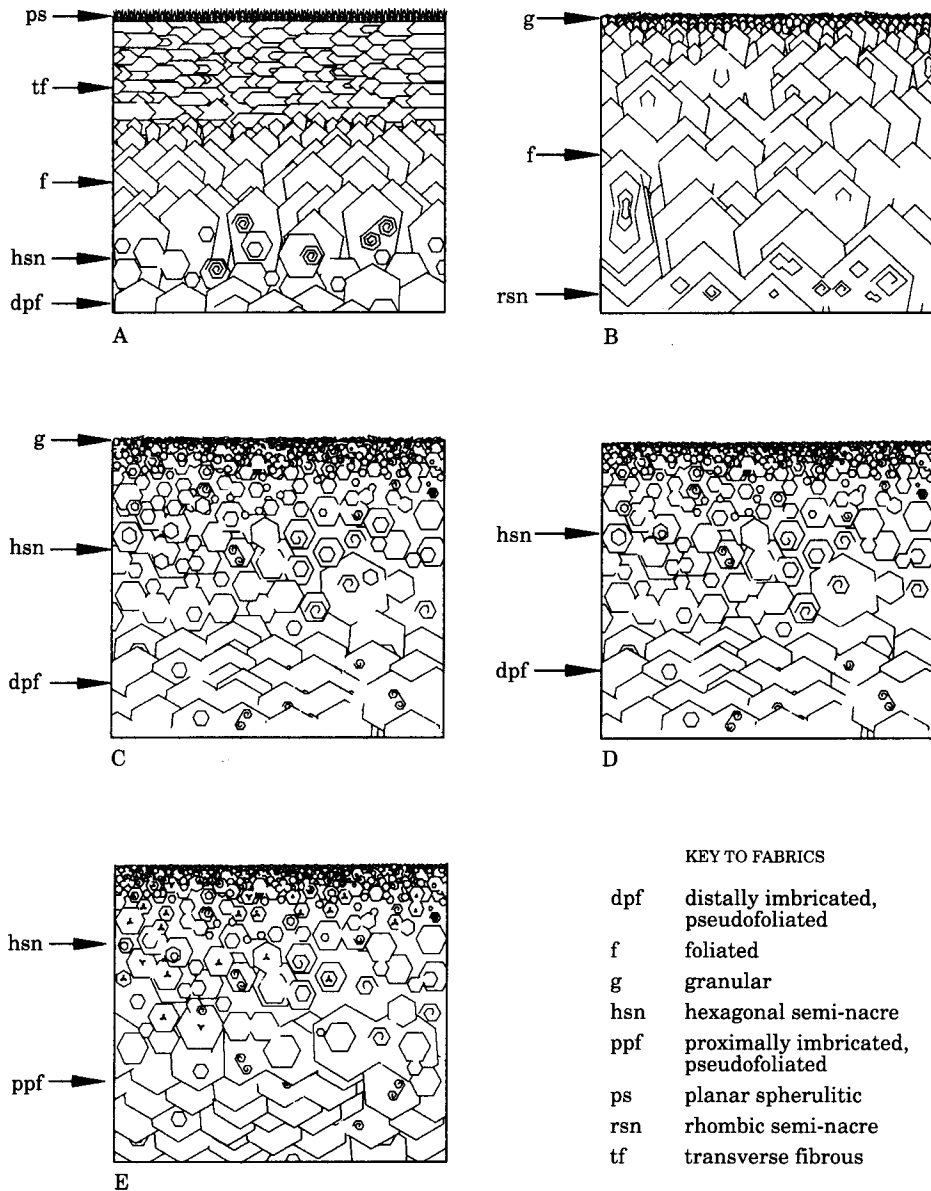


Figure 12. Diagrammatic representations of the distal parts of accreting interior walls, showing the succession of the fabrics constituting five fabric suites. Wall growing edges are at the top of each block diagram, later-formed fabrics appearing towards the bottom of the diagrams. A, interior fabric suite 1. B, interior fabric suite 2. C, interior fabric suite 3. D, interior fabric suite 4. E, interior fabric suite 5.

There is an increase in the frequencies of crystallite splitting and in screw dislocations. Transverse fibres broaden in width and change growth direction by about 90° so that most grow parallel to wall growth direction and become distally imbricated. This transition does not involve a change in crystallographic axis orientation; instead,

only the predominant direction of crystallite growth changes. Individual crystallites can sometimes be observed with newly growing foliated fabric continuing directly from the edge of a transverse fibre (Fig. 4E).

(4) *Semi-nacre grading to distally-imbricated pseudofoliated fabric*. This is the final fabric in the suite and comprises irregular, flat-lying sheets of flattened, laterally fusing tablets which are ideally six-sided. On older areas of the wall seeding of new tablets is less frequent, and the combination of screw dislocations and tablet fusion produces continuous sheets which may develop very wide crystallite fronts of pseudofoliated fabric. The thickness of the hexagonal semi-nacre fabric layer in cyclostomes with this fabric suite is highly variable. In some species (e.g. *Mecynoecia delicatula*) it is the dominant layer in the wall, whereas in others (e.g. *Tubulipora notomale*) it is reduced to a thin zoecial lining a few laminae thick on top of the dominant layer of transverse fibres.

Interior wall fabric suite 2 (predominantly distally-imbricated foliated). This suite characterizes the interior walls of all rectangulate species studied, all apart from two cerioporines (which have suite 1), and four species of tubuliporines (Fig. 12B; Appendix 1). The skeletal succession is:

(1) *Granular fabric*. In most species and wall types studied this fabric has the typical wedge-shaped structure described above. However, in others (e.g. apertural spines of some rectangulates) the granular fabric is irregular or 'blebby'. There is a gradation between wedge-shape granular fabric and the succeeding foliated fabric.

(2) *Foliated fabric*. This is the dominant fabric of the suite. There is some variation in the degree of regularity of foliated fabric, with well-developed interfacial angles predominating in tubuliporine and heteroporid cerioporines, whereas irregular, rather anhedral crystallites, with a fibrillar subtexture and poorly-developed interfacial angles, comprise the bulk of foliated fabric in the studied species of rectangulates and non-heteroporid cerioporines. Crystallite boundaries characteristically become indistinct on the older surfaces of walls where crystallite growth direction is also less regular. The lack of clearly imbricated crystallites on these surfaces contrasts with the strongly imbricated pseudofoliated fabrics of older wall surfaces in fabric suites 3–5.

Interior fabric suite 3 (predominantly hexagonal semi-nacre). Occurring in many tubuliporine species (Fig. 12C; Appendix 1), the skeletal succession here consists of:

(1) *Granular fabric*. This precursory fabric is fundamentally similar to that in cyclostomes having fabric suite 1.

(2) *Hexagonal semi-nacre*. The bulk of the wall in species with interior fabric suite 3 comprises sheets of semi-nacre. Seeding is most common distally, with older wall surfaces having more screw dislocations and maturing to predominantly distally-imbricated pseudofoliated fabric.

Interior fabric suite 4 (hexagonal semi-nacre and distally-imbricated pseudofoliated fabric). This fabric suite occurs in the tubuliporine "*Stomatopora*" sp. and all studied articulates (Fig. 12D; Appendix 1) apart from *Crisulipora* which has interior fabric suite 1. The suite is essentially identical to fabric suite 3 with the important exception that there is no precursory granular layer. Instead, tablets of hexagonal semi-nacre are seeded directly onto exterior walls. Newly-formed interior walls consisting of semi-nacre only one crystallite thick can be observed, clearly demonstrating the absence of a

granular precursory layer. Walls develop in the same way as the walls of fabric suite 3, with mature walls showing distally-imbricated pseudofoliated fabric.

Interior fabric suite 5 (predominantly proximally-imbricated pseudofoliated fabric). This fabric suite characterizes cancellates (Fig. 12E; Appendix 1). It is also the likely fabric suite of the tubuliporine *Fenestulipora*, although the lack of material with pristine growing edges means that the full succession of fabrics is unknown in this genus. In cancellates with fabric suite 5 there is no precursory granular or planar spherulitic layer. The first-formed crystallites of the skeleton are tiny tablets of hexagonal semi-nacre, often with single or more commonly triple spikes in the tablet centres (see above). Seeding of new tablets is most frequent near to the distal edge of the wall. Further proximally, screw dislocations become more common, and there is a transition to predominantly proximally-imbricated pseudofoliated fabric (see above). Fractured walls and thin sections, show that wall laminae diverge in a proximal direction (aborally) owing to the dominance of proximally-imbricated crystallites. This contrasts with the other fabric suites where laminae either parallel wall surfaces or diverge in a distal direction (orally).

Frontal exterior walls

The exterior-walled, frontal wall complex—comprising frontal walls *sensu stricto*, peristomes and terminal diaphragms—of cyclostomes has its own distinct fabric suites. In all cases the succession of laminar fabrics, which form the greatest thickness of the wall, follow the same fabric suite as the corresponding interior walls. The main differences lie in the outermost granular/planar spherulitic layers; i.e., in presence/absence of the planar spherulitic layer and the direction of growth of the constituent strip-like units of the outer layers.

Four exterior fabric suites have been recorded: (1) precursory granular → planar spherulitic → transverse fibrous → foliated → hexagonal semi-nacre; (2) precursory granular → planar spherulitic → foliated; (3) precursory granular → hexagonal semi-nacre and pseudofoliated; (4) precursory granular → foliated fabric → hexagonal semi-nacre.

Exterior fabric suite 1 (with transverse fibres). In most tubuliporines, a thin outer layer of precursory granular fabric is succeeded by a layer of distally-growing strips of planar spherulitic fabric, particularly well seen in specimens slightly etched during the bleaching process. The planar spherulitic layer is succeeded by fabrics of transverse fibres, foliated crystallites and hexagonal semi-nacre, as outlined above for interior wall fabric suite 1.

Exterior fabric suite 2 (predominantly distally-imbricated, foliated). This fabric suite is similar to the first but lacks transverse fibres. Therefore, distally-growing strips of planar spherulitic fabric are directly succeeded by distally-imbricated foliated fabric and/or semi-nacreous ultrastructure. In the tubuliporine *Fasciculipora ramosa*, the fascicle-bounding frontal walls are similar, but the planar spherulitic units do not originate at the transverse growth checks. Instead, the units originate along the zooidal boundaries and grow obliquely distally at about 45° to the boundaries. Units growing from either side of the zooid meet to form a suture along the midline of the zooid. Hiatuses in the growth of the advancing front of the planar spherulitic layer are marked out by irregularly-spaced, v-shaped growth bands. Pseudopores are elongated

parallel to the growth direction of the planar spherulitic units (i.e. obliquely to the long axis of the zooid). The planar spherulitic layer is succeeded immediately by the distally growing foliated fabric which constitutes the remainder of the frontal wall skeleton.

Exterior fabric suite 3 (lacking planar spherulitic fabric, predominantly distal-imbricated foliated/hexagonal semi-nacre). Frontal walls with an entirely granular fabric outer layer occur in tubuliporines such as *Plagioecia dorsalis*, *P. patina*, *Platonea stoechas*, and '*Cardioecia watersi*'. Pristine walls show the densely-packed, finely granular precursory fabric which was deposited directly against the cuticle. In some species (e.g. *Plagioecia patina*), this fabric comprises discrete, wedge-shaped crystallites, with triangular cross-sections and three-angled terminations. In other species, the constituent crystallites are more irregular in shape or have a rounded outline. This fabric forms a very thin exterior layer only a few crystallites deep, and in many specimens is wholly or partly lost during bleaching and cleaning. In *Plagioecia patina* there are striations, or fine ridges, parallel to wall growth direction and spaced 7–10 µm apart. The ridges mark the boundaries between strip-like units of calcification which resemble those seen in frontal walls with a planar spherulitic fabric as described below. The granular fabric is succeeded directly by foliated or hexagonal semi-nacreous fabric.

Protoecium

The protoecium may be conveniently divided into two parts: the flattened base, here called the 'floor', and the dome-shaped 'roof'. Although skeletal walls are effectively continuous between floor and roof, the ultrastructural fabrics are distinct in the two areas and are consistent in every species studied regardless of post-protoecial fabric suite (Weedon, 1998).

The fabric suite found in all protoecial roofs consists of: precursory granular → hexagonal semi-nacre/foliated. The roof of the protoecium has a two layered skeletal ultrastructure comprising a thin outer coarse granular layer (often of wedge-shaped crystallites), accreted directly against the cuticle, and an inner lining of irregular semi-nacreous fabric, maturing to pseudofoliated fabric. Planar spherulitic fabric does *not* occur in this part of the protoecium. Note that this fabric suite is the same as exterior fabric suite 3 for adult skeletons. The granular outer fabric occurs in strips, defined by tiny raised ridges (Fig. 1E, F). These strips pass from the outer edge of the roof (at the junction with the floor) and continue to the contact with the tubular distal part of the ancestrula. They are 10–15 µm wide at the outer edge, becoming narrower (2.5–5 µm) where they join this distal tube. This granular layer is succeeded by a fabric of typical hexagonal semi-nacre which is transitional to pseudofoliated fabric with laminae imbricated towards the middle of the protoecium roof or in a slightly distal direction.

The protoecium floor differs from the roof by incorporating a layer of planar spherulitic fabric so that the full fabric suite is: precursory granular → planar spherulitic → hexagonal semi-nacre/foliated. Growth of the planar spherulitic layer is centripetal, proceeding from the contact with the roof toward the centre of the floor. The floor is lined internally by hexagonal semi-nacreous fabric, continuous with the roof lining, which also matures to pseudofoliated fabric.

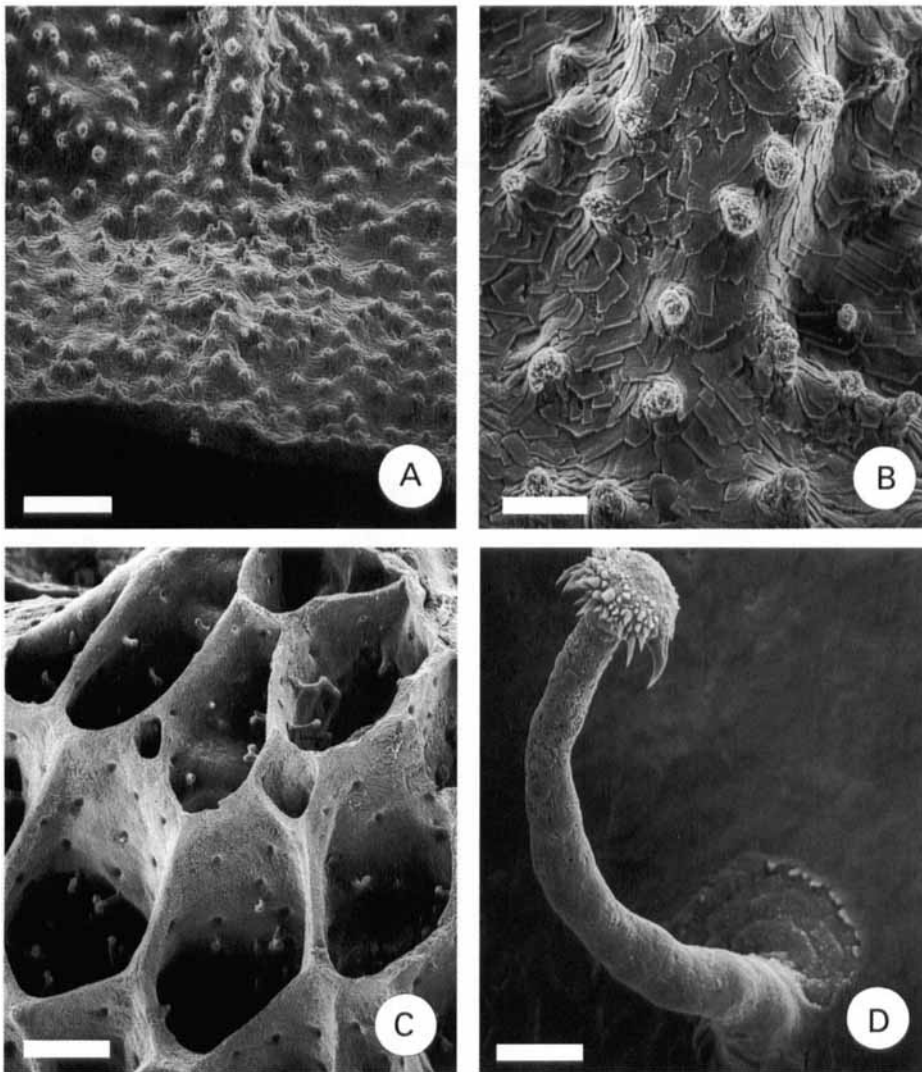


Figure 13. Pustules and mural spines in cyclostome skeletal walls. A, B, *Disporella gordonii*; basal exterior wall with developing septum (incipient interior wall); note distally-imbricated foliated fabric and abundant pustules. C, *Heteropora neozelanica*; abundant long mural spines projecting into zooidal chambers. D, *Heteropora neozelanica*; mural spine with a crown covered by minute spikes constituting a moulded fabric. (Scale bars: 30 μm in A; 7.5 μm in B; 75 μm in C; 6 μm in D).

Fine-scale structures

Fine-scale skeletal structures of cyclostome bryozoans have received relatively little attention (see Hinds, 1973; Farmer, 1979). These structures include interzooidal pores (with associated spinelets), pseudopores, pustules, apertural spines and mural spines, as well as still finer structures such as tiny spikes borne on crystallite surfaces.

Some of the fine-scale structures occur only on certain skeletal wall types, whereas others are less specific in their distribution. Pustules (Fig. 13A, B) surficial spikes,

and mural spines (Fig. 13C, D) may grow everywhere on the wall surface or may be confined to local areas. Interzooidal pores only occur in interzooidal walls and the roofs of gonozooids with interior walls. Pseudopores are restricted to frontal exterior walls, exterior walled diaphragms, the roofs of gonozooids with exterior walls, some protoecia, and occasionally basal walls. Mural hoods are only found on basal walls (see Weedon, 1997).

Mural spines

Fine-scale structures such as interzooidal pores and pseudopores are ubiquitous across all the suborders (and their respective wall types). Their phylogenetic usefulness is very restricted owing to this ubiquity combined with the similarity of the respective structures across all groups. However, mural spines ('zoocial spines' of Farmer, 1979) occur widely though not universally, and vary considerably in their sub-structure among different taxa. Hence they have potential as characters for phylogenetic analysis, and will receive a little further attention here. Mural spines vary between simple tubercular pustules (Fig. 13A, B) through longer spinose projections to more complex structures with an extended stem or shaft capped by crown-like structures with varying arrays of sharply pointed spinelets (Fig. 13C, D).

The smallest, most abundant spinose structures are simple pustules, which form dome shaped projections. They may have a fine granular 'core' with an outer layer formed by disruption of the laminar fabric of the wall. Longer, more spinose pustules may project perpendicularly (or be slightly curved) from the wall surface to a length of more than 10 μm . The crystallites of the surrounding laminar fabric may accrete up the pustule.

There is a considerable variety of mural spines with more complex spinose 'crowns'. Spine morphologies are often characteristic of particular species. The simplest, non-pustular spines, have single spike-like terminal projections comprising a single homogeneous ('moulded') fabric (e.g., *Diaperoecia purpurascens*, see Weedon & Taylor, 1997). Most commonly, such spines are not wall perpendicular but curve to point proximally. In some species, the proximal-pointing spines develop extra spinelets with maturity, and may grow to have a flattened crown or head with proximally-pointing spinelets. In other species, the spines can become quite elongate, and have a variety of crown-like structures (see Taylor *et al.*, 1995; Weedon & Taylor, 1996, 1997, 1998). These vary from flattened heads surrounded by downward curving claw-shaped spinelets (Fig. 13C, D), through multiple rows of spines covering a more rounded head, and even multiple headed spines (three-headed spines are common in, for example, *Heteropora magna*). Spines vary in length, and may be very long, exceeding 50 μm in shaft length. In a few species, notably *Tervia irregularis*, the spine consists of a comb-like structure with multiple slightly proximally-directed tooth-like spinelets arranged in a blade which is perpendicular to the wall surface and transverse to zooidal growth direction.

In all crowned mural spines, the outer fabric of the shaft of the spine comprises an extension of the imbricated crystallites of the main wall ultrastructure. The crown, however, usually has a more granular fabric in the central region, with 'moulded' fabric spinelets (Fig. 13C, D).

Summary and new findings

The mineralized component of all cyclostome bryozoan skeletons consists of microcrystalline calcite. Based on the morphology of the calcite crystallites, six

fundamental fabrics can be distinguished: granular, planar spherulitic, transverse fibrous, foliated, rhombic semi-nacre, and hexagonal semi-nacre/pseudofoliated. The first two fabrics always form very thin layers in the early parts of walls, whereas the last four fabrics form the bulk of the walls and comprise the layers of stacked or imbricated crystallites which are responsible for the distinctly lamellar appearance of cyclostome skeletal walls. Although planar spherulitic fabric has been recognized previously in exterior skeletal walls, the current paper reports its occurrence in interior walls for the first time. Crystallographic orientations inferred from measurements of interfacial angles imply that all of the lamellar fabrics have the c-axes of the crystallites oriented at 45° to the wall surface (contrary to earlier inferences) with the exception of semi-nacre/pseudofoliated where the c-axes are oriented at 90° to the wall surface. In contrast to cheilostome bryozoans, there are no known examples in living cyclostomes of fabrics consisting of fibrous crystallites growing perpendicular or subperpendicular to wall surfaces.

Individual skeletal walls are constructed of one to five different fabrics, the succession of fabrics constituting a fabric suite. Previous papers on particular cyclostome suborders (e.g. Weedon & Taylor, 1997) recognized and named specific fabric suites for particular suborders. The more comprehensive synthesis presented in the current paper distinguishes five different fabric suites in interior walls, and three in exterior frontal walls applicable across all suborders of cyclostomes. Within a single fabric suite, transitions from one fabric to another sometimes entail the seeding and growth of new crystallites with a different crystallographic orientation (e.g. foliated to semi-nacreous fabric). On other occasions, however, the transition involves only a change in the dominant direction of growth of the crystallites (e.g. transverse fibrous to foliated fabric).

PHYLOGENETIC ANALYSIS

Taxa selected

There are about 350 nominal genera of cyclostomes, approximately 20% of which are extant. Not only is adequate information on character states unavailable for the great majority of these genera, but inclusion of all cyclostome genera in a single phylogenetic analysis would both greatly exceed computational capabilities and preclude acceptable resolution without far more characters than the 46 skeletal characters used below. Therefore, a selection of 29 cyclostome genera was made for the analysis presented here. At least two genera from each of the five extant suborders were chosen. Selected genera were those for which a maximum number of character states are known, plus two fossil genera (*Cuffeyella* and *Reptomultisparsa*) which, together with a generalized trepostome, were coded for potential use as outgroups. Three other fossil genera (*Collapora*, *Meliceritites* and *Foricula*) were included in order to address the phylogenetic position of the aberrant 'melicerititids' which some bryozoologists (e.g., Viskova, 1992) have regarded as a separate suborder of cyclostomes.

Characters from the type species of each genus were used for coding purposes except for the following genera: *Borgiola* (coding based on *B. otagoensis* Taylor, Schembri & Cook, 1989), *Diaperoecia* (coding based on *D. purpurascens* (Hutton)),

Favosipora (coding based on unpublished species from New Zealand), *Foricula* and *Meliceritites* (generalized codings based on Taylor, 1994 and unpublished data), *Platonea* (coding based on *P. stoechas* Harmelin, 1976a), and *Reptomultisparsa* (coding based on the oldest recorded species, *R. hybensis* (Prantl), see Taylor & Michalik, 1991). Three species of the cerioporine *Heteropora sensu lato* were coded because of some important differences in colony-form and skeletal ultrastructure previously demonstrated (see Weedon & Taylor, 1996). Two codings were employed for the tubuliporine genus *Stomatopora sensu lato* in view of the contrasts between Jurassic (see Illies, 1963) and Recent species (see Harmelin, 1974, 1979); the former includes *Stomatopora sensu stricto* (Family Stomatoporidae) and the latter '*Stomatopora*' *sensu lato* (provisionally Family Oncouseciidae). Following a revision (Gordon & Taylor, 1997) of the type species of *Lichenopora*, the little-used genus *Patinnella* is provisionally resurrected for Recent species generally assigned to *Lichenopora*.

Characters

As noted above (p. 341), soft part characters have been described in very few cyclostomes. Furthermore, some of these characters are currently autapomorphic for particular taxa, while others seem to be universally present and primitive for the order. Characters belonging to both of these categories are uninformative when attempting to infer phylogenetic relationships between taxa of cyclostomes. Hayward & Ryland (1985: 12) commented: "The soft part morphology of cyclostomes is essentially identical in all species but skeletal structures differ markedly throughout the Order . . ." While the work of Boardman (1998) in particular has since shown this statement to be an over-simplification, the most striking and easily observable differences between cyclostome taxa do appear to reside in the skeleton. Therefore, the analysis presented here is based entirely on morphological characters observable in the skeleton, including colony- and zooid-level characters, as well as the skeletal ultrastructural characters which were discussed in greater detail above. An obvious advantage of using only skeletal characters is that fossil taxa can be included in the analysis with almost the same completeness of coding as recent taxa. Tree rooting can then be undertaken with stratigraphically old fossil taxa as outgroups. The alternative approach—rooting on the ctenostome outgroup—would be less satisfactory because of the severely reduced number of shared characters available in this entirely soft-bodied order.

Codings for ultrastructural characters were obtained exclusively from the research summarized above. Other character states were derived from the literature, supplemented by SEM and other studies of specimens mainly in the collections of The Natural History Museum, London. Key references dealing with cyclostome skeletal morphology in the coded genera are: Boardman (1998), Boardman *et al.* (1992), Borg (1926, 1933, 1941, 1944), Harmelin (1974, 1976a, 1979), Hayward & Ryland (1985), Kluge (1975), Nielsen (1970), Osburn (1953), Robertson (1910), Schäfer (1991), Silén (1977a), Taylor & Gordon (1997), Taylor & Michalik (1991), Taylor & Wilson (1996), Taylor *et al.* (1989), Walter (1970).

With one exception, characters present in only one genus and likely to constitute autapomorphies have been omitted because they are uninformative with respect to relationships between genera. Character 33—primary nanozooids—is the only autapomorphic character listed. This has been included because of possible linkages

with character 34—secondary nanozooids—which occurs in more than one of the selected genera.

Character descriptions

The characters used in this analysis can be divided into three groups: characters 1–13 are colonial, 14–37 are zooidal, and 38–46 are ultrastructural. No explanatory annotation is given for ultrastructural characters as they are reviewed above (pp. 342–373). Wherever possible, multistate characters were avoided to avoid assumptions of ordering.

1. *Colony type* (0) encrusting; (1) erect

A basic distinction can be made between encrusting colonies which are closely adpressed to a substratum throughout their growth, and erect colonies which use an initial encrusting base as a platform for arborescent growth away from the substratum such that most of the zooids in the colony are not in direct contact with the substratum. Although this trait sometimes can vary intragenerically and even intraspecifically (e.g. Harmelin, 1976a), it is apparently fixed in many species, genera, families and even suborders of cyclostomes. For example, all cyclostomes customarily assigned to the Suborder Rectangulata have encrusting colonies, whereas all those assigned to the Suborder Cancellata have erect colonies.

2. *Seriality of adnate parts of colony* (0) uniserial; (1) multiserial

Entirely encrusting colonies as well as the basal adnate parts of erect colonies may have their zooids arranged in single rows (uniserial) or in more than one row (multiserial).

3. *Branching of adnate parts of colonies* (0) absent; (1) present

Uniserial and some multiserial adnate parts of colonies develop bifurcations at distal branch budding zones. However, in other multiserial taxa branching is absent and colonies are typically subcircular in outline with a circumferential budding zone.

4. *Seriality of erect parts of colonies* (0) uniserial; (2) biserial; (3) multiserial

Zooids in narrow-branched erect species are typically arranged in a relatively constant number of series according to the species. Uniserial taxa have autozooids opening in a single series along the delicate branch, whereas biserial taxa comprise two rows of autozooids which generally open alternately on the left- and right-hand sides of the branch. A third state is here recognized for taxa with three or more rows of autozooids. As this state tends to be more variable within taxa, further subdivision is impractical.

5. *Articulations* (0) absent; (1) present

Erect colonies may be rigid or articulated. The latter possess internodes linked by nodes or joints which are elastic and permit some degree of flexing of the colony. Joints apparently form by the progressive resorption from within of the calcareous skeleton (Borg, 1926: 259) to be replaced by an annulus of elastic material (Nielsen & Pedersen, 1979).

6. *Autozooidal apertures in longitudinal rows* (0) no; (1) yes

7. *Autozooidal apertures in transverse rows* (0) no; (1) yes

Autozooidal apertures are arranged on the colony surface in characteristic patterns.

These patterns relate at least in part to interactions between the feeding currents of individual zooids to produce colonial patterns of water flow (see McKinney, 1990). In some taxa, apertures are evenly distributed over the colony surface, but in others they are unevenly distributed, sometimes grouped such that adjacent peristomes are touching (connate). Uneven arrangements may be categorized into those with apertures aligned in longitudinal rows parallel to growth direction, and those with apertures aligned in transverse rows perpendicular or almost so to growth direction. Harmelin (1976b) hypothesized evolutionary trends from primitive species with evenly-distributed apertures to advanced species with increasingly greater levels of aggregation of apertures, from non-connate to connate rows to bundles or fascicles.

8. Distribution of autozooidal apertures on erect branches (0) circumferential; (1) one side only

In erect colonies, autozooidal apertures can open everywhere around the circumference of the branches, or be confined to one side of the branch (frontal or obverse) with no autozooids on the opposite side (dorsal or reverse). Functionally, this difference is understandable in terms of feeding currents: species with autozooids opening on only one side of branches establish directional feeding currents in which water is drawn towards one side of the branch, filtered of particles, and exits at the other side. Such 'unilaminar' branches usually have a flow direction from obverse to reverse, although some species create a reverse to obverse flow direction (McKinney, 1991).

9. Endozonal budding (0) absent; (1) present

All cyclostomes exhibit at least some zoecial budding from exterior walls, including the basal lamina and, in certain taxa, the walls forming reverse sides of erect branches. However, zoecial budding can also occur in the endozone independently of exterior walls. Such endozonal budding sometimes has its locus on the two opposite sides of a distinct budding lamina but more often it is unlocalized, with new buds appearing at triple junctions between existing interior walls (see McKinney, 1975). All of the taxa with endozonal budding included in this analysis are of the latter type.

10. Intersection angle of zooids with colony surface (0) low angle; (1) high angle

Cyclostome zoecia are typically shaped like parabolically curved tubes. In some taxa, the parabola is almost complete such that the axis of the zooid changes orientation by approximately 90° along its length and the zooid consequently has a high angle of intersection (*c.* 70–90°) with the colony surface. In other taxa, the parabola is partial and the zooid intersects the colony surface at a low angle (< 60°). This distinction is reflected in the two names Rectangulata and Parallelata, coined by Waters (1887) in an early classification of cyclostomes. It must be stressed that the coding employed for this character is essentially qualitative because precise intersection angles are seldom available from the literature.

11. Peristomial budding (0) absent; (1) present

An unusual type of budding has been recorded by Harmelin (1974, 1979) in which a new bud arises at or near the top of the peristome of an autozooid. Although originally identified only in tubuliporines, budding from the erect ancestrula in articulate cyclostomes is also peristomial (Silén, 1977a).

12. *Maculae* (0) absent; (1) present

Maculae are regularly-spaced patches (subcolonies) on the colony surface recognizable by having lower densities of autozooidal apertures, concentrations of immature zooids or non-feeding polymorphs, or barren expanses of skeleton. Sometimes the apertures of feeding zooids are arranged in a radial pattern around the maculum which functions as a chimney of excurrent water flow. Extensive sheet-like colonies in all bryozoan groups may possess maculae because venting of exhalent currents at the colony perimeter becomes impossible as diameter increases (McKinney, 1986, 1990).

13. *'Extrazoooidal' calcification* (0) absent; (1) present

Calcification which is not readily attributed to particular zooids is termed extrazoooidal (Boardman, 1983: 103). In some free-walled cyclostomes, thick extrazoooidal calcification develops on branch surfaces so that older branches, particularly those close to the colony base, become noticeably thicker than younger branches.

14. *Autozooid skeletal organization* (0) fixed-walled; (1) free-walled

Probably the most striking contrast in autozooidal skeletons among cyclostomes is between species in which the autozooids develop calcified frontal exterior walls and those in which such walls are lacking. Species with calcified frontal walls were termed single-walled by Borg (1926) but are usually now referred to as 'fixed-walled'; species without calcified frontal walls, termed double-walled by Borg, are now called 'free-walled'. In free-walled cyclostomes, epithelial and pseudocoelomic continuity between adjacent zooids is maintained over the distal ends of the interior walls. Fixed-walled skeletal organization entails continued growth of the interior walls until they contact the terminal membrane (outer body wall), allowing fusion between the epithelium of the interior wall and that of the terminal membrane. A calcified layer, anchored to the ends of the calcified interior wall, can then be secreted by the epithelium directly beneath the cuticle of the outer body wall. The resultant calcified exterior frontal wall invariably contains pseudopores.

15. *Autozooidal aperture diameter* (0) mean value less than 110 μm ; (1) mean value 110–250 μm ; (2) mean value over 250 μm

The coded taxa show a fairly continuous range of autozooidal aperture diameters which are here divided into three somewhat arbitrary categories based on frequency distribution. McKinney & Boardman (1985) have demonstrated a strong correlation between apertural diameter and various quantitative attributes of the lophophore (e.g. number of tentacles) in cyclostomes, enhancing the credence of apertural diameter as a useful character in phylogeny.

16. *Exterior-walled peristomes* (0) absent; (1) present

17. *Peristome length* (0) short; (1) long

Cuticle-covered, exterior-walled peristomes are distal, tubular prolongations of the zooidal skeleton which surround the terminal skeletal aperture. In most cyclostomes they grow from the frontal exterior wall, represent a change from skeletal growth transverse to the major long axis of the zooid to growth parallel to this axis, and have a lower density of pseudopores than frontal walls. In some cyclostomes, however, peristomes develop directly from vertical interior walls, either at their distal edge or further proximally (e.g. the 'immersed peristomes' of *Cinctipora*, see

Boardman *et al.*, 1992). Two peristome characters are recognized here in view of the fairly clear distinction between taxa lacking any semblance of an exterior-walled peristome, taxa with short peristomes (length less than skeletal aperture diameter), and taxa with long peristomes which represent significant extensions of the zooidal living chamber.

18. *Exterior-walled terminal diaphragms* (0) absent; (1) present

During late ontogeny cyclostome zooids may become sealed by exterior-walled terminal diaphragms secreted from within (Silén & Harmelin, 1974; note that Harmer, 1891: 143 records resorption of terminal diaphragms in *Crisia ramosa* after winter dormancy). Most terminal diaphragms are located at about the level of the frontal wall, i.e. at the base of the peristome in taxa which have these structures. Terminal diaphragms are accreted centripetally and generally have radially elongated pseudopores, less evenly-spaced than those of frontal walls and peristomes. Whereas terminal diaphragms are almost ubiquitous in taxa with fixed-walled autozooids, exterior-walled terminal diaphragms can be present or absent in free-walled taxa where old autozooids either remain open or are occluded by interior wall calcification.

19. *Apertural spines* (0) absent; (1) present

Spines growing parallel to the long axis of the zooid are present encircling the apertures of autozooids in some cyclostomes. These apertural spines are constructed of interior wall and occur only in free-walled autozooids without peristomes. Often there is only one apertural spine per aperture and this is commonly located on the proximal side of the aperture, as in some rectangulates where Brood (1972) termed such structures 'pseudolunaria'.

20. *Opercula* (0) absent; (1) present

An analogue of the hinged opercula characteristic of cheilostome bryozoans occurs in the Cretaceous-Palaeocene meliceritid cyclostomes (Taylor, 1993). The meliceritid operculum is always calcified, in contrast to cheilostome opercula which are calcified in only a small minority of species. These exterior walls have a more-or-less straight proximal edge, articulating with a hingeline on the proximal rim of the aperture, and an arched or semicircular distal edge. Pseudopores are either scattered evenly across the surface or, more commonly, form a crescent of slit-like holes parallel to the distal edge of the operculum. Two vertical ridges (sclerites) are developed on the inner side of the operculum.

21. *Gonozooids* (0) absent; (1) non-peristomial; (2) peristomial

Brooding polymorphs (gonozooids) are developed in most cyclostome species (see Schäfer, 1991). They are usually budded among the other zooids of the colony and open on the frontal colony surface along with these zooids. However, peristomial gonozooids are budded high on the peristomes of autozooids, above the frontal colony surface (Harmelin, 1974, 1979), and tend to be smaller than basal gonozooids. The recognition of peristomial gonozooids is a problem in fossils because of the likelihood of breakage and loss of peristomes. At least some of the fossil cyclostomes in which gonozooids have never been discovered may have had peristomial gonozooids.

22. *Gonozooid position on erect branches* (0) frontal side; (1) reverse side

The position of gonozooids can vary in erect cyclostome species with branches that have differentiated frontal and reverse sides. In some genera gonozooids occur on frontal sides of branches; in others they are situated on reverse sides, although

the oeciostome may be bent forwards so that the oeciopore is directed frontally.

23. *Gonozooid skeletal organization* (0) not applicable; (1) fixed-walled; (2) free-walled

Like autozooids, gonozooids may be fixed-walled or free-walled. The roof in fixed-walled gonozooids consists of a calcified exterior wall with a density of pseudopores characteristically greater than that present in autozooidal frontal walls. Free-walled gonozooids are roofed by a calcified interior wall. This tends to have a much rougher, more rugose surface than fixed-walled gonozooids, often with ridges or tubercles, and pores situated at the bottoms of deep pits.

24. *Gonozooid outline shape* (0) equidimensional; (1) longitudinally elongate; (2) transversely elongate

Differences in gonozooid morphology have often been accorded considerable value in cyclostome taxonomy, especially for recognizing families and genera of tubuliporines. While the merits of this suite of characters in taxonomy have been challenged (e.g. Hillmer, 1968; Brood, 1972), there can be no doubting the utility of gonozooids in permitting superficially very similar taxa to be distinguished. Proximally, most gonozooids are indistinguishable from autozooids. Distally, however, gonozooids become dilated and often bulbous. Three basic character states can be recognized for the outline shape of this prominent distal part of the gonozooid according to whether their diameter parallel to growth direction is the same as (equidimensional), longer than (longitudinally elongate) or shorter than (transversely elongate) diameter transverse to growth direction.

25. *Gonozooid roof integrity* (0) unpierced; (1) pierced

The integrity of the roof of gonozooids varies between taxa. In some cyclostomes the roof is entire, but in other taxa isolated autozooids or small groups of autozooids pass through the chamber of the gonozooid so that their apertures are scattered across the surface of the gonozooid and their peristomes support the fragile roof. The pattern of growth and calcification of the roof in pierced gonozooids is often radially outwards from the vertical walls of the autozooids which penetrate and surround the gonozooid, with sutures marking the junctions between different growth fronts (e.g. Weedon & Taylor 1996: fig. 6c).

26. *Ooeciostome location* (0) terminal; (1) lateral; (2) central

In most cyclostomes the oeciostome and oeciopore (the aperture through which the larvae are released) is situated on the medial axis of the gonozooid, at or very close to the distalmost extremity of the frontal wall. This terminal position can be contrasted with two other character states, one in which the oeciopore is located on the lateral edge of the gonozooid, and the other in which it is approximately in the centre of the dilated frontal wall. Some variability in this character occurs within species (Ostrovsky, 1998b).

27. *Ooeciopore diameter* (0) less than 100 μm ; (1) 100–150 μm ; (2) more than 150 μm

Based on published and new measurements of oeciopore diameter, three size classes are distinguished for the genera coded here.

28. *Ooeciostome length* (0) short; (1) long

Ooeciostomes vary greatly in length and shape among cyclostome species (e.g. Harmelin, 1976a), and sometimes within a species (Ostrovsky, 1998b). However, it is difficult to obtain a full data set covering all such variations because of the frequent breakage of the very fragile oeciostome. Therefore, a simple twofold division of

cyclostomes with oeciostomes is employed here, founded on length and similar to the distinction between short and long peristomes (character 17). Long oeciostomes are often strongly or weakly curved, and may taper or flare distally.

29. *Atrial ring* (0) not applicable; (1) absent; (2) present

A structure termed the 'atrial ring' by Levinsen (1912) and 'valve' by Harmer (1891, 1893) is present in the gonozooids of a few cyclostome genera. The atrial ring is a narrow, ring-like partial diaphragm which encircles the distal gonozooidal chamber just proximally of the oeciostome (Taylor & Weedon, 1996). Atrial rings become visible only when gonozooids are fractured open or are sectioned.

30. *Kenozooids interspersed between autozooids* (0) absent; (1) present

Kenozooids are polymorphs known or inferred to lack a functional feeding polymorph and other interior organs (Silén, 1977b). Invariably smaller than autozooids, kenozooids in cyclostomes with fixed-walled autozooids often lack an open aperture and are sealed by calcified exterior wall, enabling straightforward recognition in material without soft parts. Kenozooids develop sporadically in some species (e.g. where a growing colony encounters an obstruction), in others they form semi-regularly as overgrowths which act to strengthen and buttress erect branches (e.g. *Idmidronea*), whereas in certain species they are intercalated regularly between the autozooids, apparently providing a means of spacing autozooidal apertures and tentacle crowns. Character 30 codes for the presence or absence of regularly interspersed kenozooids of this third type. Such kenozooids have received different names according to suborder: cancelli (Cancellata), alveoli (Rectangulata) or simply kenozooids (Cerioporina). Without evidence to the contrary, and following the opinion of Brood (1972: 52), these polymorphs are assumed to be homologous and are all classified as kenozooids.

31. *Spinose kenozooids* (0) absent; (1) present

Long spine-like kenozooids are present in most articulate cyclostomes. These polymorphs, sometimes known as 'processus spiniformes' and related functionally to other spinozooids by Silén (1977b), were regarded by Borg (1926) as modified internodes reduced to a single zooid.

32. *Rhizooids* (0) absent; (1) present

Rhizooids (or rhizooids) grow downwards towards the substratum, where they may bud rows of adnate zooids, from the erect branches of most articulate cyclostomes. They originate from a small hemispherical chamber partitioned off within an autozooid (Silén, 1977a: fig. 3).

33. *Primary nanozooids* (0) absent; (1) present

Dwarf zooids with a tiny skeletal aperture and a polypide with a single tentacle occur scattered among the autozooids in the cyclostome genus *Diplosolen* (Silén, 1977b). These primary nanozooids apparently function to clean particles of mud from the colony surface, the single tentacle performing a sweeping motion (Silén & Harmelin, 1974).

34. *Secondary nanozooids* (0) absent; (1) present

Although primary nanozooids have a restricted taxonomic distribution, secondary nanozooids are found more widely among cyclostomes (Silén & Harmelin, 1974; Moyano, 1982), and comparable structures also occur in some extinct cyclostomes (Voigt, 1982) and other stenolaemates (Bancroft, 1986). Secondary nanozooids

develop during the late ontogeny of autozooids and represent an example of ontogenetic polymorphism. For example, in some species of *Plagioecia*, the terminal diaphragms secreted across the apertures of degenerated autozooids are incomplete and contain a miniature peristome-like tubule near the centre (Silén & Harmelin, 1974). A single tentacle can be protruded through the tiny aperture at the top of this tubule.

35. *Eleozooids* (0) absent; (1) present

In the operculate meliceritid cyclostomes, there are usually polymorphic zooids in which the operculum (and aperture) differs in size and shape from those of autozooids in the same colony. These polymorphs, which are morphologically and probably functionally comparable to cheilostome avicularia, have been termed eleozooids (Taylor, 1986, 1993). Sometimes the operculum (mandible) of the eleozooid is hypertrophied but in a few instances it is reduced in size. It is usually elongated relative to an autozooid operculum and may be spatulate or pointed.

36. *Ancestrula tube* (0) adnate; (1) erect

The distal tube of the ancestrula can emerge either from the side of the protoecium and grow adnate to the substratum, or from the top of the protoecium and grow erect and perpendicular to the substrate (Nielsen, 1970). Intermediate, semi-erect orientations are uncommon (e.g. Taylor & Sequeiros, 1982) and do not occur in any of the taxa considered here. As noted by Borg (1926) and Silén (1977a), erect ancestrular tubes are characteristic of articulates and hornerid cancellates.

37. *Protoecium diameter* (0) less than 350 μm ; (1) more than 350 μm

A few cyclostomes (including *Cinctipora* and *Hornera*) have protoecia with particularly large diameters. Protoecia over 350 μm in diameter are here recognized as a separate character state. Given that the protoecium is formed more-or-less directly from the newly settled and metamorphosed larva (Nielsen, 1970), a strong correlation between protoecial diameter and larval size is expected, although this relationship has yet to be demonstrated empirically.

38. *Mural spines and pustules* (0) absent; (1) present

39. *Long mural spines* (0) absent; (1) present

40. *Planar spherulitic fabric in frontal walls* (0) absent; (1) present

41. *Transverse fibrous fabric* (0) absent; (1) present

42. *Granular fabric* (0) absent; (1) present

43. *Semi-nacre/pseudofoliated fabric* (0) absent; (1) present

44. *Spiked crystallites* (0) absent; (1) present

45. *Distally foliated fabric* (0) absent; (1) present

46. *Proximally foliated fabric* (0) absent; (1) present

Tree rooting

Among Palaeozoic cyclostomes, Crownoporidae (=Kukersellidae) is inferred to be most closely-related to the crown-group cyclostomes of the post-Palaeozoic

(Taylor & Wilson, 1996; Taylor, in press). There are three crownporid genera: *Kukersella* (= *Crownopora*), *Voightia* and *Cuffeyella*. Of these, *Cuffeyella* from the Ordovician has the most generalized morphology and most closely resembles the earliest post-Palaeozoic cyclostomes (stomatoporids and multisparisids) which appear in the Upper Triassic (Bizzarini & Braga, 1981; Taylor & Michalik, 1991; Taylor, 1993). Therefore, *Cuffeyella* was chosen as the principal outgroup taxon to root the trees generated by PAUP 3.1 (Swofford, 1993). A full morphological description of *Cuffeyella* was given by Taylor & Wilson (1996).

An alternative rooting on a hypothetical trepostome was undertaken to evaluate the effects on tree topology and character transitions of rooting on this extinct stenolaemate order which has been previously suggested as ancestral to at least some post-Palaeozoic cyclostomes (Boardman, 1984, 1998; Viskova, 1992).

Results

Analysis of the data matrix (Appendix 2) using a heuristic search procedure (with 10 random addition sequences) and omitting the taxon trepostome and the autapomorphic character primary nanozooids, gave a single most parsimonious tree (Fig. 14) of length 142 steps. The consistency index (CI) is 0.430, retention index (RI) 0.663, and rescaled consistency index (RC) 0.285. To ascertain the existence of structure in the data, one million trees were sampled randomly and found to have a mean length of 263.54 (SD=8.5, $g1 = -0.44$, $g2 = 0.26$). The random trees considerably exceeded the length of the most parsimonious trees, thereby demonstrating structure.

Relative degrees of homoplasy can be compared in colony vs zooid vs ultrastructural characters. The approach used to do so is similar to that adopted by Smith, Littlewood & Wray (1996) when comparing larval vs adult vs molecular characters in echinoids. The values of three metrics (CI, RI, RC) describing levels of character homoplasy for the three character types are summarized in Figure 15. Using both CI and RC, ultrastructural characters are found to be the most homoplastic, followed by zooidal characters and finally colonial characters. However, zooidal characters are the most homoplastic for the RI metric, followed by ultrastructural and then colonial characters.

Reweighting using RC yields 15 equally parsimonious trees, a strict consensus of which is broadly similar to the original tree except that the *Diplosolen* + *Plagioecia* clade is located further crownwards.

Rooting the tree on a trepostome outgroup gave 2 equally parsimonious trees, each of length 146 steps (no significance should be accorded to the greater length of these trees compared to those rooted on *Cuffeyella* because they include one extra taxon). The tree (Fig. 16) retains most of the clades seen in the trees rooted on *Cuffeyella*.

Comments on some character state transitions

A few of the more important character state transitions implied by the cladogram are discussed here:

1. *Skeletal organization* (characters 14 and 23). By rooting the cladogram on the

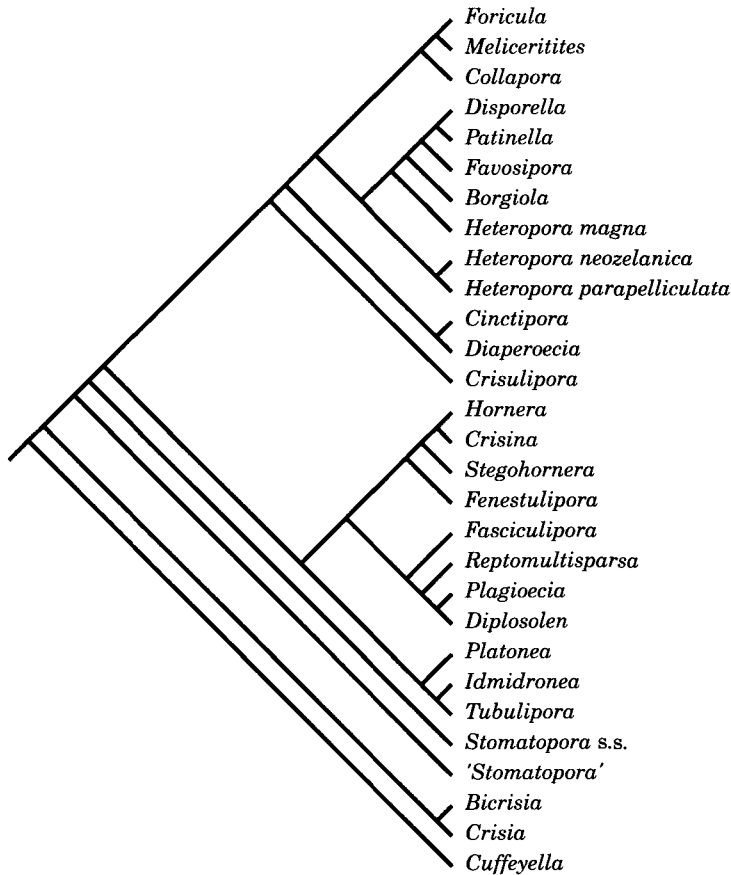


Figure 14. Single most parsimonious tree for 28 post-Palaeozoic cyclostome taxa rooted on the Palaeozoic cyclostome *Cuffeyella*. Tree length is 142 steps.

paleotubuliporine *Cuffeyella*, the primitive condition for skeletal organization is set at fixed-walled. There are four transitions from fixed- to free-walled autozooids and no reversals (Fig. 17). Theoretically, such transitions can be accomplished through ontogenetic paedomorphosis, with exterior frontal walls being omitted from the late ontogeny of the skeleton in zooids of descendant species (Taylor, in press). In two of the four clades with free-walled autozooids, gonozooids have subsequently undergone a fixed- to free-walled transition.

Using a trepostome outgroup (Fig. 16) changes the primitive state of this character from fixed- to free-walled because all trepostomes are free-walled. This produces one transition from free- to fixed-walled, followed by three reversals back to free-walled autozooids. Free- to fixed-walled transitions may be explained conceptually by astogenetic paedomorphosis in which exterior frontal walls are retained in post-ancestral zooids of descendant species (Taylor, in press). In addition, gonozooid skeletal organization switches from fixed- to free-walled in two clades already with free-walled autozooids.

2. *Articulation* (character 5). The favoured tree interprets articulation as a character which has evolved twice in cyclostomes, once in the *Crisia* + *Bicrisia* clade and a second

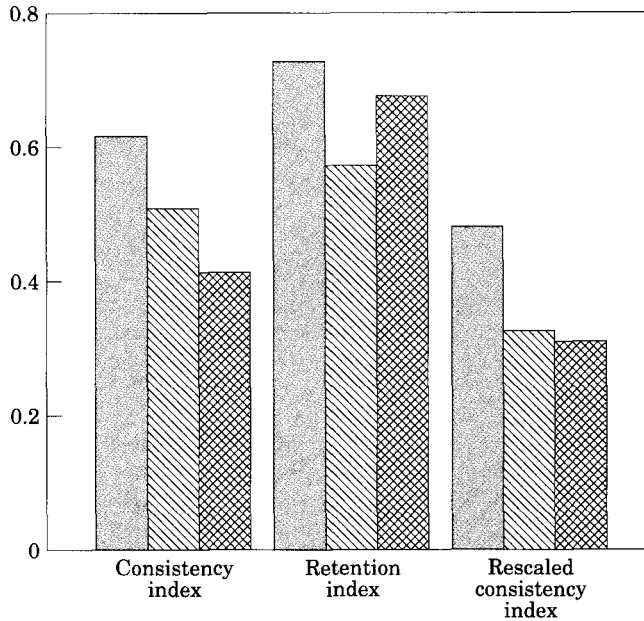
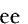




Figure 15. Histogram comparing three measures of homoplasy in colonial ; zooidal  and ultrastructural  characters from the single most parsimonious tree (Fig. 14).

time in *Crisulipora*. The relationship of *Crisulipora* to other articulated cyclostomes has long been a matter of debate, with some authors (e.g. Borg, 1926; Osburn, 1953; Soule, Soule & Chaney, 1995) regarding the genus as belonging to the Suborder Articulata, but others (e.g. Robertson, 1910; Canu & Bassler, 1920) placing it in the Tubuliporina. Evidence from skeletal ultrastructure, together with details in the morphology of the skeletal articulations, recently led Weedon & Taylor (1998) to favour the latter. This is further supported by the new phylogenetic analysis. The position of *Crisulipora* within the Tubuliporina has yet to be determined but it may be significant that the characteristic sieve-like closure plates in the pseudopores (Weedon & Taylor, 1998: fig. 6A–C) closely resemble structures illustrated in the tubuliporine genus *Tetrastomatopora* by Moyano (1991: pl. 2, fig. 5).

3. *Distribution of autozooidal apertures on erect branches* (character 8). An unexpected finding of the analysis is that all of the genera with autozooidal apertures opening circumferentially around erect branches group as a single clade derived from the primitive condition of having apertures restricted to one side of the branch. A common assumption for erect cyclostomes (and other stenolaemates) has been that taxa with apertures only on one side of erect branches represent an advanced state (e.g. Taylor, 1987). In a broader context, McKinney (1986) has demonstrated a repeated trend through geological time towards a higher proportion of unilaminar species in bryozoan faunas, a macroevolutionary trend which is explicable in terms of the greater hydrodynamic efficiency obtained from having feeding zooids opening only on one side of erect branches. Inclusion of additional taxa in future phylogenetic analyses can be anticipated therefore to reveal a more complex pattern of change in this functionally important character.

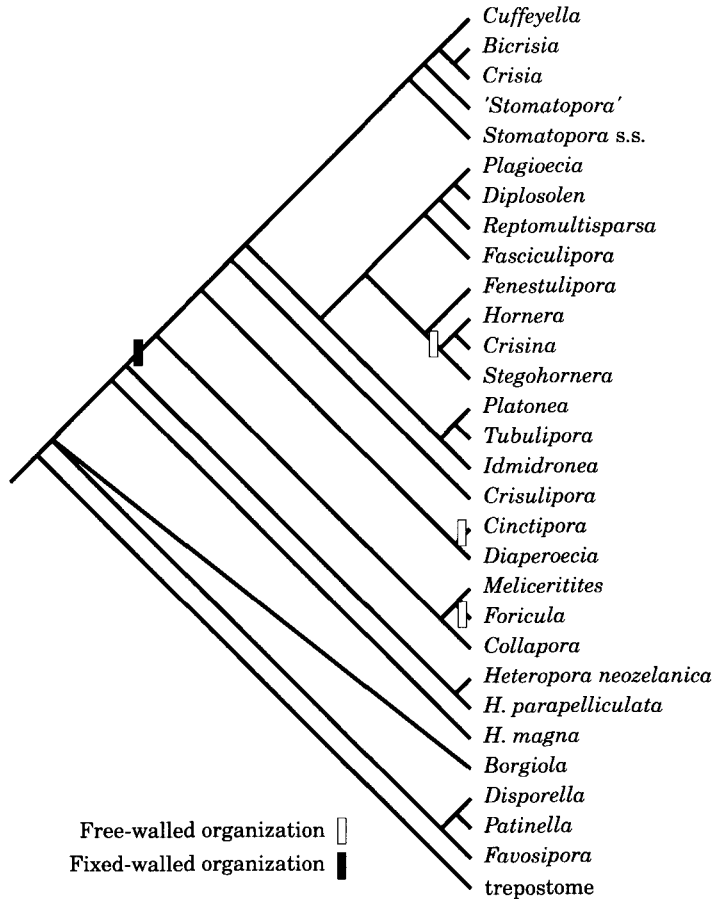


Figure 16. Semi-strict consensus of two trees for 28 post-Palaeozoic cyclostomes and the Palaeozoic cyclostome *Cuffeyella*, rooted on a hypothetical trepostome. Tree length is 146 steps. Transitions between skeletal organizations (free- and fixed-walled) are marked.

4. *Gonozooid roof integrity* (character 25). Morphoserries-based evolutionary schemes typically show a progression from simple gonozooids with unpierced roofs to complex gonozooids with roofs penetrated by autozooidal peristomes (Harmelin, 1976b; Schäfer, 1991). Although the favoured cladogram identifies two such changes (at nodes defining the *Diplosolen* + *Plagioecia* clades, and the clade encompassing *Crisulipora* to *Borgiola*), it also shows an apparent reversal from a pierced to an unpierced roof in the *Collapora* + *Meliceritites* + *Foricula* clade. Given the lack of evidence for any appropriate ancestors with pierced roofs in the Jurassic fossil record, this latter transition must be treated with some scepticism.

5. *Principal ultrastructural fabrics* (characters 41, 42, 45 and 46). Ultrastructural fabrics are unknown in the out-group paleotubuliporine *Cuffeyella*, but the favoured cladogram predicts a skeleton of semi-nacre/pseudofoliated fabric. This primitive, widely-distributed fabric is interpreted to have been lost twice, once in *Fasciculipora* and a second time in the *Heteropora magna* + *Favosipora* + *Patinella* + *Disporella* + *Borgiola* clade. Distally foliated fabric is inferred to have evolved twice and been secondarily

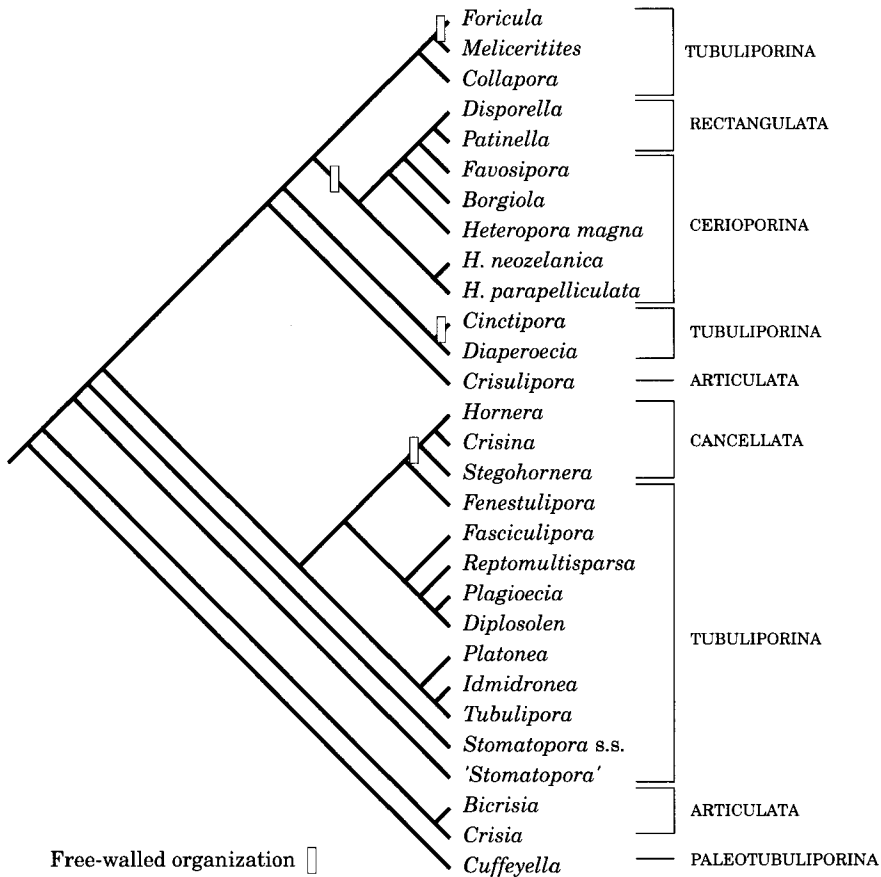


Figure 17. Traditional suborders superimposed on single most parsimonious tree for 28 post-Palaeozoic cyclostome taxa rooted on the Palaeozoic cyclostome *Cuffeyella*. Also shown are transitions between skeletal organizations (free- and fixed-walled).

lost once, and proximally foliated fabric to have evolved once (in the *Fenestulipora* + *Stegohornera* + *Crisina* + *Hornera* clade). The distribution of transverse fibres is more complex, with origin of this fabric close to the base of the tree (between Recent *'Stomatopora'* and Jurassic *Stomatopora* s.s.) and its subsequent loss on three separate occasions (in *Platonea*, and in the *Diplosolen*-*Hornera* clade and the *Heteropora magna*-*Borgiola* clade).

Suborders and their inter-relationships

Most modern classifications distinguish five suborders of extant cyclostomes: Tubuliporina (=Acamptostega), Articulata (=Camptostega), Cerioporina (=Heteroporina), Rectangulata (=Calyptrostega) and Cancellata (=Pachystega). Tubuliporines with zoecia gathered together into fascicles are sometimes separated as a sixth suborder, Fasciculina (e.g. Ryland, 1982). Three additional extinct suborders

are usually recognized: Hederelloidea, Paleotubuliporina and Salpingina (or Meliceritida). The Hederelloidea is not considered further here because of doubts about its bryozoan identity, and the Paleotubuliporina is excluded from discussion as the sole genus included in the analysis was used to root the tree. A preliminary assessment of the extant suborders and their main features has been made by Taylor (in press).

Albeit based on a limited sample of genera, the favoured cladogram rooted on *Cuffeyella* (Fig. 14) permits the following assessments to be made of each extant cyclostome suborder with respect to monophyly, paraphyly and polyphyly:

(1) Articulata are diphyletic, with *Crisulipora* (Crisuliporidae) not closely related to the two genera of Crisiidae (*Crisia* and *Bicrisia*).

(2) Tubuliporina are paraphyletic, having Cerioporina, Rectangulata, Cancellata, and *Crisulipora* nested within the suborder.

(3) Cerioporina are paraphyletic, having Rectangulata nested within the suborder.

(4) Rectangulata are monophyletic.

(5) Cancellata are monophyletic.

The monophyletic status of the extinct Salpingina (Meliceritida), previously regarded as nesting within Tubuliporina (Taylor, 1994; Taylor & Weedon, 1996), is also supported by the present analysis in as much as the two genera (*Meliceritites* and *Foricula*) included are shown to be sister taxa.

These findings are in broad agreement with preliminary phylogenetic interpretations based mainly on studies of skeletal ultrastructure (Weedon & Taylor, 1996, 1997, 1998). The main difference is that the cladogram does not support the inference (Weedon & Taylor, 1996) that Cerioporina are diphyletic, comprising separate clades with transverse fibrous and distally foliated skeletons (i.e. respectively interior fabric suite 1 and 2 see Fig. 12A, B).

Subordinal inter-relationships implied by the cladogram reveal some expected and some unexpected groupings. Using the very limited number (five) of informative characters given by Borg (1944) in his diagnoses of cyclostome suborders, Taylor (in press) found two equally parsimonious trees with a PAUP analysis rooted on tubuliporines. Both trees contained a Cerioporina + Rectangulata clade, and an Articulata + Cancellata clade was present in one. The new cladogram (Fig. 17) corroborates the close relationship between rectangulates and cerioporines, but does not recognize an Articulata + Cancellata clade.

Comparisons with earlier, non-cladistic phylogenies

Very few publications have considered cyclostome phylogeny at subordinal or lower taxonomic levels, and none has used cladistic methods. Figure 18 shows three published evolutionary trees depicting the inter-relationships of cyclostome suborders, together with a tree based on the cladogram found in the current study.

The Brood (1972) and Schäfer (1991) trees are similar in depicting the Tubuliporina as a suborder from which all of the other suborders evolved, either directly or indirectly. Therefore, the Tubuliporina are strongly paraphyletic in both of these schemes. Brood implicitly interpreted all other suborders as monophyletic. However, the Cerioporina are also paraphyletic in Schäfer's tree having given rise to Cancellata and Rectangulata (a suborder subsumed within the cerioporines by Brood). A very different interpretation of cyclostome relationships was published by Viskova (1992) who viewed the Cyclostomata as diphyletic. One of Viskova's two clades of

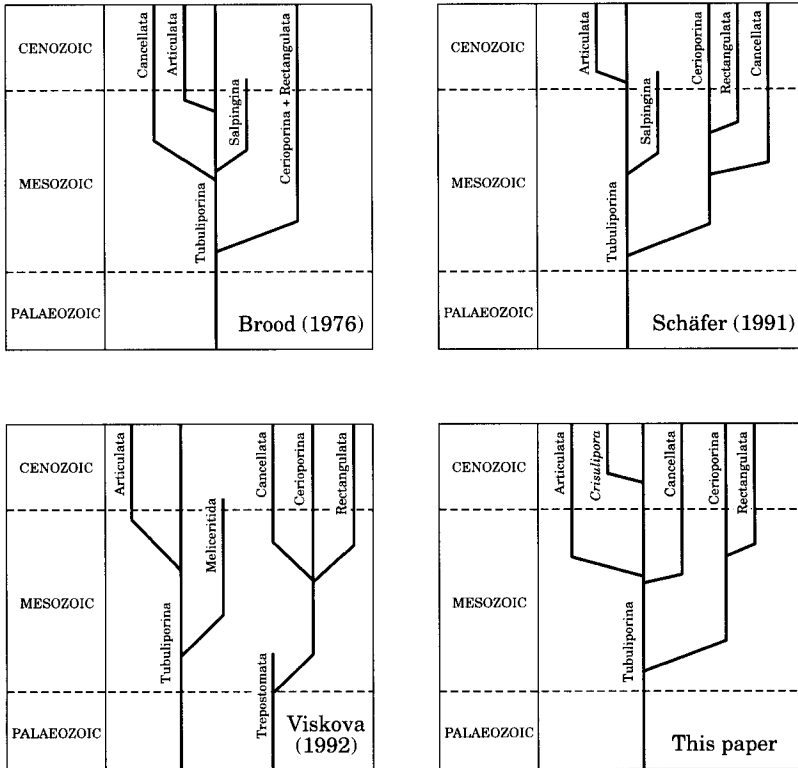


Figure 18. Three published phylogenetic trees (redrawn) of cyclostome suborder relationships and a new, simplified tree based on results from the current study. Ranges for the new tree are approximate and are derived from data in Taylor (1993); jointed colony-form defining the suborder Articulata is first seen in the Lower Cretaceous but the cladogram infers the earlier presence of stem group, unjointed articulates which would be indistinguishable from ‘tubuliporines’.

‘cyclostomes’ comprises the implicitly paraphyletic Tubuliporina and its two monophyletic derivatives, Meliceritida and Articulata. The other clade originates from the Palaeozoic-Triassic trepostomes and comprises the implicitly paraphyletic Cerioporina from which evolved the monophyletic Cancellata and Rectangulata.

Phylogenetic relationships found in the present study are most similar to those inferred by Schäfer (1991), especially in the interpretation of tubuliporines as highly paraphyletic and of rectangulates as nesting within the paraphyletic cerioporines. A principal difference is that Schäfer’s tree implies a cerioporine sister-group for the cancellates whereas the current analysis proposes a tubuliporine sister-group.

DISCUSSION

Recent research, reviewed and expanded upon here, on the ultrastructure of the cyclostome skeleton has advanced our understanding of the microarchitecture of the skeleton and how it varies between taxa. In all known species skeletal walls have a dominantly lamellar structure, with layers of calcite crystallites in the plane of the

wall surface or gently imbricated and subparallel to this surface. Through the growth of existing crystallites and the formation of new crystallites, walls lengthen distally and become thicker. Individual walls are usually constructed from a combination of two or more fabric types, deposited successively as the wall develops. Six fundamental fabrics can be recognized. As seen on wall growing surfaces, these fabrics differ in the morphology of the calcite crystallites, their prevailing growth directions and crystallographic orientations. Fabric suites are defined by combinations of specific fabrics. It is possible to distinguish five fabric suites in interior walls (i.e. walls partitioning body cavities) and four in exterior walls (i.e. walls at the boundary between the bryozoan and the external environment). Although the diversity of morphological patterns of skeletal ultrastructures is now much more fully recorded in cyclostomes than it was a decade ago, much remains to be learnt about the chemistry and mineralogy of the skeleton, its organic inter- and intracrystallite components, and the cellular processes controlling biomineralization. For example, do the different fabrics correlate with differences in organic or inorganic components, and how are switches from one fabric to another achieved during wall growth? The relative mechanical properties of different fabrics are as yet totally unknown.

Knowledge of cyclostome soft-part anatomy is so poor that it is pragmatically impossible to gather data on a sufficient number of taxa for use in phylogenetic analysis—much more histological work of the kind described in Boardman (1998) needs to be done. Consequently, we have reconstructed cyclostome phylogeny based entirely on characters of the skeleton, including ultrastructure as well as characters which are manifested in the skeleton but are of more general relevance (e.g. colony shape). An inherent advantage of this approach is that fossil taxa can be (1) coded without an excessively large number of question marks in the data matrix, and (2) used as out groups for rooting the trees resulting from PAUP analysis.

The preferred tree, rooted on the Ordovician cyclostome *Cuffeyella*, is the first computer-generated phylogeny of cyclostome genera. While some of the suprageneric groupings used in traditional classifications of cyclostomes are found to be monophyletic (e.g. suborders Cancellata and Rectangulata), others appear to be polyphyletic (Articulata) or paraphyletic, 'grade groups' (Tubuliporina, Cerioporina). In common with some previous findings, the cladogram shows Rectangulata nesting within Cerioporina. Contrary to expectations, however, Cancellata nest within Tubuliporina rather than Cerioporina or Rectangulata. The cladogram interprets calcified frontal walls in post-ancestrular zooids to have been lost independently four times, each loss corresponding to a transition from fixed- to free-walled skeletal organization. There is no evidence for acquisition of calcified frontal walls *de novo* in any of the genera considered, i.e. no transitions from free- to fixed-walled organization. This finding has broader implications. Firstly, it questions the likelihood of polyphyletic hypotheses for the origin of post-Palaeozoic cyclostomes which demand convergent acquisition of calcified exterior walls in one or more clades of free-walled Palaeozoic stenoelamates. Secondly, it provides a pointer to the origin of the enigmatic free-walled genus *Cinctipora*. The cladogram interprets *Cinctipora* as nesting within a clade of fixed-walled cyclostomes, thus supporting phylogenetic model 2 of Boardman *et al.* (1992: fig. 90) as opposed to model 1 (*ibid.*, fig. 87; see also Boardman, 1998: fig. 111). Of the genera included in the current analysis, *Diaperocia* was found to be the most-closely related to *Cinctipora*, regardless of rooting (compare Figs 14 and 16). The annular to spiral budding pattern, and corresponding arrangement of zooids on the branch surface, seen in *Diaperocia*, which like *Cinctipora*

is an Australasian Cenozoic genus, closely resembles the pattern seen in *Cinctipora* and other cinctiporids but contrasts with the alternating pattern occurring in *Filicea*, the free-walled European Cretaceous genus at the base of the tree in phylogenetic model 1. Cinctiporids are unusual among post-Palaeozoic cyclostomes in apparently lacking polymorphic gonozooids. The cladogram implies that this lack of gonozooids is due to secondary loss. It may be significant that cinctiporids have very large autozooids, possibly large enough to brood larvae without the need of voluminous polymorphs.

Silén's theory (1977a; see also Ostrovsky, 1998a) of a close relationship between stomatopod tubuliporines and crisiid articulates receives some support from the current cladistic analysis. The two groups are positioned close together at the base of the cladogram. However, the stomatopods are located anomalously crownward of the crisiids in view of the considerably earlier appearance in the fossil record (Taylor, 1993) of stomatopods (Upper Triassic) than crisiids (Lower Cretaceous). A possible explanation for this anomaly is that some of the gracile erect 'tubuliporine' cyclostomes (see Walter, 1970), abundant in the Mesozoic but seldom studied, are non-articulated, stem-group crisiids, precursors to the first recognizably articulated taxa. For example, Canu & Bassler (1927) recognized a non-articulated, supposed crisiid genus (*Crisiona*) represented by two species in the Cretaceous plus three younger species.

A more surprising result of the phylogenetic analysis concerns the relative values for colonial, zooidal and ultrastructural characters of various metrics (CI, RI, RC) of homoplasy (Fig. 15). It is generally assumed in cyclostome (and other bryozoans) that colony-level characters are very plastic and subject to high degrees of convergence, zooidal characters less so, and ultrastructural characters least plastic and carrying the strongest phylogenetic signal. There can be little doubting that homeomorphy in colony-form has been a dominant theme of bryozoan evolution (e.g. Taylor & McKinney, 1996), whereas homeomorphy has seldom been shown in zooidal characters (cf. Taylor & Badve, 1995) and has yet to be fully demonstrated in ultrastructural characters (although interphyletic convergences in ultrastructural fabrics have long been recognized). Therefore, the finding that colonial characters have the highest values for all three metrics, indicating the least homoplasy, and ultrastructural characters the lowest values for two of the three metrics (CI and RC), indicating the most homoplasy, is very unexpected. Taken at face value the result suggests that more emphasis should be placed on colonial characters in cyclostome phylogeny (and classification). However, it may be an artefact correlating with the diminishing relative importance accorded to colonial, zooidal and ultrastructural characters in delineating traditional cyclostome genera. The use of correlated colony-level characters for generic definition contrasts with the total neglect of ultrastructural characters for this purpose. This might be biasing the analysis towards finding minimal homoplasy in congruent colonial characters but maximal homoplasy in non-congruent ultrastructural characters. Had cyclostome genera been defined on the basis of ultrastructural characters, the results may have been the opposite.

An important caveat to all of the conclusions about the standings and inter-relationships of the suborders is that inclusion of additional genera in future analyses may have a profound effect. For example, a suborder recognized here as monophyletic can potentially become polyphyletic on addition of further genera which have been previously, though incorrectly, assigned to it in conventional classifications. The

preferred cladogram (Fig. 14) is the phylogeny which best explains the distribution of a small sample of phenotypic characters in a limited number of taxa. With such a small sample of cyclostome genera (<10%) and a tiny fraction of the total phenotypic characters which must be expressed, sampling artefacts could be expected to play an overwhelming role in the resulting phylogenetic pattern. It would be extremely premature to use the cladogram as the basis for a major overhaul of cyclostome classification. Nevertheless, the cladogram does point to problem areas in the current classification, as well as providing a more objective benchmark against which to evaluate future cladograms generated using soft part characters and genetic sequence data.

ACKNOWLEDGEMENTS

Marcello Ruta, Andrew Smith, Peter Forey and Paul Kenrick are thanked for assistance with PAUP analyses and general discussions about phylogeny. We are grateful for grants from the NERC, during which this work was commenced, and the JSPS and Leverhulme Foundation, during which it was completed. J.-G. Harmelin kindly provided material for ultrastructural study. Nodosaka san is thanked for SEM assistance in Japan, and Chris Jones for SEM at the NHM.

REFERENCES

- Bancroft AJ. 1986.** Secondary nanozoecia in some Upper Palaeozoic fenestrate Bryozoa. *Palaeontology* **29**: 207–212.
- Bigey F. 1977.** Application du microscope électronique a balayage (M.E.B.) a la paléontologie et a la sédimentologie. *Travaux du Laboratoire de Micropaléontologie Université Pierre-et Marie Curie* **7**: 189–215.
- Bigey F. 1982.** Bryozoaires tubulaires paléozoïques et actuels: morphologie et microstructure squelettiques (Trepostomida Cyclostomida). *Bulletin de la Société Zoologique de France* **107**: 297–306.
- Bizzarini F, Braga G. 1981.** Prima segnalazione de genere *Stomatopora* (Bryozoa Cyclostomata) nel Trias Superiore delle Dolomiti Orientali (Italia). *Lavori Società Veneziana di Scienze Naturali* **6**: 135–144.
- Boardman RS. 1983.** General features of the Class Stenolaemata. In: Boardman RS, Cheetham AH, Blake DB, Utgaard J, Karklins OL, Cook PL, Sandberg PA, Lutaud G, Wood TS. Bryozoa (revised). Volume 1. *Treatise on invertebrate paleontology. Part G*, Boulder and Lawrence: Geological Society of America and University of Kansas, 49–137.
- Boardman RS. 1984.** Origin of the post-Triassic Stenolaemata (Bryozoa): a taxonomic oversight. *Journal of Paleontology* **58**: 19–39.
- Boardman RS. 1998.** Reflections on the morphology, anatomy, evolution, and classification of the Class Stenolaemata (Bryozoa). *Smithsonian Contributions to Paleobiology* **86**: 1–60.
- Boardman RS, Cheetham AH, Cook PL. 1983.** Introduction to the Bryozoa. In: Boardman RS, Cheetham AH, Blake DB, Utgaard J, Karklins OL, Cook PL, Sandberg PA, Lutaud G, Wood TS. Bryozoa (revised). Volume 1. *Treatise on invertebrate paleontology. Part G*, Boulder and Lawrence: Geological Society of America and University of Kansas, 3–48.
- Boardman RS, McKinney FK, Taylor PD. 1992.** Morphology, anatomy, and taxonomy of the Cinctiporidae, new family (Bryozoa: Stenolaemata). *Smithsonian Contributions in Paleobiology* **70**: 1–81.
- Borg F. 1926.** Studies on Recent cyclostomatous Bryozoa. *Zoologiska Bidrag från Uppsala* **10**: 181–507.
- Borg F. 1933.** A revision of the Recent Heteroporidae (Bryozoa). *Zoologiska Bidrag från Uppsala* **14**: 253–394.
- Borg F. 1941.** On the structure and relationships of *Crisina* (Bryozoa Stenolaemata). *Arkiv för Zoologi* **33A** (11): 1–44.
- Borg F. 1944.** The stenolaematous Bryozoa. In: Bock S, ed. *Further Zoological Results of the Swedish Antarctic Expedition 1901–1903*. Stockholm: Norstedt and Söner, 1–276.

- Brood K.** 1972. Cyclostomatous Bryozoa from the Upper Cretaceous and Danian in Scandinavia. *Stockholm Contributions in Geology* **26**: 1–464.
- Brood K.** 1976. Wall structure and evolution in cyclostomate Bryozoa. *Lethaia* **9**: 377–389.
- Brunton CHC.** 1972. The shell structure of chonatacean brachiopods and their ancestors. *Bulletin of the British Museum (Natural History), Geology Series* **21**: 1–26.
- Bryan WH, Hill D.** 1941. Spherulitic crystallization as a mechanism of skeletal growth in the hexacorals. *Proceedings of the Royal Society of Queensland* **52**: 78–91.
- Busk G.** 1852. An account of the Polyzoa, and sertularian Zoophytes, collected in the Voyage of the Rattlesnake, on the Coasts of Australia and the Loisiade Archipelago, &c. In: MacGillivray J, ed. *Narrative of the Voyage of the H.M.S. Rattlesnake, . . . during the years 1846–1850, Volume 1*. London: Boone, 343–402.
- Canu F, Bassler RS.** 1920. North American Early Tertiary Bryozoa. *Bulletin of the United States National Museum* **106**: 1–876.
- Canu F, Bassler RS.** 1927. Bryozoaires des Iles Hawaï. *Bulletin de la Société des Sciences de Seine- $\&$ -Oise* **7**: 1–67.
- Carter JG, Bandel K, de Buffr enil V, Carlson SJ, Castanet J, Crenshaw MA, Dallingwater JE, Francillon-Vieillot H, G eraudie J, Meunier FJ, Mutvei, H, de Ricql es A, Sire JY, Smith AB, Wendt J, Williams A, Zylberberg L.** 1990. Glossary of skeletal biomineralization. In: Carter JG, ed. *Skeletal biomineralization: patterns, processes and evolutionary trends. Volume 1*. New York: Van Nostrand Reinhold, 609–627.
- Carter JG, Clark GR II.** 1985. Classification and phylogenetic significance of molluscan shell microstructure. In: Broadhead TW, ed. *Mollusks, notes for a short course*. University of Tennessee, Department of Geological Sciences, Studies in Geology, 50–71.
- Dick MH, Williams LP, Coggeshall-Burr M.** In press. Use of 16S mitochondrial ribosomal DNA sequences to investigate sister-group relationships among gymnolaemate bryozoans. *Proceedings of the 11th Conference of the International Bryozoology Association*, Panama, January 1998.
- Farmer JD.** 1979. Morphology and function of zoecial spines in cyclostome Bryozoa: implications for paleobiology. In: Larwood GP, Abbott MB, eds. *Advances in bryozoology*. London: Academic Press, 219–246.
- Gordon DP.** In press. Towards a phylogeny of the Cheilostomata. *Proceedings of the 11th Conference of the International Bryozoology Association*, Panama, January 1998.
- Gordon DP, Taylor PD.** 1997. The Cretaceous-Miocene genus *Lichenopora* (Bryozoa), with a description of a new species from New Zealand. *Bulletin of The Natural History Museum, London, Geology Series* **53**: 71–78.
- Harmelin J-G.** 1973. Morphological variations and ecology of the Recent cyclostome bryozoan “*Idmonea*” *atlantica* from the Mediterranean. In: Larwood GP, ed. *Living and Fossil Bryozoa*. London: Academic Press, 95–106.
- Harmelin J-G.** 1974. A propos d’une forme stomatoporienne typique, *Stomatopora gingrina* Jullien, 1882 (Bryozoaires, Cyclostomes) et de son gonozoide. *Journal of Natural History* **8**: 1–9.
- Harmelin J-G.** 1976a. Le sous-ordre des Tubuliporina (Bryozoaires Cyclostomes) en M diterran e. *M moires de l’Institut o c nographique, Monaco* **10**: 1–326.
- Harmelin J-G.** 1976b. Evolutionary trends within three Tubuliporina families (Bryozoa, Cyclostomata). *Documents des Laboratoires de G ologie de la Facult  des Sciences de Lyon, Hors S rie* **3**(2): 607–616.
- Harmelin J-G.** 1979. On some stomatoporiform species (Bryozoa Cyclostomata) from the bathyal zone of the northeastern Atlantic Ocean. In: Larwood GP, Abbott MB, eds. *Advances in Bryozoology*. London: Academic Press, 403–422.
- Harmelin J-G, d’Hondt J-L.** 1982. Bryozoaires Cyclostomes bathyaux des compagnes o c nographiques de l’ “Atlantis II”, du “Chain” et du “Knorr” (1967–1972). *Bulletin du Mus um d’Histoire Naturelle, Paris*, (4), **4**: 3–23.
- Harmer SF.** 1891. On the British species of *Crisia*. *Quarterly Journal of Microscopical Science* **32**: 127–181.
- Harmer SF.** 1893. On the occurrence of embryonic fission in cyclostomatous Polyzoa. *Quarterly Journal of Microscopical Science* **34**: 199–241.
- Hayward PJ, Ryland JS.** 1985. Cyclostome bryozoans. *Synopses of the British Fauna (New Series)* **34**: 1–147.
- Hillmer G.** 1968. On the variation of gonozoecia of encrusting “*Berenicea*”-forms (Lower Cretaceous) (Bryozoa). *Atti della Societ  Italiana di Scienze Naturali e del Museo Civico di Storia Naturale di Milano* **108**: 64–70.
- Hinds RW.** 1973. Intrazoecial structures in some tubuliporinid cyclostome Bryozoa. In: Larwood GP, ed. *Living and fossil Bryozoa*. London: Academic Press, 299–306.

- Horowitz AS, Pachut JF. 1996.** Diversity of Cenozoic Bryozoa: A preliminary report. In: Gordon, DP, Smith AM, Grant-Mackie JA, eds. *Bryozoans in space and time*. Wellington: NIWA, 133–137.
- Illies G. 1963.** Über *Stomatopora dichotoma* (LAMX.) und *St. dichotomoides* (d'ORB.) [Bryoz. Cycl.] aus dem Dogger des Oberrheingebietes. *Oberrheinische Geologische Abhandlungen* **12**: 45–80.
- Kluge GA. 1975.** *Bryozoa of the northern seas of the USSR*. New Delhi: Amerind Publishing Co. Ltd.
- Lee DE, Brunton CHC. 1986.** *Neocrania* n. gen., and a revision of Cretaceous–Recent brachiopod genera in the family Craniidae. *Bulletin of the British Museum (Natural History), (Geology Series)* **40**: 141–160.
- Levinsen GMR. 1912.** Studies on the Cyclostomata Operculata. *Det Kgl. Danske Videnskabernes Selskabs Skrifter, Raekke 7, Copenhagen* **10**: 1–52.
- Lidgard S, McKinney FK, Taylor PD. 1993.** Competition, clade replacement and a history of cyclostome and cheilostome bryozoan diversity. *Paleobiology* **19**: 352–371.
- McKinney FK. 1975.** Autozoecial budding patterns in dendroid stenolaemate bryozoans. *Documents des Laboratoires de Géologie de la Faculté des Sciences de Lyon, Hors Série* **3**(1): 65–76.
- McKinney FK. 1986.** Historical record of erect bryozoan growth forms. *Proceedings of the Royal Society of London* **B228**: 133–148.
- McKinney FK. 1990.** Feeding and associated colonial morphology in marine bryozoans. *Reviews in Aquatic Sciences* **2**: 255–280.
- McKinney FK. 1991.** Colonial feeding currents of *Exidmonea atlantica* (Cyclostomata). *Bulletin de la Société des Sciences Naturelles de l'Ouest de la France Mémoire HS* **1**: 263–270.
- McKinney FK, Boardman RS. 1985.** Zooidal biometry of Stenolaemata. In: Nielsen C, Larwood GP, eds. *Bryozoa: Ordovician to Recent*. Fredensborg: Olsen and Olsen, 193–203.
- McKinney FK, Lidgard S, Sepkoski JJ, Taylor PD. 1998.** Decoupled temporal patterns of evolution and ecology in two post-Paleozoic clades. *Science* **281**: 807–809.
- Moyano GHI. 1982.** Genero *Disporella* Gray, 1848: dos nuevas especies para la fauna Chilena (Bryozoa, Cyclostomata, Disporellidae). *Boletín de la Sociedad de Biología Concepción* **53**: 71–77.
- Moyano GHI. 1991.** Bryozoa from deep-sea waters in Chile: Cyclostomata. *Bulletin de la Société des Sciences Naturelles de l'Ouest de la France Mémoire HS* **1**: 281–290.
- Nielsen C. 1970.** On metamorphosis and ancestrula formation in cyclostomatous bryozoans. *Ophelia* **7**: 217–256.
- Nielsen C. 1987.** Structure and function of metazoan ciliary bands and their phylogenetic significance. *Acta Zoologica* **68**: 205–262.
- Nielsen C. 1995.** *Animal Evolution*. Oxford: Oxford University Press
- Nielsen C, Pedersen KJ. 1979.** Cystid structure and protrusion of the polypide in *Crisia* (Bryozoa, Cyclostomata). *Acta Zoologica* **60**: 65–88.
- Nielsen C, Riisgård HU. 1998.** Tentacle structure and filter-feeding in *Crisia eburnea* and other cyclostomatous bryozoans, with a review of upstream-collecting mechanisms. *Marine Ecology Progress Series* **168**: 163–186.
- Osburn RC. 1953.** Bryozoa of the Pacific coast of America. Part 3, Cyclostomata, Ctenostomata, Entoprocta, and addenda. *Allan Hancock Pacific Expeditions* **14**(3): 613–841.
- Ostrovsky A. 1998a.** The genus *Anguisia* as a model of a possible origin of erect growth in some Cyclostomatida (Bryozoa). *Zoological Journal of the Linnean Society* **124**: 355–367.
- Ostrovsky A. 1998b.** Variability of oocciostome shape and position in Antarctic idmidroniform bryozoans (Bryozoa: Cyclostomatida). *Zoologischer Anzeiger* **237**: 97–106.
- Probert PK, Batham EJ, Wilson JB. 1979.** Epibenthic macrofauna off southeastern New Zealand and mid-shelf bryozoan dominance. *New Zealand Journal of Marine and Freshwater Research* **13**: 379–392.
- Riisgård HU, Manriquez P. 1997.** Filter-feeding in fifteen marine ectoprocts (Bryozoa): particle capture and water pumping. *Marine Ecology Progress Series* **154**: 223–239.
- Robertson A. 1910.** The cyclostomatous Bryozoa of the west coast of North America. *University of California Publications in Zoology* **6**: 225–284.
- Ross JRP. 1975.** Organization of calcified tissues in stenolaemate ectoprocts. *Documents des Laboratoires de Géologie de la Faculté des Sciences de Lyon, Hors Série* **3**(1): 179–186.
- Ross JRP. 1976.** Body wall ultrastructure of living cyclostome ectoprocts. *Journal of Paleontology* **50**: 350–353.
- Ross JRP. 1977.** Microarchitecture of body wall of extant cyclostome ectoprocts. *American Zoologist* **17**: 83–105.
- Runnegar B. 1984.** Crystallography of the foliated calcite shell layers of bivalve molluscs. *Alcheringa* **8**: 273–290.

- Ryland JS. 1982.** Bryozoa. In: Parker SP, ed. *Synopsis and classification of living organisms* New York: McGraw-Hill, 743–769.
- Sandberg PA. 1983.** Ultrastructure and skeletal development in cheilostome Bryozoa. In: Boardman RS, Cheetham AH, Blake DB, Utgaard J, Karklins OL, Cook PL, Sandberg PA, Lutaud G, Wood TS. Bryozoa (revised). Volume 1. *Treatise on invertebrate paleontology. Part G*, Boulder and Lawrence: Geological Society of America and University of Kansas, 238–286.
- Schäfer P. 1986.** On the gizzard in the bryozoan genus *Diaperocia* Canu (Order Tubuliporata). *Senckenbergiana Maritima* **17**: 253–277.
- Schäfer P. 1991.** Brutkammern der Stenolaemata (Bryozoa): Konstruktionsmorphologie and phylogenetische Bedeutung. *Courier Forschungsinstitut Senckenberg* **136**: 1–263.
- Silén L. 1977a.** Structure of the adnate colony portions in Crisiidae. *Acta Zoologica* **58**: 227–244.
- Silén L. 1977b.** Polymorphism. In: Woollacott RM, Zimmer RL, eds. *Biology of bryozoans*. New York: Academic Press, 183–231.
- Silén L, Harmelin J-G. 1974.** Observations on living Diastoporidae (Bryozoa Cyclostomata), with special regard to polymorphism. *Acta Zoologica* **55**: 81–96.
- Smith AB, Littlewood DTJ, Wray GA. 1996.** Comparative evolution of larval and adult life-history stages and small subunit ribosomal RNA amongst post-Palaeozoic echinoids. In: Harvey PH, Brown AJL, Maynard Smith J, Nee S, eds. *New uses for new phylogenies*. Oxford: Oxford University Press, 234–253.
- Söderqvist T. 1968.** Observations on extracellular body wall structure in *Crisia eburnea*. *Atti della Società Italiana di Scienze Naturali e del Museo Civico di Storia Naturale di Milano* **108**: 115–118.
- Soule DF, Soule JD, Chaney HW. 1995.** The Bryozoa. In: Blake JA, Chaney HW, Scott PH, Lissner AL, eds. *Taxonomic atlas of the Santa Maria Basin and Western Santa Barbara Channel* **13**: 1–344. Santa Barbara Museum of Natural History, California.
- Suzuki S. 1979.** Mineralization of the regenerated organic membrane shell in *Mytilus edulis* (Pelecypoda). *Journal of the Geological Society of Japan* **85**: 669–678.
- Swofford DL. 1993.** *PAUP: Phylogenetic Analysis Using Parsimony*. Version 3.1. Champaign: Illinois Natural History Survey.
- Tavener-Smith R, Williams A. 1972.** The secretion and structure of the skeleton of living and fossil Bryozoa. *Philosophical Transactions of the Royal Society of London* **B264**: 97–159.
- Taylor PD. 1986.** Polymorphism in meliceritid cyclostomes. In: Nielsen C, Larwood GP, eds. *Bryozoa: Ordovician to Recent*. Fredensborg: Olsen and Olsen.
- Taylor PD. 1987.** Fenestrate colony-form in a new meliceritid bryozoan from the U. Cretaceous of Germany. *Mesozoic Research* **1**: 71–77.
- Taylor PD. 1993.** Bryozoa. In: Benton MJ, ed. *The Fossil Record 2*. London: Chapman & Hall, 465–489.
- Taylor PD. 1994.** Systematics of the meliceritid cyclostome bryozoans; introduction and the genera *Elea*, *Semielea* and *Reptomulteia*. *Bulletin of The Natural History Museum, London, Geology Series* **50**: 1–103.
- Taylor PD. In press.** Cyclostome systematics: phylogeny, suborders and the problem of skeletal organization. *Proceedings of the 11th Conference of the International Bryozoology Association*, Panama, January 1998.
- Taylor PD, Badve R. 1995.** A new cheilostome bryozoan from the Cretaceous of India and Europe: a cyclostome homeomorph. *Palaeontology* **38**: 627–657.
- Taylor PD, Gordon DP. 1997.** *Fenestulipora* gen. nov., an unusual cyclostome bryozoan from New Zealand and Indonesia. *Invertebrate Taxonomy* **11**: 689–703.
- Taylor PD, Jones CG. 1993.** Skeletal ultrastructure in the cyclostome bryozoan *Hornera*. *Acta Zoologica* **74**: 135–143.
- Taylor PD, Larwood GP. 1990.** Major evolutionary radiations in the Bryozoa In: Taylor PD, Larwood GP, eds. *Major evolutionary radiations*. Systematics Association Special Volume No. 42. Oxford: Oxford University Press, 209–233.
- Taylor PD, McKinney FK. 1996.** An *Archimedes*-like cyclostome bryozoan from the Eocene of North Carolina. *Journal of Paleontology* **70**: 218–229.
- Taylor PD, Michalik J. 1991.** Cyclostome bryozoans from the late Triassic (Rhaetian) of the West Carpathians, Czechoslovakia. *Neues Jahrbuch für Geologie und Paläontologie* **182**: 285–302.
- Taylor PD, Schembri PJ, Cook PL. 1989.** Symbiotic associations between hermit crabs and bryozoans from the Otago region, southeastern New Zealand. *Journal of Natural History* **23**: 1059–1085.
- Taylor PD, Sequeiros L. 1982.** Toarcian bryozoans from Belchite in north-east Spain. *Bulletin of the British Museum (Natural History), Geology Series* **37**: 117–129.

- Taylor PD, Weedon MJ. 1996.** Skeletal ultrastructure and affinities of eleid (meliceritid) cyclostomate bryozoans. In: Gordon DP, Smith AM, Grant-Mackie JA, eds. *Bryozoans in space and time*. Wellington: NIWA, 341–350.
- Taylor PD, Weedon MJ, Jones CG. 1995.** Skeletal ultrastructure in some cyclostome bryozoans of the Family Lichenoporidae. *Acta Zoologica* **76**: 205–216.
- Taylor PD, Wilson MA. 1996.** *Cuffeyella*, a new bryozoan genus from the Late Ordovician of North America, and its bearing on the origin of the post-Paleozoic cyclostomes. In: Gordon DP, Smith AM, Grant-Mackie JA, eds. *Bryozoans in space and time*. Wellington: NIWA, 351–360.
- Todd JA. In press.** The central role of ctenostomes in bryozoan phylogeny. *Proceedings of the 11th Conference of the International Bryozoology Association*, Panama, January 1998.
- Travis DF. 1968.** The structure and organization of, and the relationship between, the inorganic crystals and the organic matrix of the prismatic region of *Mytilus edulis*. *Journal of Ultrastructure Research* **23**: 183–215.
- Viskova LA. 1992.** Marine post-Paleozoic-Bryozoa. *Trudy Paleontological Institute* **250**: 1–187. [In Russian]
- Voigt E. 1882.** Heteromorphie und taxonomischer Status von *Lopholepis* v. Hagenow, 1851, *Cavarinella* Marsson, 1887 und ähnlichen Cyclostomata-Genera (Bryozoa, ob. Kreide). *Nachrichten der Akademie der Wissenschaften in Göttingen. II. Mathematisch-Physikalische Klasse* **1981**: 39–91.
- Walter B. 1970.** Les bryozoaires jurassiques en France. *Documents des Laboratoires de Géologie de la Faculté des Sciences de Lyon* **35**[for 1969]: 1–328.
- Wasson K, Newberry AT. 1997.** Modular metazoans: gonochoric, hermaphroditic, or both at once? *Invertebrate Reproduction and Development* **31**: 159–175.
- Waters AW. 1887.** On Tertiary cyclostomatous Bryozoa from New Zealand. *Quarterly Journal of the Geological Society of London* **43**: 337–350.
- Weedon MJ. 1997.** Mural “hoods” in the basal walls of cyclostome bryozoans and their taxonomic distribution. *Species Diversity* **2**: 105–119.
- Weedon MJ. 1998.** Skeletal ultrastructure of the early astogenetic stages of some cyclostome bryozoans. *Acta Zoologica* **79**: 163–174.
- Weedon MJ, Taylor PD. 1995.** Calcitic nacreous ultrastructures in bryozoans: implications for comparative biomineralization of lophophorates and molluscs. *Biological Bulletin* **188**: 281–292.
- Weedon MJ, Taylor PD. 1996.** Skeletal ultrastructures in some cerioporine cyclostome bryozoans. *Acta Zoologica* **77**: 249–265.
- Weedon MJ, Taylor PD. 1997.** Skeletal ultrastructure in some tubuliporine cyclostome bryozoans. *Acta Zoologica* **78**: 107–122.
- Weedon MJ, Taylor PD. 1998.** Skeletal ultrastructures in some articulate cyclostome bryozoans. *Acta Zoologica* **79**: 133–148.
- Williams A. 1966.** Growth and structure of the shell of living articulate brachiopods. *Nature* **211**: 1146–1148.
- Williams A. 1968a.** Evolution of the shell structure of articulate brachiopods. *Special Papers in Palaeontology* **2**: 1–55.
- Williams A. 1968b.** A history of skeletal secretion among articulate brachiopods. *Lethaia* **1**: 268–287.
- Winston JE. 1986.** An annotated checklist of coral-associated bryozoans. *American Museum Novitates* **2859**: 1–39.
- Zabala M, Maluquer P. 1988.** Illustrated keys for the classification of Mediterranean Bryozoa. *Treballs del Museu de Zoologia, Barcelona* **4**: 1–294.

APPENDIX 1

Summary of interior wall fabric suites found in modern and fossil (*) cyclostome species, arranged according to conventional suborder and family classification.

Suborder	Family	Species studied	Fabric suite
Tubuliporina	Annectocymidae	<i>Annectocyma tubulosa</i> (Busk)	1
		<i>Entalophoreocia deflexa</i> (Couch)	3
Cinctiporidae		* <i>Attinopora campbelli</i> Boardman <i>et al.</i>	1
		<i>Attinopora zealandica</i> (Mantell)	1
		<i>Cinctipora elegans</i> Hutton	1
Diaperoeciidae		<i>Diaperoecia purpurascens</i> (Hutton)	1
		<i>Diaperoecia</i> sp. 1 (of Weedon, 1997)	3
		<i>Diaperoeciforma californica</i> (d'Orbigny)	1
Diastoporidae (= Plagioeciidae)		' <i>Cardioecia watersi</i> (O'Donoghue & de Watteville)	3
		' <i>Desmoplagioecia amphorae</i> Harmelin	3
		<i>Diplosolen obelia</i> (Johnston)	3
		* <i>Hyporosopora dilatata</i> (d'Orbigny)	1
		* <i>Hyporosopora</i> aff. <i>parvipora</i> (Canu & Bassler)	
		* <i>Hyporosopora</i> aff. <i>typica</i> Canu & Bassler	1
		* <i>Hyporosopora</i> sp. [Albian]	1
		<i>Plagioecia dorsalis</i> (Waters)	3
		<i>Plagioecia patina</i> (Lamarck)	3
		<i>Plagioecia sarniensis</i> (Norman)	3
<i>Platonea stoechas</i> Harmelin	3		
Eleidae (= Melicerititidae)		*? <i>Semielea</i> sp. (of Taylor & Weedon, 1996)	1
		* <i>Elea triangularis</i> (Michelin)	1
		* <i>Foricula pustulosa</i> (d'Orbigny)	1
		* <i>Meliceritites divergens</i> (d'Orbigny)	1
Fron diporidae		<i>Fron dipora verrucosa</i> (Lamouroux)	1
		<i>Fasciculipora ramosa</i> d'Orbigny	2
		<i>Telopora watersi</i> (Harmer)	1
Mecynoeciidae		<i>Mecynoecia delicatula</i> (Busk)	1
Multisparsidae		* <i>Collapora straminea</i> (Phillips)	1
		* <i>Collapora tetragona</i>	1
Oncosoeciidae		' <i>Stomatopora</i> ' sp.	3
Semiceidae		* <i>Filicea</i> sp. [Santonian]	1
Stomatoporidae		* <i>Stomatopora cunningtoni</i> (Gregory)	1
		* <i>Stomatopora</i> sp. [Oxfordian]	1
Terviidae		<i>Tervia irregularis</i> (Meneghini)	1
Tubuliporidae		<i>Idmidronea atlantica</i> (Forbes in Johnston)	1
		<i>Idmidronea coerulea</i> Harmelin	1
		<i>Idmidronea obtecta</i> Borg	2
		<i>Fenestulipora cassiformis</i> (Harmer)	5
		<i>Tubulipora hemiphragmata</i> Harmelin	1
		<i>Tubulipora liliacea</i> (Pallas)	1
		<i>Tubulipora notomale</i> (Busk)	1
		<i>Tubulipora plumosa</i> Thompson in Harmer	1
		<i>Tubulipora</i> (p. 3 of Weedon, 1998)	2

continued

APPENDIX 1—*continued*

Suborder	Family	Species studied	Fabric suite
Articulata	Crisiidae	<i>Bicrisia</i> cf. <i>edwardsiana</i> d'Orbigny	4
		<i>Crisia fistulosa</i> (Heller)	4
		<i>Crisia oranensis</i> Waters	4
		<i>Crisia sigmoidea</i> Waters	4
		<i>Crisia</i> sp. 1 (of Weedon & Taylor, 1998)	4
		<i>Crisia</i> sp. 2 (of Weedon & Taylor, 1998)	4
		<i>Crisia</i> sp. 3 (of Weedon & Taylor, 1998)	4
		<i>Crisia</i> sp. 4 (of Weedon & Taylor, 1998)	4
		<i>Crisia</i> sp. 5 (of Weedon & Taylor, 1998)	4
		<i>Filicrisia</i> sp. 1 (of Weedon & Taylor, 1998)	4
	<i>Filicrisia</i> sp. 2 (of Weedon & Taylor, 1998)	4	
	Crisulporidae	<i>Crisulpora occidentalis</i> Robertson	1
	Cerioporina	Cerioporidae	* <i>Clausia</i> sp. [Albian]
<i>Heteropora</i> cf. <i>pacifica</i> Borg			2
<i>Heteropora</i> cf. <i>pelliculata</i> Waters			2
<i>Heteropora magna</i> O'Donoghue & O'Donoghue			2
<i>Heteropora neozelanica</i> Busk			1
<i>Heteropora parapelliculata</i> Taylor <i>et al.</i>			1
* <i>Heteropora tennesseensis</i> Canu & Bassler			1
<i>Neofungella claviformis</i> (Waters)			2
* <i>Tetrocycloecia</i> sp. [Albian]			1
Densiporidae			<i>Borgella pustulosa asiaticus</i> Androsova
<i>Borgiella otagoensis</i> Taylor <i>et al.</i>		2	
<i>Densipora corrugata</i> MacGillivray		2	
<i>Favosipora</i> sp. (of Weedon & Taylor 1996)		2	
incertae sedis	<i>Coronopora truncata</i> (Fleming)	2	
Rectangulata	Lichenoporidae	<i>Disporella</i> sp. ('blue <i>Disporella</i> ' of Taylor <i>et al.</i> , 1995)	2
		<i>Disporella gordonii</i> Taylor <i>et al.</i>	2
		<i>Disporella</i> sp. 1 (of Taylor <i>et al.</i> , 1995)	2
		<i>Disporella</i> sp. 2 (of Taylor <i>et al.</i> , 1995)	2
		<i>Disporella</i> sp. 3 (of Taylor <i>et al.</i> , 1995)	2
		<i>Disporella</i> sp. 4 (<i>D</i> sp. 1 of Weedon, 1998)	2
		<i>Disporella</i> sp. 5 (<i>D</i> sp. 2 of Weedon, 1998)	2
		<i>Patinella radiata</i> (Audouin)	2
		<i>Patinella verrucaria</i> (Fabricius)	2
		Cancellata	Calvetiidae
Crisinidae	<i>Crisina radians</i> (Lamarck)		5
Horneridae	<i>Hornera frondiculata</i> (Lamouroux)		5
	<i>Hornera lichenoides</i> (Linnaeus)		5
	<i>Hornera robusta</i> MacGillivray		5
	<i>Hornera squamosa</i> Hutton		5
	* <i>Siphodictyum gracile</i> Lonsdale		1
<i>Stegohornera violacea</i> (Sars)	5		
Pseudidmoneidae	<i>Pseudidmonea fissurata</i> (Busk)		5

APPENDIX 2

Character matrix used in the phylogenetic analysis. See text (pp. 375–381) for character descriptions and codes.

	1	2	3	4	5	6	7	8	9	10	11	12	13	14	15	16	17	18	19	20	21	22	23	
<i>Cuffeyella</i>	0	0/1	1	?	0	0	0	?	0	0	?	0	0	0	0	1	0	1	0	0	?	?	?	
<i>Bicrisia</i>	1	0	1	2	1	0	0	1	0	0	1	0	0	0	0	1	0	1	0	0	1	0	0	
<i>Borgiola</i>	0	1	0	?	0	0	0	?	0/1	1	0	1	0	1	1	0	?	0	0	0	1	?	0	
<i>Cinctipora</i>	1	1	1	1	0	0	1	0	1	0	0	0	0	1	2	1	0	1	0	0	0	?	?	
<i>Collapora</i>	1	1	0	1	0	0	0	0	1	0/1	0	0	0	0	1	1	0	1	0	0	1	?	0	
<i>Crisia</i>	1	0	1	2	1	0	0	1	0	0	1	0	0	0	0	1	0	1	0	0	1	0	0	
<i>Crisina</i>	1	1	0	1	0	0	1	1	1	0	0	0	1	1	0	0	?	0	1	0	1	0	1	
<i>Crisulipora</i>	1	?	?	1	1	0	0	1	0	0	?	0	0	0	1	1	1	1	0	0	1	0	0	
<i>Diaperocia</i>	1	1	1	1	0	0	0/1	0	1	0	0	0	0	0	0	1	1	0	1	0	0	1	?	0
<i>Diplosolen</i>	0	1	0	?	0	0	0	?	0	0	0	0	0	0	1	1	1	1	0	0	1	?	0	
<i>Disporella</i>	0	1	0	?	0	0/1	0	?	0	1	0	1	0	1	1	0	?	0	1	0	1	?	1	
<i>Fasciculipora</i>	1	1	0	1	0	0	0	0	1	0	0	0	0	2	1	1	?	0	0	2	?	?	0	
<i>Favosipora</i>	0	1	0	?	0	1	0	?	0	1	0	1	0	1	1	0	?	1	0	0	1	?	0	
<i>Fenestulipora</i>	1	?	?	2	0	0	0	1	0	0	0	0	0	0	0	1	1	1	0	0	1	0	0	
<i>Foricula</i>	1	1	0	1	0	0	0	0	1	1	0	0/1	0	1	1	1	0	1	0	1	1	?	0	
<i>Heteropora magna</i>	1	1	0	1	0	0	0	0	1	1	0	1	0	1	1	1	0	1	0	0	?	?	?	
<i>H. neozelanica</i>	1	1	0	1	0	0	0	0	1	1	?	1	0	1	0	1	0	1	0	0	1	?	0	
<i>H. parapelliculata</i>	0	1	0	?	0	0	0	?	0	1	0	1	0	1	0	1	0	1	0	0	1	?	0	
<i>Homera</i>	1	1	0	1	0	0	0	1	1	0	0	0	1	1	0	0	?	0	1	0	1	1	1	
<i>Idmidronea</i>	1	1	1	1	0	0	1	1	0	0	0	0	0	0	0	1	1	1	0	0	1	0	0	
<i>Meliceritites</i>	1	1	0	1	0	0	0	0	1	0/1	0	0	0	0	1	1	0	1	0	1	1	?	0	
<i>Patnella</i>	0	1	0	?	0	1	0	?	0	1	0	1	0	1	0	0	?	0	1	0	1	?	1	
<i>Plagioecia</i>	0	1	0	?	0	1	0	?	0	0	0	1	0	0	0	1	1	1	0	0	1	?	0	
<i>Platonea</i>	1	1	1	1	0	0	1	1	0	0	0	0	0	0	0	1	1	?	0	0	1	?	0	
<i>Stegohomera</i>	1	1	0	1	0	0	0	1	1	0	0	0	1	1	1	0	?	0	1	0	1	1	0	
<i>Stomatopora</i> (Jurassic)	0	0	1	?	0	0	0	?	0	0	?	0	0	0	1	1	1	1	0	0	?	?	?	
' <i>Stomatopora</i> ' (Recent)	0	1	0	0	0	1	0	0	1	0	0	0	1	1	1	1	0	0	2	0	0	0	1	
<i>Reptomultisparsa</i>	0	1	0	?	0	0	0	?	0	0	0	0	0	0	1	1	0	1	0	0	1	?	0	
<i>Tubulipora</i>	0	1	1	?	0	0	1	?	0	0	0	0	0	0	1	1	1	1	1	0	0	1	?	0
trepostome	1	1	0	1	0	0	0	0	1	1	0	1	0	1	?	0	?	0	0/1	0	0	?	0	

continued

